

**GENETIC STUDY OF HEMATOPOIESIS IN ZEBRAFISH
— CHARACTERIZATION OF ZEBRAFISH UDU MUTANT,
POSITIONAL CLONING AND FUNCTIONAL STUDY OF UDU GENE**

LIU YANMEI

NATIONAL UNIVERSITY OF SINGAPORE

2006

**GENETIC STUDY OF HEMATOPOIESIS IN ZEBRAFISH
— CHARACTERIZATION OF ZEBRAFISH UDU MUTANT,
POSITIONAL CLONING AND FUNCTIONAL STUDY OF UDU GENE**

LIU YANMEI

(Master of Medicine, Peking University, China)

**A THESIS SUBMITTED
FOR THE DEGREE OF DOCTOR OF PHILOSOPHY
INSTITUTE OF MOLECULAR AND CELL BIOLOGY
DEPARTMENT OF BIOLOGICAL SCIENCES
NATIONAL UNIVERSITY OF SINGAPORE**

Acknowledgements

I would like to express my sincere gratitude to my supervisor Dr. Zilong Wen for his great guidance, encouragement, support and patience during my Ph.D studies. I am also deeply grateful to my Ph.D committee members, Dr. Jinrong Peng, Dr. Sudipto Roy and Dr. Yun-Jin Jiang for their constructive discussions and valuable advice.

I greatly appreciate the past and present lab members for their kind concern, helpful discussions and invaluable friendship. Especially I want to thank Linsen Du and Bernard Teo for their excellent cooperation with me in this project. Special thanks also go to Dr. Motomi Osato (Lab of molecular oncology), who made great contribution to cell cycle and cytology analysis of hematopoietic cells. I also would like to express my heartfelt gratitude to our genetic screen team, both in our lab: Feng Qian, Hao Jin, Fenghua Zhen, Jin Xu and Dr. Peng's group: Lin Guo and Honghui Huang. I also appreciate Dr. Haiwei Song for protein domain analysis, Dr. Chengjin Zhang for her pioneer work in our lab.

I am deeply grateful to fish facility, sequence facility as well as administration of IMCB and TLL (ex-IMA) for their great service. I appreciate the high level training of Ph.D program provided by TLL (ex-IMA) and IMCB and thank all the teachers in the graduate courses. Many thanks go to my dear friends and all the people ever helped me in TLL (ex-IMA) and IMCB. Especially, I want to thank my best friend, Meipei She for her kind help in my studies, work and life.

I owe my every progress to my dearest parents for their self-giving love, constant encouragement, inculcation and understanding. Especially, during my thesis writing and also pregnancy period, my mother comes to take care of me and make me concentrating on the thesis writing. I would like to give my loving gratitude to my husband Jifeng. Although he is studying in Germany and not around me, he never stops supporting me, encouraging me and discussing with me in my project. Lastly, I also want to thank my baby daughter, whose coming brings me great courage to deal with all the difficulties.

Table of Contents

Acknowledgement	i
Table of Contents	iii
Summary	vi
List of Tables	viii
List of Figures	ix
List of Abbreviations	xi
List of Publication	xiv

Chapter I Introduction.....	1
1.1 Hematopoiesis in mammals.....	1
1.1.1 Hematopoiesis: definition and significance.....	1
1.1.2 Two waves of hematopoiesis: primitive and definitive	2
1.1.2.1 Hematopoietic stem cells derive from ventral mesoderm	2
1.1.2.2 Primitive hematopoiesis	5
1.1.2.3 Definitive hematopoiesis.....	6
1.1.3 Putative hemangioblast.....	9
1.1.4 Hematopoietic stem cells.....	9
1.1.4.1 Origin of Hematopoietic stem cells.....	9
1.1.4.2 Lineage differentiation of Hematopoietic stem cell	11
1.1.5 Erythropoiesis.....	15
1.1.6 Myeloid lineage development	18
1.1.7 T Lymphocyte development	20
1.1.7.1 T lymphopoiesis	20
1.1.7.2 Thymus organogenesis	23
1.2 Genetic study of hematopoiesis in Zebrafish	25
1.2.1 Zebrafish is a powerful model to study hematopoiesis	25
1.2.2 Primitive hematopoiesis in zebrafish.....	26
1.2.2.1 Primitive erythropoiesis	26
1.2.2.2 Primitive myelopoiesis	28
1.2.3 Definitive hematopoiesis in zebrafish	29
1.2.4 Genetic methods to study hematopoiesis in zebrafish.....	32
1.2.4.1 Mutagenesis Screening.....	32
1.2.4.1.1 Zebrafish Genomics	34
1.2.4.1.2 Principles of Positional Cloning.....	35
1.2.4.2 Morpholinos	37

1.2.4.3 Transgenic Reporters	37
1.2.4.4 Targeting Induced Local Lesions In Genomes (TILLING)	38
1.2.5 Important zebrafish hematopoietic mutants	39
1.2.5.1 HSC mutants	39
1.2.5.2 Erythroid progenitor mutants	41
1.2.5.3 Late stage erythrocyte mutants	43
1.3 Aims of the study	45
Chapter II Materials and Methods.....	46
2.1 Zebrafish maintenance and embryo culture	46
2.2 Whole-mount <i>in situ</i> hybridization (WISH) and <i>o</i> -dianisidine staining.....	46
2.2.1 Digoxigenin (DIG)-labeled RNA probe synthesis.....	46
2.2.2 WISH procedure for <i>rag1</i> screening	47
2.2.3 High-resolution WISH protocol	48
2.2.4 <i>o</i> -Dianisidine staining of hemoglobin	49
2.3 Genetic Screen	51
2.3.1 ENU mutagenesis.....	51
2.3.2 Generation of F1 fish and F2 families	51
2.3.3 <i>rag1</i> screen	52
2.3.4 Outcrossing to generate F3, F4, and F5 progeny.....	52
2.4 Positional cloning of <i>wz260</i>	53
2.4.1 Generation of mapping families and collection of the embryos.....	53
2.4.2 DNA preparation	53
2.4.3 Bulk segregation analysis (BSA)	54
2.4.4 Linkage analysis with single mutant embryos.....	54
2.4.5 Searching for the contigs and clones containing the mutant gene.....	58
2.4.6 Identification of the mutant gene by sequencing analysis	59
2.5 Amplification of <i>udu</i> cDNA and the related plasmid construction.....	59
2.5.1 Total RNA extraction from embryos	59
2.5.3 Cloning of <i>udu</i> cDNA constructs containing the wild type allele and the <i>udu</i> ^{<i>sq1zl</i>} allele (pcDNA3.1- <i>udu</i> -wt, pcDNA3.1- <i>udu</i> -T2976A)	61
2.5.4 Cloning of Flag-tagged and HA-tagged <i>udu</i> cDNA constructs (pcDNA3.1-N-Flag- <i>udu</i> -wt and pcDNA3.1-C-HA- <i>udu</i> -wt) and SANT-L domain deficient mutant construct (pcDNA3.1- <i>udu</i> - Δ SANT-L)	62
2.6 <i>udu</i> cRNAs rescue experiments	62
2.6.1 Synthesis of <i>udu</i> cRNAs.....	62
2.6.2 microinjection.....	64
2.6.3 Evaluation of the rescue efficiency and genotyping analysis	64
2.7 Morpholino knockdown	64
2.8 Acridine orange staining.....	68
2.9 FACS, cytology, and cell cycle analysis.....	68
2.10 Cell transplantation	69
2.11 Northern blot analysis of <i>udu</i> transcripts.....	70
2.11.1 RNA Preparation	70
2.11.2 Dig-labeled RNA Probe Preparation	70

2.11.3 Northern blot	70
2.12 Generation of rabbit anti-udu antibodies.....	72
2.12.1 GST-fusion protein expression and purification.....	72
2.12.2 Immunization of rabbits with GST-Udu-N/C-Antigen.....	73
2.12.3 Antibody affinity purification.....	73
2.13 Western blot analysis of Udu protein expression in transfected cells.....	74
2.13.1 Extraction of proteins from cultured cells transfected with udu constructs	74
2.13.2 Western blot.....	75
2.14 Immunohistochemistry staining	75
2.15 Affymetrix Array	76
2.16 Real time PCR and Semi-quantitative RT-PCR.....	76
Chapter III Genetic Screen for T lymphocyte deficient mutants.....	78
3.1 Results.....	78
3.1.1 Genetic screen for <i>rag1</i> -deficient mutants	78
3.1.2 Data management.....	80
3.1.3 Preliminary characterization of the <i>rag1</i> -deficient mutants	82
3.2 Discussion	87
Chapter IV Characterization of <i>udu</i> mutant embryo, positional cloning and functional study of <i>udu</i> gene	91
4.1 Results.....	91
4.1.1 Characterization of <i>udu</i> mutant	91
4.1.1.1 Morphological phenotype of <i>wz260</i> and complementary test between <i>wz260</i> and <i>ugly duckling (udu^{u24})</i>	91
4.1.1.2 Primitive hematopoietic hypoplasia in <i>udu</i> ^{-/-} mutant.....	93
4.1.1.3 Abnormal proliferation and differentiation of hematopoietic cells in <i>udu</i> ^{-/-}	94
4.1.2 Identification of the <i>udu</i> mutant gene.....	100
4.1.2.1 Positional cloning of <i>udu</i> gene	100
4.1.2.2 Confirmation of identity of the <i>udu</i> gene by cRNA rescue and morpholino knockdown	111
4.1.3 Functional study of <i>udu</i> gene	111
4.1.3.1 Expression pattern of <i>udu</i>	111
4.1.3.2 Cell-autonomous erythroid defect in the <i>udu</i> ^{-/-} mutant.....	115
4.1.3.3 The <i>udu</i> gene encodes a putative transcriptional modulator.....	118
4.1.3.4 The <i>udu</i> ^{-/-} erythroid defect is mediated by a <i>p53</i> -dependent pathway	119
4.2 Discussion	130
4.2.1 Analysis of the hematopoietic phenotype of <i>udu</i> mutant	130
4.2.2 Cell-autonomous role of <i>udu</i> gene in erythropoiesis.....	131
4.2.3 The putative molecular mechanism involving Udu protein	132
4.2.4 The possible relationship between Udu and p53	133
4.2.5 The Udu homologue GON4L may be associated with tumor development	135
4.2.6 Essential role of Udu in proliferation and differentiation of erythroid lineage	136
Reference list.....	137

Summary

Vertebrate hematopoiesis is a highly conserved process that requires a series of cell specification, proliferation and differentiation. The underlying mechanisms governing these cellular events are, however, not fully understood. Recently, zebrafish (*Danio rerio*) has emerged as a good genetic model organism to study the early events of blood formation during vertebrate development.

In order to study hematopoiesis, we carried out a whole-mount *in situ* hybridization (WISH) based forward genetic screen to isolate the *rag1*-deficient mutants. From screening 540 genomes, we identified 86 *rag1*-deficient mutants from 540 mutagenized genomes. By observing blood circulation, *wz260* mutant was identified as the only mutant that also had defects in primitive erythropoiesis. Therefore I selected *wz260* for detailed characterization and found that it was a new allele (*udu^{sq1zl}*) of *ugly duckling* (*udu^{tu24}*), which was first isolated from the 1996 Tuebingen large-scale screen as a mutation affecting morphogenesis during gastrulation and tail formation. WISH to detect the hematopoietic markers indicated that both primitive erythropoiesis and myelopoiesis were impaired in *udu^{sq1zl}* homozygous mutants. Cell cycle, cytology, and transplantation analyses showed that the primitive erythroid cells in the *udu^{sq1zl}* homozygous mutants were severely defective in proliferation and differentiation in a cell-autonomous fashion. Positional cloning revealed that the *udu* gene encodes a novel protein of 2055 amino acids (aa) that contained several

conserved regions, including two Paired Amphipathic-Helix like (PAH-L) repeats and a putative SW13, ADA2, N-Cor and TFIIB-like (SANT-L) or a Myb-like DNA binding domain (This domain is referred as SANT-L thereafter). I further found that the Udu protein is predominantly localized in the nucleus and deletion of the putative SANT-L domain abolishes its function. Moreover, robust elevations of the tumor suppressor *p53* expression as well as several *p53* downstream targets were observed in the *udu*^{-/-} mutant embryos. Knockdown of *p53* protein expression by *p53* antisense morpholino oligos (MO) could correct the mutant phenotype to the same extent as *udu* RNA injections in mutant embryos. Thus, these results indicate that the Udu protein plays a crucial role in regulating the proliferation and differentiation of erythroid cells through a *p53*-dependent pathway.

List of Tables

Table 2.1	List of Constructs for antisense RNA Probes	50
Table 2.2	Duration of Proteinase K Permeabilization for Zebrafish WISH	50
Table 2.3	300 pairs of SSLP markers used for BSA	55
Table 2.4	The polymorphic SSLP/SNP markers used for <i>udu</i> mapping	60
Table 2.5	Primers for 5' and 3' RACE of <i>udu</i> gene	63
Table 2.6	Primers for cloning of <i>udu</i> cDNA constructs	63
Table 3.1	Summary of <i>rag1</i> genetic screen	81
Table 4.1	Rescue results	112
Table 4.2	Summary of cell transplantation analysis	117
Table 4.3	Summary of down-regulated genes in <i>udu</i> ^{-/-} mutant	123
Table 4.4	Summary of up-regulated genes in <i>udu</i> ^{-/-} mutant	126

List of Figures

Figure 1.1	The hematopoietic hierarchy	13
Figure 1.2	Hematopoietic program in zebrafish	31
Figure 1.3	Outline of forward genetic screen in zebrafish	33
Figure 1.4	Bulk segregation analysis to isolate linked SSLP	36
Figure 2.1	Cloning strategy of <i>udu</i> constructs	65
Figure 3.1	Expression of <i>rag1</i> in zebrafish	79
Figure 3.2	Detection of <i>rag1</i> expression in wild type and mutant embryos	79
Figure 3.3	Database management of <i>rag1</i> screen	83
Figure 3.4	<i>o</i> -dianisidinstaining of 2dpf wild type and mutant <i>wz260 (udu)</i> embryos	84
Figure 3.5	Expression of <i>hoxa3</i> and <i>foxn1</i> in zebrafish	85
Figure 3.6	<i>foxn1</i> condensed expression pattern in some mutant embryos	86
Figure 3.7	Twelve <i>rag1</i> -deficient mutants with relatively normal morphology.	88
Figure 4.1	Morphological phenotype of <i>udu (wz260)</i> mutant	92
Figure 4.2	Primitive erythropoiesis is impaired in the <i>udu</i> ^{-/-} mutant	95
Figure 4.3	Myelopoiesis is defective in the <i>udu</i> ^{-/-} mutant	96
Figure 4.4	Extensive cell deaths in the CNS but not in the ICM in the <i>udu</i> ^{-/-} mutant	98
Figure 4.5	The <i>udu</i> ^{-/-} erythroid cells are defective in cell proliferation and differentiation	99
Figure 4.6	BSA identified that the <i>udu</i> mutation was linked to SSLP marker z10036 (A) and z1215 (B) on linkage group 16	102

Figure 4.7	Single embryo linkage analyses of marker z10036 (A) and z1215	103
Figure 4.8	The genetic map T51 and MGH provided by ZFIN	104
Figure 4.9	Fine mapping using z17246 and SSLP-S16	105
Figure 4.10	Alignment of North Contig #9751 and South Contig #10178	107
Figure 4.11	Positional cloning and gene structure of <i>udu</i> gene	108
Figure 4.12	The nonsense mutation in Ensemble Gene ENSDARG00000005867 (<i>udu</i> gene) in <i>udu^{tu24}</i> and <i>udu^{sq1zl}</i> mutants	108
Figure 4.13	<i>udu</i> cDNA sequence	109
Figure 4.14	Confirmation of the <i>udu</i> gene by cRNA rescue and morpholino knockdown	112
Figure 4.15	The temporal and spatial expression of the <i>udu</i> gene during early zebrafish development	114
Figure 4.16	Northern blot analysis of <i>udu</i> mRNA expression at different stages of zebrafish	114
Figure 4.17	Western blot examination of purified anti-Udu-N and C-Antigen polyclonal antibodies by recognizing the untagged Udu-N-Antigen and Udu-C-Antigen.	116
Figure 4.18	Western blot analysis of the ectopic expressed Udu protein in 293T cells.	116
Figure 4.19	Sequence alignment of the zebrafish Udu, human and mouse GON4L proteins	120
Figure 4.20	The Udu protein is a putative transcriptional modulator	122
Figure 4.21	Verification of elevated <i>p53</i> and its target gene expressions in the <i>udu^{-/-}</i> mutant embryos by semi-quantitative RT-PCR	128
Figure 4.22	The hematopoietic phenotype of the <i>udu^{-/-}</i> mutant is mediated by a <i>p53</i> -dependent pathway	129

List of Abbreviations

aa	amino acid
AGM	aorta-gonad-mesonephros
ALM	anterior lateral mesoderm
AO	acridine orange
AP	alkaline phosphatase
BAC	bacterial artificial chromosome
BCIP	5-bromo-3-chloro-3-indolyl phosphate
BCS	bovine calf serum
BFU-E	bust-forming unit-erythroid
BL-CFC	blast colony-forming cells
<i>bls</i>	<i>bloodless</i>
BM	Bone marrow
BMP	Bone morphogenetic factor
bp	base pair
BPA	Burst promoting activity
BSA	bulk segregation analysis
<i>cdy</i>	<i>chardonnay</i>
CFU-E	colony forming unit-erythroid
CFU-S	colony-forming unit-spleen
<i>cha</i>	<i>chablis</i>
<i>cia</i>	<i>chianti</i>
<i>clo</i>	<i>cloche</i>
CLP	common lymphoid progenitor
cM	centimorgan
CMP	common myeloid progenitor
CNS	central nervous system
DEPC	diethylpyrocarbonate
Dhh	Desert hedgehog
DIG	digoxigenin
DN	Double-negative
DNA	deoxyribonucleic acid
dNTP	deoxyribonucleotide triphosphate
DP	Double-positive
dpc	day <i>postcoitum</i>
dpf	days post fertilization
<i>drc</i>	<i>dracula</i>
<i>dsm</i>	<i>desmodius</i>
DTT	dithiothreitol
ECM	extracellular matrix
EDTA	ethylenediaminetetraacetic acid
EGFP	enhanced green fluorescent protein

EKLF	Erythroid Kruppel-like Factor
ENU	N-ethyl-N-nitrosourea
EPO	Erythropoietin
ES	embryonic stem
FACS	fluorescence-activated cell sorting
FBS	fetal bovine serum
FGF	fibroblast growth factor
FOG	Friend of GATA-1
<i>frx</i>	<i>freixinet</i>
GATA-1	GATA-binding protein 1
G-CSF	granulocyte colony-stimulating factor
GFP	green fluorescent protein
GM-CSF	granulocyte macrophage-colony stimulating factor
GMP	granulocyte-monocyte progenitor
HEB	Hela E-box Binding protein
HEPES	4-(2-hydroxyethyl)-1-piperazineethanesulfonic acid
hpf	hours post fertilization
hr	hour
HSC	hematopoietic stem cell
ICM	intermediate cell mass
Ihh	Indian hedgehog
IL-3	interleukin-3
IPTG	isopropyl b-D-thiogalactopyranoside
kb	kilo base pair
<i>kgg</i>	<i>kugelig</i>
Lin ^{-/lo}	lineage marker ^{-/lo}
Lmo2	lim-only protein 2
LTR	long-term multilineage repopulating
M	mole per liter
M-CSF	macrophage colony-stimulating factor
MEP	megakaryocyte-erythrocyte progenitor
mg	milligram
min	minute
ml	milliliter
MO	morpholino oligo nucleotides
<i>mon</i>	<i>moonshine</i>
<i>mot</i>	<i>merlot</i>
<i>mpo</i>	<i>myeloperoxidase</i>
mRNA	messenger ribonucleic acid
NBT	nitroblue tetrazolium
NK	nature killer
nl	nanolitre
NTP	ribonucleotide triphosphate
O/N	overnight

PAH-L	<u>P</u> aired <u>A</u> mphipathic- <u>H</u> elix like
PBS	phosphate-buffered saline
PCR	polymerase chain reaction
PFA	paraformaldehyde
PLM	posterior lateral mesoderm
PTU	1-phenyl-2-thiourea
<i>rag1</i>	<i>recombination activating gene 1</i>
RBI	rostral blood island
<i>ret</i>	<i>retsina</i>
<i>ris</i>	<i>riesling</i>
RT	room temperature
RT-PCR	reverse transcription polymerase chain reaction
SANT-L	<u>S</u> W13, <u>A</u> DA2, <u>N</u> -Cor and <u>T</u> FIIB-like
<i>sau</i>	<i>sauternes</i>
SCF	stem cell factor
SCL	stem cell leukemia hematopoietic transcription factor
SDF-1	stromal cell-derived factor-1
SDS	sodium dodecyl sulfate
SNP	single nucleotide polymorphism
<i>spt</i>	<i>spadetail</i>
SSC	sodium chloride-trisodium citrate solution
SSLP	simple sequence length polymorphism
TCR	T-cell receptor
TdT	Terminal deoxynucleotidyl transferase
TEC	thymic epithelial cells
TECK	thymus-expressed chemokine
TGF- β	transforming growth factor- β
<i>TIF1γ</i>	<i>transcriptional intermediary factor 1γ</i>
TILLING	Targeting Induced Local Lesions In Genomes
TPO	thrombopoietin
<i>udu</i>	<i>ugly duckling</i>
UROD	uroporphyrinogen decarboxylase
UV	ultraviolet
VE	visceral endoderm
<i>vlt</i>	<i>vlad tepes</i>
<i>weh</i>	<i>weissherbst</i>
WGS	whole genome shotgun
WISH	whole-mount in situ hybridization
wt	wild-type
YC	yolk sac
<i>yqe</i>	<i>yquem</i>
μ g	microgramme
μ l	microlitre

List of Publication

Yanmei Liu, Linsen Du, Motomi Osato, Eng Hui Teo, Feng Qian, Hao Jin, Fenghua Zhen, Jin Xu, Lin Guo, Honghui Huang, Jun Chen, Robert Geisler, Yun-Jin Jiang, Jinrong Peng and Zilong Wen. The Zebrafish *udu* Gene Encodes a Novel Nuclear Factor and Is Essential for Primitive Erythroid Cell Development. *Blood*. In press.

Chapter I Introduction

1.1 Hematopoiesis in mammals

1.1.1 Hematopoiesis: definition and significance

Hematopoiesis is the development of blood cells and other formed elements of blood. Hematopoietic cells consist of erythrocytes, monocytes, neutrophils, basophils, eosinophils, mast cells, megakaryocytes, natural killer (NK) cells, T and B lymphocytes. And they display distinctive functions, for example, erythrocytes deliver oxygen, platelets form blood clot, some myeloid cells scavenge debris as well as pathogens, and lymphocytes regulate the host specific immune reactions. Despite their wide functional diversities, all of the blood cells are derived from a common precursor cell — hematopoietic stem cell (HSC) (Kondo et al., 2003). So, hematopoiesis embraces two aspects: the development of the first HSCs from nonhematopoietic tissue in embryonic and fetal life, as well as differentiation of multipotent, self-renewing HSCs into all lineages of the blood.

Hematopoiesis research has been always at the forefront of basic science, helping us to understand cell biology, molecular biology, genetics, and protein structure and formation. On the other hand, from the clinical point of view, a basic understanding of the biology of blood cells is essential for developing new therapeutic approaches for treatment of the hematopoietic diseases, such as thalassemia, immunodeficiency and leukemia. For instance, HSC or bone marrow transplantation has been used to treat the leukemia patients efficiently. Therefore, hematopoiesis study definitely provides a promising future for basic science as well as clinical medicine.

In the past few decades, studies in several species, including mammals, birds, and amphibians, have shown that hematopoiesis is considerably conserved throughout vertebrate evolution. The best understood vertebrate hematopoietic system is that of the laboratory mouse (*Mus musculus*), and recently the zebrafish (*Danio rerio*) has emerged as another excellent model organism for studying hematopoiesis (Lensch and Daley, 2004). Thus, I will mainly introduce hematopoiesis in the mouse and zebrafish in this chapter.

1.1.2 Two waves of hematopoiesis: primitive and definitive

Vertebrate hematopoiesis has two successive waves, primitive and definitive, that differ in anatomic location and the cell types produced. In mammals, the first or primitive wave of hematopoiesis, is transitory, occurs in the extraembryonic structure-yolk sac (YS), and produces nucleated primitive erythrocytes, some macrophages and rare megakaryocytes (Palis and Yoder, 2001; Xu et al., 2001; Medvinsky et al., 1993; Moore and Metcalf, 1970). The second or definitive wave of hematopoiesis is persistent, initiates from the aorta-gonad-mesonephros (AGM) region, then transits to the liver, thymus, spleen, and finally, moves to the bone marrow. Definitive hematopoiesis generates all mature blood cells (Johnson and Moore, 1975; Lensch and Daley, 2004; Medvinsky et al., 1993; Godin et al., 1993).

1.1.2.1 Hematopoietic stem cells derive from ventral mesoderm

HSCs are specified early in embryogenesis from ventral mesoderm. As the undifferentiated, self-renewing cells, mesoderm will give rise to stem cells for the blood, mesenchyme, kidney, muscle, and notochord (from ventral to dorsal) (Zon, 1995). The understanding of ventral mesoderm induction comes mainly from studies

in *Xenopus*. The unfertilized *Xenopus* egg is radially symmetric with a dark pigmented animal hemisphere and a lightly colored yolky vegetal hemisphere. Sperm entry initiates a rotation of the cortex of the egg with respect to the internal cytoplasm. This cortical rotation results in the dorsal side being defined by the formation of the Nieuwkoop center in the vegetal region on the side opposite sperm entry (Huber and Zon, 1998; De Robertis and Kuroda, 2004). At blastula stage, vegetal signals, which are maternally derived and separated into ventral-vegetal and dorsal-vegetal signals, induce the equatorial cells (known as the marginal zone) to form dorsal and ventral mesoderm. Fibroblast growth factor (FGF) may be the ventral-vegetal signal that induces mesoderm with ventro-lateral character. Vg-1, activin, two members of the transforming growth factor- β (TGF- β) family, and Wnt11, a member of the Wg/Wnt proteins (Heasman, 2006), are likely to be the main dorsal-vegetal signals, through which the Nieuwkoop center specifies the Spemann's organizer and the dorsal mesoderm (Huber and Zon, 1998; De Robertis and Kuroda, 2004). At the gastrula stage, bone morphogenetic factor 4 (BMP4), another TGF- β family member, is expressed in the ventral and lateral marginal zones as a ventral mesoderm-patterning factor. *BMP4* RNA and cDNA injections ventralize embryos while dominant negative BMP4 receptor injections dorsalize embryos. In combination with mesoderm inducers, such as FGF and activin, BMP4 yields abundant hematopoietic mesoderm. BMP4 activity is inhibited by at least three factors, chordin, follistatin and noggin, secreted from the Spemann's organizer, the dorsal gastrula center (De Robertis and Kuroda, 2004; Huber and Zon, 1998). The ventral-mesoderm patterning by BMP4 is mediated, at least in part, by members of the Mix and Vent families of homeobox transcription factors. Following gastrulation, a subset of ventral mesoderm is specified to become HSCs (Davidson and Zon, 2000).

In mouse, mesoderm is formed from cells migrating through the primitive streak between the presumptive ectoderm and the endoderm. The same layer of mesoderm extends both into the embryo and extraembryonically, into the YS. In mouse, around 7.0-7.5 day *postcoitum* (dpc), the extraembryonic mesodermal cells in association with the visceral endoderm (VE) form the blood islands, where primitive hematopoiesis takes place. Structurally, blood islands consist of clusters of hematopoietic cells surrounded by endothelial cells (Lensch and Daley, 2004). TGF- β 1 and BMP4 have been shown to be required for blood-island formation in the mouse embryo. In *TGF- β 1* and *BMP4* mutant embryos, both blood and endothelial cell developments are compromised (Dickson et al., 1995; Winnier et al., 1995).

Tissue recombination experiments performed in the mouse establish more directly that VE is required for induction of hematopoiesis in the gastrulation embryo (Belaoussoff et al., 1998). Around the onset of gastrulation, induction of primitive hematopoiesis from ectoderm (more specifically, nascent mesoderm cells arising from the primitive streak) requires the presence of VE. And this VE signaling is only required in a relatively narrow window of time, since blood formation is autonomous to mesoderm by mid-streak stage. Surprisingly, VE signals can respecify the anterior epiblast (prospective neural ectoderm) to posterior cell fates, formation of blood and endothelial cells (Belaoussoff et al., 1998). Recently, Indian hedgehog (Ihh), expressed in VE of gastrulating mouse embryos and mature yolk sacs, was identified to be the VE secreted signal sufficient to induce formation of hematopoietic and endothelial cells. Strikingly, Ihh can also respecify anterior epiblast along hematopoietic and endothelial lineages. Bmp4, upregulated in response to Ihh signals,

may mediate activation of hematopoietic and vascular development. Although *Ihh* alone is sufficient to induce the development of hematopoiesis and vasculogenesis, analysis of mice deficient in *Ihh* shows that *Ihh* is not essential in these processes, suggesting that another hedgehog protein, perhaps Desert hedgehog (Dhh), or a distinct pathway must at least partially compensate for *Ihh* function (Dyer et al., 2001).

1.1.2.2 Primitive hematopoiesis

As mentioned above, murine primitive or embryonic wave of hematopoiesis occurs at around 7-7.5 dpc in the YS blood islands derived from ventral mesoderm, and produces primitive erythrocytes, macrophages and rare megakaryocytes (Palis and Yoder, 2001; Xu et al., 2001; Medvinsky et al., 1993; Moore and Metcalf, 1970). Compared with the definitive red blood cells, the primitive erythroid cells are larger and remain nucleated (Lensch and Daley, 2004). These cells express 3 hemoglobin tetrameric complexes known as EI ($\zeta_2\varepsilon_2$), EII ($\alpha_2\varepsilon_2$), and EIII ($\alpha_2\beta H1_2$). ε and $\beta H1$ are embryonic forms of β -globin-like hemoglobin; ζ and α are embryonic and adult forms of α -globin-like hemoglobin, respectively (Fantoni et al., 1967). The embryonic forms of hemoglobin are uniquely adapted to the diffusion-limited, oxygen-poor microenvironment of the embryo prior to circulation (Leder et al., 1980). This early erythroid cells require the stimulation of burst promoting activity (BPA), a erythroid growth factor intrinsic produced by the YS (Labastie et al., 1984). In the contrast, erythropoietin (Epo), which is important for definitive erythroid cell survival and proliferation, is not required for this early red blood cell activity and not provided by the YS environment (Lin et al., 1996; Wu et al., 1995).

Prior to the emergence of primitive erythroblast, several genes important for hematopoiesis begin to express in the YS. These genes include stem cell leukemia hematopoietic transcription factor (*Scl*), the receptor tyrosine kinase *Flk-1*, which are expressed in both endothelial and hematopoietic progenitors (Shalaby et al., 1995; Shalaby et al., 1997; Shivdasani et al., 1995), and the transcription factors GATA-binding protein 1 (*Gata-1*) and *Brachyury* that are specifically expressed in the hematopoietic cells (Palis et al., 1999). Knockout of *Flk-1* abolishes the formation of both vascular and hematopoietic lineages, although mesoderm formation appears intact (Shalaby et al., 1995; Shalaby et al., 1997). Targeted disruption of *Scl* results in absence of embryonic hematopoietic cells, while the initiation of endothelial cell and vascular formation are normal. However, yolk sac vessel patterning is perturbed (Shivdasani et al., 1995). The studies of the hematopoietic potential of homozygous mutant embryonic stem (ES) cells in chimeric mice demonstrate that both *Flk-1* and *Scl* are also required for adult hematopoiesis (Porcher et al., 1996; Robb et al., 1996; Shalaby et al., 1997). Mutation of *Gata-1* affects both primitive and definitive erythropoiesis (Fujiwara et al., 1996; Pevny et al., 1991).

With development of the embryonic vasculature and initiation of cardiac contractions at 8.25dpc, the nucleated primitive red blood cells enter the circulation around 8.5dpc, persisting beyond the establishment of liver hematopoiesis (10.0dpc) and nearly absent at 15dpc (Ji et al., 2003).

1.1.2.3 Definitive hematopoiesis

Definitive hematopoiesis is believed to originate from the AGM region, which is derived from the intraembryonic lateral plate mesoderm, as early as 9dpc in mouse

(Medvinsky et al., 1993). At 10dpc, the AGM region possesses the long-term multilineage repopulating (LTR)-HSCs ability, able to rescue long-term blood formation in transplant recipients (Muller et al., 1994). Between 9.5 and 11dpc, the HSCs exit the AGM region and seed the fetal liver presumably through blood circulation (Garcia-Porrero et al., 1995). The liver remains an active hematopoietic organ until the neonatal period, where HSCs expand and differentiate to various cell types (Sasaki and Sonoda, 2000). The splenic rudiment is colonized by HSCs at 12dpc, becoming fully hematopoietic at 14.5dpc. The spleen aids in the transition from fetal liver to bone marrow hematopoiesis, and its activity persists throughout the life span of mouse (Sasaki and Matsumura, 1988). HSCs derived lymphoid progenitor cells appear to enter the thymic rudiment continuously from 11dpc and the thymus remains a lymphopoietic organ throughout life, fundamental to the development of the T lymphocytes (Douagi et al., 2002). Bone marrow (BM) is colonized by HSCs at 16dpc, and serves as the major organ producing blood cells in the juvenile and adult mouse (Delassus and Cumano, 1996).

Additionally, definitive hematopoiesis activity was also found in the YS. Firstly, before onset of the circulation, small-enucleated cells expressing adult globin, named as burst-forming unit-erythroid (BFU-E) cells are discovered in the YS at 8dpc (Palis et al., 1999). These BFU-E cells are then found in blood circulation by 9dpc, and later in the liver around 11dpc, suggesting this activity comes from the YS (Palis et al., 1999). Secondly, multipotent progenitors capable of generating myeloid and lymphoid cells can be detected in the YS at 8.5-9dpc (Galloway and Zon, 2003; Yoder et al., 1997a). And the YS-derived hematopoietic cells are able to form spleen colonies (colony-forming unit-spleen, CFU-S activity) after 9dpc. Finally, by 11dpc, the YS

harbors LTR-HSCs, which are able to reconstitute all aspects of long-term hematopoiesis when transplanted into a lethally irradiated host (Yoder et al., 1997b; Yoder and Hiatt, 1997). Therefore, the YS has the potential of definitive hematopoiesis.

As mentioned above, *Scf* and *Flk-1* are necessary for both primitive and definitive hematopoiesis, and *Gata-1* is required for both primitive and definitive erythropoiesis (Pevny et al., 1991; Fujiwara et al., 1996). In contrast, *Runx1* and *c-Myb* are required for definitive hematopoiesis but not primitive hematopoiesis (Wang et al., 1996; Mukoyama et al., 1999; Mucenski et al., 1991; North et al., 1999). Both *Runx1* and *c-Myb* deficient mice display the same hematopoietic phenotype: no hematopoietic cells generated in the AGM region, fetal liver anemia but normal YS-derived erythropoiesis (Wang et al., 1996; Mucenski et al., 1991; North et al., 1999). This indicates that these two genes are involved in the definitive HSCs generation, maintenance, and proliferation or self-renew. Considering the migratory feature of definitive hematopoietic cells, some homing molecules must play a role during this early process. *β -1-integrin* has been identified to be necessary for the migration of the hematopoietic cells to the fetal liver as well as to thymus and bone marrow (Fassler and Meyer, 1995). Additionally, mutations in *Jak2* (Neubauer et al., 1998), *Epo/EpoR* (Wu et al., 1995; Lin et al., 1996) and *Erythroid Kruppel-like Factor (Eklf)* (Perkins et al., 1995) genes disrupt predominately the definitive erythropoiesis. Taken together, the molecular regulation of hematopoiesis is complex and the differences between primitive and definitive hematopoiesis may be because of the two anatomically separated hematopoietic sites: the YS and the AGM region.

1.1.3 Putative hemangioblast

Hematopoietic and endothelial cells have a close relationship. These cells concurrently emerge in the YS and express overlapping sets of genes, including *Flk1*, *CD34*, *Scl*, *Flt1* and *Gata-2*, indicating that both of these two cell types are derived from a common precursor, hemangioblast (Cumano and Godin, 2001; Keller et al., 1999). Targeted disruption of *Flk-1* or *TGF- β 1*, resulting in absence of both hematopoietic and endothelial cell lineages, provides additional evidence for the existence of hemangioblast (Dickson et al., 1995; Shalaby et al., 1995; Shalaby et al., 1997). Furthermore, using the ES cell differentiation culture system, the blast colony-forming cells (BL-CFCs), which are isolated within embryoid bodies generated from differentiated ES cells, can generate both hematopoietic and endothelial cells upon culture with appropriate cytokines. Therefore, the BL-CFC represents the putative hemangioblast. Additionally the BL-CFCs are lost quickly during the embryoid body development, which may also be the feature of hemangioblast that makes it difficult to be identified (Choi et al., 1998; Kennedy et al., 1997). In addition, *in vitro* culture system shows that TEK⁺ cells isolated from AGM and Flk⁺ cells sorted from ES cells and 9.5dpc YS also have the hemangiogenic potential (Hamaguchi et al., 1999; Nishikawa et al., 1998). Thus all of this evidence indicate the existence of hemangioblast.

1.1.4 Hematopoietic stem cells

1.1.4.1 Origin of Hematopoietic stem cells

HSCs are defined by their two abilities: pluripotency and self-renewal. Pluripotency means that HSCs are able to create progeny of all blood cell lineages. Self-renewal is that HSCs can undergo cell divisions and generate the daughter cells identical to the

parent stem cells, maintaining the stem cell pool as well as the proliferative capacity of HSCs (Kondo et al., 2003). Currently HSCs have been purified using fluorescence-activated cell sorting (FACS) and characterized as the lineage marker^{-/lo} (Lin^{-/lo}), c-Kit⁺, Sca-1⁺ subset of marrow cells (Uchida et al., 1996). Single HSC of the Thy1.1^{lo} Lin⁻, c-Kit⁺, Sca-1⁺ subset is able to self-renew and reconstitute all lineages of the blood in long term when transplanted into irradiated mice (Smith et al., 1991; Wagers et al., 2002b).

As we have known, the primitive hematopoiesis derives from the YS, whereas the definitive wave occurs at the AGM region. What is the relationship between the primitive HSCs in YS and the definitive HSCs from AGM remains controversial. Some studies support the notion that the two waves of hematopoiesis are independently derived from two different HSC pools occurring in two distinct sites (Dieterlen-Lievre, 1975; Medvinsky and Dzierzak, 1996), whereas others indicate that the early HSCs which give rise to both primitive and definitive waves are originated from one anatomic site, and then migrate to the other (Johnson and Moore, 1975; Moore and Metcalf, 1970). The most convincing evidence to support the first argument comes from studies in birds, where chick yolk sacs were transplanted onto quail embryos before the onset of circulation, and the host quail cells were found to be the sole contributors to definitive hematopoiesis (Dieterlen-Lievre, 1975). In contrast, the studies aiming to demonstrate that YS cells possess at least the capacity of transition to definitive blood cells give a support to the second theory. Matsuoka and colleagues observed that by co-culture with AGM-derived stromal cells, both early YS and AGM, isolated before the onset of circulation, can generate definitive HSCs with a similar repopulating potential (Matsuoka et al., 2001). The other experiment

showed that enforced expression of HoxB4 combined with culture on hematopoietic stroma induces the YS cells to become the definitive HSCs with the long-term, multilineage hematopoiesis repopulation activity (Kyba et al., 2002). Both of these studies indicate that the precirculation YS hematopoietic tissues have the potential of definitive HSCs activity when given the proper induction. But the critical point is whether this proper induction also exists *in vivo*. In another experiment, YS cells isolated from 9 dpc embryos were found capable to provide long-term multilineage reconstitution in primary neonatal recipients, suggesting that YS HSCs are available to seed the fetal liver on 10.0 dpc when definitive hematopoiesis is initiated (Yoder et al., 1997b).

Currently, three models describing the origin of definitive HSCs have been proposed (Galloway and Zon, 2003). The first theory states that all the HSCs are derived from the YS, and the AGM provides the appropriate microenvironment to enable the primitive YS cells to mature into definitive HSCs, capable of seeding the fetal liver and then bone marrow. The second model asserts that both the YS and the AGM generate HSCs independently, and these two sources of HSCs colonize the fetal liver, contributing to the definitive hematopoiesis together. In the third model, the AGM is the only source of HSCs, and the definitive activity observed in the YS comes from the AGM cells through circulation.

1.1.4.2 Lineage differentiation of Hematopoietic stem cell

Differentiation of HSCs to various blood cell types is believed to undergo a series of commitment steps to generate multipotent progenitors, lineage specific precursors and finally to terminal differentiated cells with a gradually restricted developmental

potential and the loss of self-renewal ability. Oligopotent progenitors, which have been identified in mouse, consist of common lymphoid progenitor (CLP) and common myeloid progenitor (CMP). CLPs develop to T, B lymphocytes and NK cells, whereas CMPs produce granulocyte-monocyte progenitor (GMP) and megakaryocyte-erythrocyte progenitor (MEP), which further differentiate to macrophage, granulocyte, and megakaryocyte, erythrocyte, respectively (Akashi et al., 2000; Kondo et al., 1997) (Figure 1.1).

What are the mechanisms governing the cell fate of HSCs? Two models have been proposed: stochastic and instructive. The stochastic hypothesis implies that HSCs randomly commit to self-renew or differentiate, whereas the instructive model infers that the external cues from the microenvironment, in which HSCs reside, drive the cell fate (Till, 1964; Socolovsky et al., 1998). Now it is believed that both extrinsic and intrinsic cellular regulators work together to determine the HSCs cell fate. Stem cells reside in their microenvironments, termed “niches”, which are believed to govern their self-renewal or differentiation. When undergoing asymmetric division, one daughter cell remains attached to the niche, receiving local signals to self renew, whereas the other daughter cell exits the niche and begins to differentiate (Wagers et al., 2002a). The extrinsic signals, provided by niches, influence HSCs through direct cell-cell or cell-extracellular matrix (ECM) interactions or through secretion of soluble mediators (Wagers et al., 2002a). In the absence of these signals, the hematopoietic cells will undergo apoptosis. The cytokines including stem cell factor (SCF), Flt3 (a tyrosine kinase receptor) ligand, and thrombopoietin (TPO) have been identified to affect the process of self-renewal and differentiation of HSCs (Nocka et al., 1989; Mackarehtschian et al., 1995; Carver-Moore et al., 1996). Recently, several

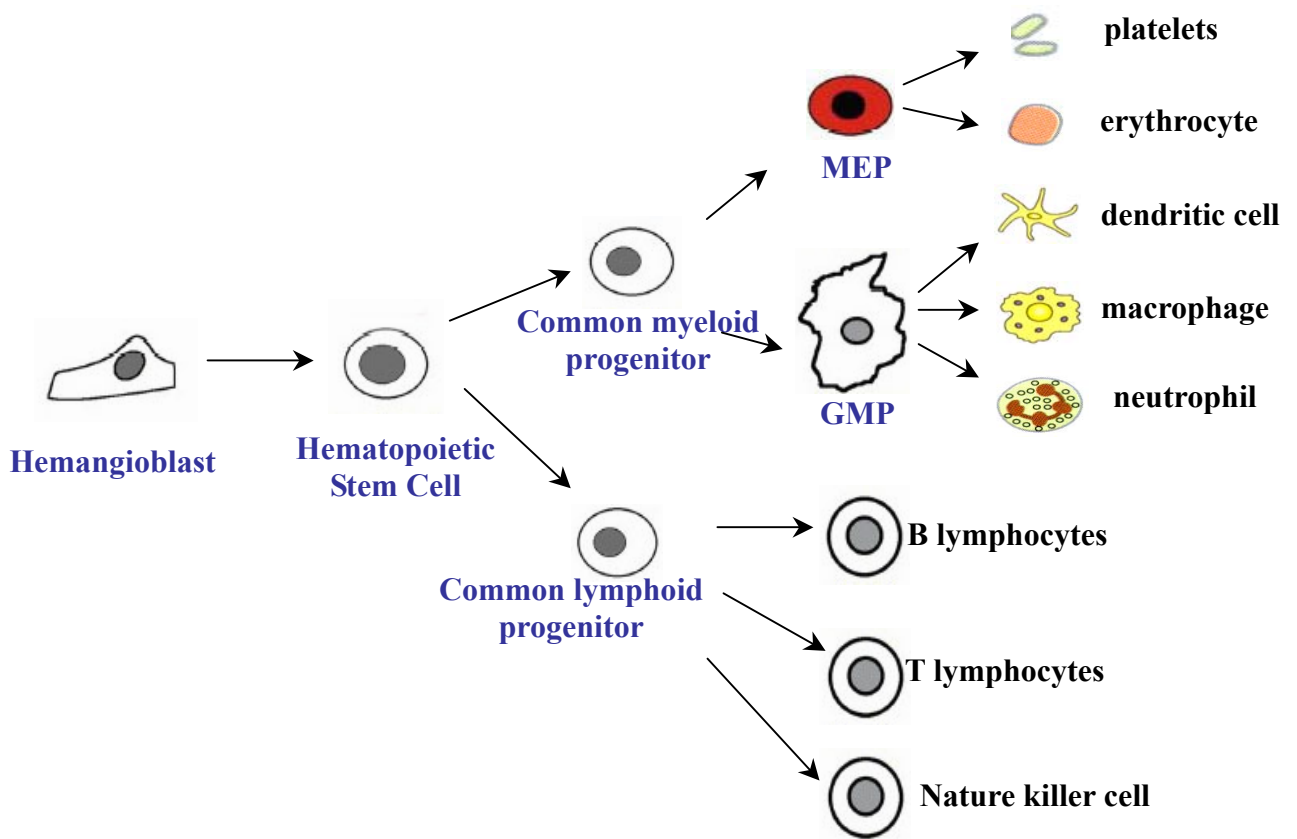


Figure 1.1 The hematopoietic hierarchy. The hematopoietic stem cells firstly give rise to common myeloid progenitors and common lymphoid progenitors, which further differentiate and eventually mature to all the blood lineages. MEP, megakaryocyte-erythrocyte progenitor; GMP, granulocyte-monocyte progenitor.

signaling pathways that determine cell fate have been shown to enhance the expansion of HSCs *ex vivo*. These include Wnts, Notch 1, Sonic hedgehog and BMP (Bhardwaj et al., 2001; Bhatia et al., 1999; Dyer et al., 2001; Reya et al., 2003; Varnum-Finney et al., 2000; Willert et al., 2003). How these environmental cues trigger the cell-intrinsic process to determine the self-renewal or differentiation of HSCs remains to be ascertained.

Intrinsic regulation of HSC cell-fate decision is predominantly via transcriptional regulation. Loss-of-function and overexpression studies have identified several genes indispensable for hematopoietic specification during embryonic development. These include *Scf*, *lim-only protein 2 (Lmo2)*, *Runx1*, *Gata-2*, *c-Myb* and *Ikaros* (Nichogiannopoulou et al., 1999; North et al., 1999; Tsai et al., 1994; Mucenski et al., 1991; Shivdasani et al., 1995; Wang et al., 1996; Warren et al., 1994). In addition, Homeobox genes also play a role in hematopoiesis. For example, *HOXA9* is important for the maintenance of the HSC pool and *HOXB4* appears to promote HSC self-renewal *in vivo* (Buske et al., 2002; Lawrence et al., 2005; Lawrence et al., 1997; Thorsteinsdottir et al., 1999; Antonchuk et al., 2002; Sauvageau et al., 1995). More interestingly, several experiments indicate that multilineage genes are co-expressed in HSCs or multipotent progenitors, preceding commitment to differentiation *per se*. These genes include *β globin*, *myeloperoxidase*, *PU.1*, *C/EBP α* and *GATA-3* (Hu et al., 1997; Ivanova et al., 2002; Phillips et al., 2000). Lineage commitment requires not only the enhancement of the appropriate gene expression but also the repression of the alternative lineage gene program (Hoang, 2004). A subtle shift in these transcription factors dosages can be caused by some “stochastic” events such as interactions with stroma, different concentration of a growth factor through activating a signaling

pathway. And this subtle shift is sufficient to disrupt the balance between different lineage genes and drive lineage commitment through the complex transcription factor interaction networks. The networks include positive and negative feedback, cooperativity, antagonism, as well as autoregulation paths (Hoang, 2004). For instance, PU.1 is essential for the development of both myeloid and lymphoid lineages, but its down-regulation is necessary for erythroid differentiation (DeKoter and Singh, 2000; DeKoter et al., 1998; Scott et al., 1994; Scott et al., 1997). In contrast, GATA-1 is the key player in erythroid and megakaryocyte development, but negatively regulates the myeloid specification (Fujiwara et al., 1996; Nerlov et al., 2000; Pevny et al., 1991; Pevny et al., 1995). Both PU.1 and GATA-1 proteins can positively autoregulate their own expression and mutually antagonize the expression of each other (Tenen et al., 1997; Chen et al., 1995). Furthermore, PU.1 and GATA-1 physically interact to reciprocally inhibit their respective function (Rekhtman et al., 1999; Zhang et al., 1999). GATA-1 blocks the binding of PU.1 co-activator, c-Jun to PU.1 and then inhibits the activation of PU.1 target genes, whereas, PU.1 inhibits GATA-1 function by binding to the GATA-1 C-finger and inhibiting GATA-1 DNA binding (Nerlov et al., 2000; Zhang et al., 2000). In summary, combination of extrinsic cues and cell-intrinsic processes not only determines the HSCs cell fate but also govern continuously the blood cell differentiation throughout the whole hematopoietic hierarchy.

1.1.5 Erythropoiesis

As discussed above, the primitive erythropoiesis occurs at YS blood islands transiently, producing nucleated primitive erythrocytes, which contain the embryonic forms of hemoglobin (Lensch and Daley, 2004). The definitive erythropoiesis happens

at fetal liver, spleen and then bone marrow sequentially, which ultimately generates enucleated mature red blood cells with adult forms of hemoglobin (Lensch and Daley, 2004). By 12dpc, smaller, anucleate, definitive erythrocytes appear in circulation and the population of primitive erythrocytes declines (Galloway and Zon, 2003). During the hierarchical ontogeny of definitive hematopoiesis, HSCs give rise to CLPs and CMPs; then CMPs generate GMPs and MEPs; MEPs further develop into megakaryocyte and erythrocyte progenitors (Kondo et al., 2003). Erythrocyte progenitors are not identifiable morphologically, but detected by *in vitro* colony assays as BFU-E (Orkin and Zon, 1997). EPO, SCF and other early acting cytokines, including interleukin-3 (IL-3), granulocyte macrophage-colony stimulating factor (GM-CSF) and TPO, are important for the synergistic expansion of BFU-E (Dai et al., 1991; Sawada et al., 1989; Ratajczak et al., 1998). Primarily dependent on EPO, BFU-E continues differentiate into the colony forming unit-erythroid (CFU-E) and subsequent matures through several erythroblastic stages (Sawada et al., 1989). The proerythroblast is the first morphologically recognizable erythroid precursor, distinguished by its large nucleus and basophilic cytoplasm as revealed by Wright-Giemsa staining (Orkin and Zon, 1997). Only small quantities of hemoglobin are present at the proerythroblast stage. During further differentiation, the chromatin condenses and hemoglobin increases gradually. Terminally, in mammalian definitive erythropoiesis, non-nucleated mature red blood cells are generated. This process is also accompanied with the loss of cell division ability and arrest of cell cycle.

The stepwise progression through erythropoiesis is tightly regulated by positive- and negative-acting transcription factors controlling genes involved in proliferation and differentiation. GATA-1, a zinc finger transcription factor is the key molecule in

erythroid development and is induced by EPO signal. GATA-binding motifs ((T/A)GATA(A/G)) have been identified in the promoters or enhancers of all the studied erythroid and megakaryocytic-specific genes (Evans et al., 1988). Mice lacking GATA-1 die around 10.5dpc from severe anemia with erythroid maturation arrest at a proerythroblast-like stage (Fujiwara et al., 1996). *In vitro* differentiated GATA-1⁻ ES cells are also developmentally arrested and succumb to apoptosis (Weiss et al., 1994; Weiss and Orkin, 1995). Thus, GATA-1 regulates the survival as well as the maturation of erythroid cells.

Biochemical studies have shown that GATA-1 interacts with multiple proteins, including Friend of GATA-1 (FOG-1), EKLF, SCL, PU.1, Sp1, CBP/p300 as well as the SWI/SNF chromatin-remodeling complex, and regulates erythroid cell development as either an activator or a repressor (Rodriguez et al., 2005). So far, the best-studied co-activator of GATA-1 is FOG-1. *FOG-1* is co-expressed with *GATA-1* during development and *FOG-1* deficient mice display similar erythroid phenotype to that of *GATA-1* null mice (Tsang et al., 1997; Tsang et al., 1998). FOG-1 contains nine zinc-fingers four of which individually mediate interactions with the N-finger of GATA-1 (Crispino et al., 1999). Activation of numerous GATA-1 target genes such as *β-globin* gene, requires the proper binding of GATA-1 with FOG-1, whereas other's, notably *FOG-1* itself and *EKLF*, are induced independent of FOG-1 (Anguita et al., 2004; Pal et al., 2004; Letting et al., 2004). In addition to FOG-1, GATA-1 forms multimeric complex with SCL, Ldb1, E2A and LMO2 and activates *glycophorin A* and the *α-globin* locus through closely spaced GATA and E-box binding motifs (Lahlil et al., 2004). Interestingly, GATA-1 can also repress the expression of *GATA-2*, *c-myc* and *c-kit*, which are expressed abundantly in HSCs and

progenitor cells but decrease in the erythroid lineage (Rylski et al., 2003). The repression of *GATA-2* and *c-kit* by GATA-1 also requires FOG-1, which recruits the nucleosome remodeling and histone deacetylase complex to repress transcription (Hong et al., 2005).

1.1.6 Myeloid lineage development

Neutrophils, basophils and eosinophils are white blood cells with granules, termed granulocytes. They share a precursor cell, GMP, with monocytes. IL-3 and GM-CSF are required for production of GMPs. Two distinct cytokines, macrophage colony-stimulating factor (M-CSF) and granulocyte colony-stimulating factor (G-CSF), support monocyte and granulocyte differentiation, respectively (Barreda et al., 2004).

HSCs are primed for multilineage gene expression including PU.1 and GATA-1. Treatment of CD34⁺ cells with GM-CSF leads to PU.1 increase and GATA-1 decrease. PU.1 positively autoregulates its own promoter and activates the gene for the GM-CSF receptor α , resulting in increases in proliferation, differentiation, and suppression of apoptosis of myeloid progenitors (Scott et al., 1994; Scott et al., 1997; Chen et al., 1995). At the same time, PU.1 downregulates GATA-1 promoter and inhibits GATA-1 function by interacting with it, leading to inhibition of erythroid pathway (Zhang et al., 2000). Analysis of PU.1-knockout mice shows that the earliest myeloid progenitors can form in the absence of PU.1, but cannot further differentiate, indicating that PU.1 is important for the further development, especially for monocyte and macrophage differentiation from the precursors (McKercher et al., 1996).

Through a relatively small region within its Ets domain, PU.1 interacts with several factors, including GATA-1, GATA-2, Runx1, C/EBP (CCAAT enhancer binding protein) and C-Jun, and mediates both positive and negative regulation of PU.1 activity (Zhang et al., 1999; Petrovick et al., 1998). As discussed earlier, GATA-1 and GATA-2 inhibit PU.1 by the interaction, whereas, Runx1 and C/EBP factors have a cooperative and/or synergistic positive function through the interaction (Zhang et al., 1999; Petrovick et al., 1998). C-Jun has been shown to be upregulated during monocytic, but not granulocytic, differentiation of GMP. Further studies found that C-Jun mediates the enhancement effect of Ras on PU.1 transactivation function as a specific coactivator, critical for activating the monocytic target promoters such as the M-CSF receptor promoter (Behre et al., 1999).

PU.1, together with its coactivator C-Jun, induces the multipotential myeloid precursors to differentiate along the default monocytic pathway, whereas, C/EBP α acts to block the default pathway and induce granulocytic differentiation (Radomska et al., 1998). C/EBP α is specifically up regulated in early granulocytic cells, down regulated in monocytic cells (Radomska et al., 1998). Consistent with this expression feature, C/EBP α deficient mice show that granulocytes are blocked at an early stage of development, all other blood cell elements appear to be normal, indicating that C/EBP α is critical for early granulocyte development (Zhang et al., 1997). The target genes of C/EBP α include G-CSF receptor, the IL-6 receptor α and primary granule protein genes (Zhang et al., 1997). Another C/EBP protein, C/EBP ϵ is essential for terminal maturation of granulocytes (Lekstrom-Himes and Xanthopoulos, 1999; Yamanaka et al., 1997). Targeted disruption of C/EBP ϵ results in a fertile viable mouse whose granulocytes block at the terminal maturation stage (metamyelocyte).

The functionally abnormal granulocytes cannot kill bacterial targets, making the C/EBP ϵ -knockout animals to develop infections in a nonsterile environment. In the C/EBP ϵ -knockouts, the secondary granule protein mRNA is selectively deficient, whereas, the primary granule mRNA is comparable to that of wild type (Lekstrom-Himes and Xanthopoulos, 1999; Yamanaka et al., 1997). Therefore, granulocyte differentiation is induced initially by C/EBP α , which is essential for primary granule protein gene expression, and subsequently by C/EBP ϵ , which is critical for secondary granule protein gene expression and terminal maturation.

1.1.7 T Lymphocyte development

1.1.7.1 T lymphopoiesis

CLPs, derived from pluripotent HSCs, are capable to differentiate into T and B lymphocytes as well as NK cells. T-cell development depends on the microenvironment of thymus. From 11dpc, CLPs enter the thymic rudiment continuously and the thymus remains a lymphopoietic organ throughout life (Douagi et al., 2002). In the thymus, CLPs lose the potential for B cell and NK cell development. These early committed T cells lack expression of T-cell receptor (TCR), CD4 and CD8, and are termed double-negative (DN; no CD4 or CD8) thymocytes. DN thymocytes are further subdivided into four sequential stages of differentiation: DN1, CD44⁺CD25⁻; DN2, CD44⁺CD25⁺; DN3, CD44⁻CD25⁺; DN4, CD44⁻CD25⁻. DN T cells give rise to the major population of $\alpha\beta$ TCR-expressing T cells and the minor population of $\gamma\delta$ TCR-expressing cells. For cells that proceed along the $\alpha\beta$ TCR pathway, DN3-stage cells first express the pre-TCR, which is composed of the non-rearranging pre-TCR α -chain and a rearranged TCR β -chain. At the cell surface, the pre-T-cell receptor forms a complex with the CD3 molecules that provide the

signaling components of T-cell receptors. The assembly of CD3: pre-T-cell receptor complex leads to cell proliferation, the expression of co-receptor proteins CD8 and CD4, and replacement of the pre-TCR α -chain with a newly rearranged TCR α -chain, which yields a complete $\alpha\beta$ TCR. The resulted large population of double-positive (DP; CD4⁺CD8⁺) $\alpha\beta$ -TCR-expressing thymocytes then interact with cortical epithelial cells that express a high density of MHC class I and class II molecules associated with self-peptides. Most DP thymocytes bear receptors that interact so poorly with the self-peptide-MHC ligands that the intracellular survival signals are not generated, which leads to death by neglect. A small fraction of DP thymocytes express TCRs that bind very well to self-antigens and the resulted too strong signals promote rapid apoptotic death (negative selection). Cells that express TCRs that recognize self MHC and generate appropriate intermediate level of signals initiate a multi-step process known as positive selection that ultimately results in lineage-specific differentiation into either CD4⁺ or CD8⁺ mature T cells (Germain, 2002).

The mechanisms controlling the commitment of HSCs to the lymphoid lineages are poorly understood. The earliest known transcription factor that regulates the lymphoid specification and differentiation is Ikaros (Georgopoulos et al., 1994). Ikaros and its molecular partners, Helios and Aiolos, are zinc finger transcription factors, which have four N-terminal and two C-terminal zinc-finger domains. The N-terminal domains are crucial for DNA binding, whereas the C-terminal zinc fingers mediate the heterodimerization between Ikaros, Aiolos and Helios (Rebollo and Schmitt, 2003). Targeted disruption of *Ikaros* gene leads to severe deficiency in B, T and NK cell development, while erythroid, megakaryocyte, and myeloid cell development is normal (Georgopoulos et al., 1994). Interestingly, Ikaros appears to function both as a

transcriptional repressor and as an activator. Ikaros binds a large number of nuclear factors, including the histone deacetylase repressor complexes NURD and SIN3, and the nucleosome-remodelling complex SWI/SNF, indicating much of the influence of Ikaros is mediated through chromatin reorganization. Ikaros may activate or repress transcription in the classical way by binding to the promoter in cooperation with other factors. Alternatively, by physically recruiting genes or repression complexes into regions of pericentromeric-heterochromatin (PC-HC), the transcriptionally-inaccessible nuclear regions, Ikaros represses or activates gene transcription respectively (Westman et al., 2002). The downstream target genes of Ikaros identified so far include recombination-activating genes (*RAG-1* and *RAG-2*, terminal deoxynucleotidyl transferase (*TdT*), immunoglobulin heavy and light chains, *Igα*, and *CD3* (Fuller and Storb, 1997; Fong et al., 2000). *RAG-1*, along with *RAG-2*, catalyzes the rearrangement of immunoglobulin genes in immature B cells and of T cell receptor genes in immature T lymphocytes, which plays an important role in B and T lymphocyte maturation. *RAG-1* knock out mice have no mature T cell or B cell (Mombaerts et al., 1992).

Several transcription factors and signal pathways have been identified to regulate T or B cell lineage determination from CLP. Notch1 signaling is believed to be necessary and sufficient to induce T-cell lineage specification in early lymphoid progenitors (Radtke et al., 2004; Radtke et al., 1999). The expression of a dominant active form of Notch1 in hematopoietic precursors results in the ectopic T cell development in BM at the expense of B cell development (Pui et al., 1999). Conversely, the inactivation of Notch 1 in newborn mice completely abrogates T cell differentiation and the thymus apparently becomes a site for B cell development (Wilson et al., 2001). The B lineage

commitment factor Pax5 is reported to repress Notch1 expression at the transcriptional level in B-cell progenitors, providing a possible mechanism to ensure B-cell development in the BM (Souabni et al., 2002). Additionally, E-box binding protein E2A dosage determines the choice between a B or T cell fate. Higher E2A activity is required for commitment into the B cell lineage and for proper B-cell differentiation (Herblot et al., 2002; Zhuang et al., 1996). And E2A also interacts with Hela E-box Binding protein (HEB), driving T cell development (Barndt et al., 2000; Sawada and Littman, 1993). Another key factor, GATA-3, expressed specifically in T and NK cells, has also been found to be required for T cell lineage commitment and differentiation (Ting et al., 1996).

1.1.7.2 Thymus organogenesis

In vertebrates, thymus plays an important role for T lymphocyte development. Thymus organogenesis in mammals requires the intercommunication of tissues from all three embryonic germ layers: ectoderm, mesoderm and endoderm (Manley, 2000). This process can be separated into three stages: formation of the thymic rudiment, the interaction between T cells and thymic epithelial cells (TECs), and fetal thymus development. In the first stage of thymic development, the third pharyngeal pouch endoderm provides the initiating signals for induction of the thymus. And the neuroectoderm-derived neural crest mesenchymal cells from the sixth hindbrain rhombomere respond to this signal and migrate to the third and fourth pharyngeal pouches, where they interact with endoderm and provide signals supporting growth and differentiation of the epithelial rudiment. During the second stage, the thymic rudiment is colonized by CLPs derived from HSCs. The interaction between CLPs and TECs leads to further patterning and differentiation of the TECs. Last, throughout

fetal development, TECs appear to progressively acquire competence to promote different stages of thymocyte maturation (Manley, 2000).

Several factors have been identified to be involved in the early stages of thymus organogenesis. Mutation of the *Hoxa3* gene, which is expressed in both the third pouch endoderm and neural crest mesenchyme, results in athymia as well as the pharyngeal region defects in mice (Manley and Capecchi, 1995). Thus *Hoxa3* may be involved in the initial induction of thymus organogenesis with a general mechanism involved in the pharyngeal pouch endoderm development. *Pax1* and *Pax9*, expressed throughout the pharyngeal endoderm, are specifically down regulated in the third pharyngeal pouch in *Hoxa3* knockouts (Manley and Capecchi, 1995). *Pax1* mutants have subtle defects in thymus development, whereas *Pax9* inactivation leads to severe thymic deficiency (Peters et al., 1998; Su and Manley, 2000). Furthermore, genetic interaction between *Hoxa3* and *Pax1* genes has been indicated by the severity of the thymic defect in *Hoxa3*^{+/-}*Pax1*^{-/-} compound mutants (Su and Manley, 2000). Therefore, *Hoxa3*, *Pax1* and potentially *Pax9* may function in the same pathway to form the endoderm of thymic rudiment.

Foxn1, also known as Whn, is essential for proper development of the thymus epithelium (Blackburn et al., 1996; Nehls et al., 1994). It is identified as the responsible gene for nude mice that are characterized by lack of fur development and thymus agenesis. Foxn1 expression is specific to epithelial cells, both in the skin and in the thymus. It is expressed already in all epithelial cells of the thymus before the entry of lymphoid progenitors (Nehls et al., 1996). Disruption of the Foxn1 gene in nude mice shows an arrest of differentiation of the thymic epithelium that prevents

colonization by CLPs (Blackburn et al., 1996; Nehls et al., 1994). The Foxn1 gene encodes for an evolutionarily highly conserved transcription factor of the winged helix domain family. The Foxn1 protein comprises a C-terminal transcriptional activation domain and a DNA-binding domain, both of which are critically required for target gene activation by Foxn1 (Boehm et al., 2003). However, the precise functions of Foxn1, i.e. its target genes, are still largely obscure. Some studies indicate that thymus-expressed chemokine (TECK), stromal cell-derived factor-1 (SDF-1) may be the target genes of the Foxn1 and loss of them in thymus of nude mice leads to failure of attracting the CLPs into thymus (Boehm et al., 2003).

1.2 Genetic study of hematopoiesis in Zebrafish

1.2.1 Zebrafish is a powerful model to study hematopoiesis

Although much advancement has been made to understand the blood forming processes, the underlying mechanisms of hematopoiesis have yet been fully revealed. The mouse system has its limitation. For example, mouse knockout techniques restrict to studying previously identified genes suspected of playing a role in hematopoiesis, but not favor to discovery of new genes involved in this process. Furthermore the small litter size makes the mouse not very well suited for forward genetic studies. Additionally, mouse embryos develop *in uteri* and it is difficult to study early hematopoiesis.

Complementary to the mouse system, the zebrafish has been proved to be an ideal genetic model for hematopoiesis studies for the following reasons: Firstly, zebrafish has a similar hematopoietic program as other vertebrate organisms (Amatruda and Zon, 1999). It consists of multilineage of blood cells, including erythroid, myeloid,

lymphoid, and platelet-equivalent cells, and has two waves of hematopoiesis (Thompson et al., 1998). Furthermore, homologues of genes critical for hematopoiesis (*gata* factors, *lmo2*, *scl*, *c-myb*, *ikaros*, *lck*, *c-fms*, *c-kit*, *globins*) and vasculogenesis (*tie1*, *tek*, *flk1*, *flt*) in mice have been isolated in zebrafish and play roles similar to their mammalian orthologues (Paw and Zon, 2000). Thus, studies in zebrafish are relevant to other vertebrate organisms. Secondly, zebrafish embryos develop externally and are transparent, so it is easy to observe and manipulate the embryos under the microscope. Finally, its short generation time, rich fecundity, and high mutagenesis efficiency by ethylnitrosourea (ENU) make zebrafish well suited for forward genetic screens (Paw and Zon, 2000). So in our lab, we use zebrafish to study hematopoiesis. In the following sections, I will discuss the current progress in hematopoiesis and methods of research in this area of zebrafish studies.

1.2.2 Primitive hematopoiesis in zebrafish

In zebrafish, primitive hematopoiesis occurs in two distinct intraembryonic locations: the intermediate cell mass (ICM) and the rostral blood island (RBI). The ICM derives from two bilateral stripes in the posterior lateral mesoderm (PLM), equivalent to the mammalian yolk sac blood islands. It produces the primitive proerythroblasts and the endothelial cells of the trunk vasculature, whereas, the RBI in the anterior lateral mesoderm (ALM) generates mainly macrophages and possibly neutrophils, as well as vasculature endothelial cells (de Jong and Zon, 2005) (Figure 1.2).

1.2.2.1 Primitive erythropoiesis

In Zebrafish, the earliest primitive hematopoietic progenitors emerge at 1-2 somite stage (11hpf) as indicated by appearance of *scl* expression as a pair of bilateral stripes

in the PLM (Porcher et al., 1996; Liao et al., 1998). Other early hematopoietic and vascular markers including *lmo2*, *gata2*, *draculin (drl)*, *hhex*, *fli1a* are also expressed by these progenitors (Davidson and Zon, 2004). Zebrafish mutants *kugelig/cdx4*, *spadetail/tbx16*, *cloche* have defects in the HSCs formation in the PLM (Davidson and Zon, 2004).

Commitment of the HSCs into erythroid lineage begins at the 4-somite stage with appearance of *gata1* expression in a subset of *scl*⁺ cells (Davidson et al., 2003; Detrich, III et al., 1995). These *gata1* positive cells in the PLM extend anteriorly and posteriorly, migrate towards the midline and then converge at the 20-somite stage to form the ICM. During these processes, erythroid precursors further develop and proliferate. By 24-26 hpf when the blood circulation begins, the ICM comprises of at least 300 proerythroblasts (Long et al., 1997). These proerythroblasts express genes required for heme and globin synthesis (α and β embryonic globins, *alas2*, *fch*, *urod*), iron utilization (*dmt1*) and membrane stability (*β -spectrin*, *protein 4.1r*, *band3*), and mature into flattened elliptical erythrocytes which retained nucleus over the next 4 days during circulating (Davidson and Zon, 2004). Transfusion experiments have demonstrated that these primitive erythrocytes are the only circulating red blood cells for the first 4 days postfertilization (dpf) and begin to decline by 6dpf, reaching 50% of the initial number at 10dpf (Weinstein et al., 1996). The *bloodless* mutant, defective in primitive erythropoiesis in the ICM, starts to restore the circulating red blood cells after 5dpf, indicating the definitive erythropoiesis begins around this time (Liao et al., 2002).

1.2.2.2 Primitive myelopoiesis

Like the primitive progenitors in the ICM, those found in the RBI also express *scl*, *lmo2*, *gata2* and *flila* at the 3-5 somite stage (11-12hpf), contributing to both blood and vascular development (Brown et al., 2000; Liao et al., 1998; Thompson et al., 1998). This is followed soon after by *pu.1* expression in a subset of *scl*⁺ RBI cells, indicating the initiation of myeloid lineage precursors in RBI (Bennett et al., 2001; Lieschke et al., 2002). These early *pu.1*⁺ myeloid cells, including macrophages and granulocytes, migrate toward the head midline during 11-15 somite stage (14-16hpf) and then migrate laterally across the yolk sac at around 22-24hpf. Then some of them enter circulation via the ducts of Cuvier, while others migrate into the head (Herbomel et al., 1999). *pu.1* is also expressed at a low level in ICM blood precursors at 10-19 somite stage (14-18hpf), then disappears due to increase of *gata1*. But the expression of *pu.1* in the ALM continues until 28 to 30hpf (Lieschke et al., 2002). Zebrafish *l-plastin*, monocytes/macrophages marker, starts to be expressed in ALM at 18hpf and by 28hpf is detected in the posterior ICM (Herbomel et al., 1999). Consistent with this, lysozyme C, also specifically expressed in monocytes/macrophages, is observed over the anterior portion of the yolk at 20hpf and in the posterior portion in the ICM by 30hpf (Liu and Wen, 2002). It is controversial whether these posterior macrophages are derived from posterior ICM or come from the circulating macrophages generated in RBI. The functional activity of these early macrophages has been observed as early as 26hpf in the ducts of Cuvier, where macrophages can be seen engulfing erythroblasts from the bloodstream. Additionally, macrophages at 30hpf can migrate to the site of infection with *Escherichia coli* and *Bacillus subtilis* and phagocytose the offending bacteria (Herbomel et al., 1999).

Zebrafish is found to have at least two types of granulocytes: neutrophilic granulocytes and eosinophilic granulocytes, the latter exhibiting characteristics of both mammalian eosinophils and basophils. The neutrophils can be morphologically detected in circulation and in loose connective tissue at 48hpf, whereas the site and time of origin of the eosinophilic granulocytes are not clear (Lieschke et al., 2001). Zebrafish *myeloperoxidase (mpo)*, the granulocyte-specific marker, is first detected at 18hpf in presumptive neutrophilic precursors within the caudal ICM. One to two hours later, *mpo* is also found in the cells scattered on the yolk sac. Some of the anterior *mpo*-expressing cells coexpress *pu.1*, suggesting their origin from RBI. However, the onset of expression of *mpo* in caudal ICM before circulation supports the argument that the ICM also gives rise to a population of myeloid progenitors (Bennett et al., 2001). Most of the *mpo*⁺ cells do not coexpress *l-plastin*, consistent with an idea that these two molecules mark distinct granulocyte and macrophage lineages respectively (Bennett et al., 2001). By 3dpf, the *mpo*⁺ cells distribute throughout the embryo and can be observed to accumulate at sites of injury (Lieschke et al., 2001). Currently it is not known how long the primitive macrophages and granulocytes persist in the embryo.

1.2.3 Definitive hematopoiesis in zebrafish

The definitive hematopoiesis in zebrafish is believed to start in the ventral wall of the dorsal aorta, the AGM equivalent, between 24-48hpf, based on the expression of *runx1* and *c-myb* (Burns et al., 2002; Thompson et al., 1998; Kalev-Zylinska et al., 2002). Studies in mice have shown that Runx1 and c-myb are essential for definitive, but not primitive hematopoiesis (North et al., 1999; Mucenski et al., 1991; Mukoyama et al., 1999; Wang et al., 1996). In zebrafish, expression of *runx1* is

firstly detected at 12hpf in the ICM colocalizing with *scl*-expressing cells. By 24hpf, expression of *runx1* in the posterior ICM is weakened, while a new domain of expression of *runx1* appears in the ventral wall of the dorsal aorta, and persists until 40hpf (Burns et al., 2002; Kalev-Zylinska et al., 2002). These *runx1* positive cells in the ventral wall of the dorsal aorta also express *c-myb*, *scl*, *lmo2* and *ikaros* (Davidson and Zon, 2004; Willett et al., 1999). Morpholino knockdown of *runx1* abolishes the definitive hematopoiesis, as well as the vasculature formation (Kalev-Zylinska et al., 2002). Thus, it is postulated that the *c-myb* and *runx1* expressing cells are the definitive HSCs that subsequently seed kidney and thymus (Figure 1.2).

By 5dpf, the definitive hematopoiesis is established in the kidney, the hematopoietic organ at adult zebrafish (Galloway and Zon, 2003; Willett et al., 1999). By 7dpf, erythroblasts, myeloblasts and neutrophilic granulocytes are easily observed in the kidney, whereas lymphoblasts are not found here until 19dpf (Danilova and Steiner, 2002; Willett et al., 1999).

Definitive erythropoiesis starts around 5dpf as indicated by the recovery of circulating red blood cells in the *bloodless* mutant at this time (Liao et al., 2002). Distinct from those in mammals, zebrafish mature definitive erythrocytes are nucleated and elliptical in shape. Similar to that in mammals, zebrafish hemoglobin is a tetrameric molecule that consists of two α -globin subunits and two β -globin subunits. These cells also undergo globin switching from primitive forms to adult forms (Brownlie et al., 2003; Chan et al., 1997).

Similar to that in mammals, in zebrafish T cell maturation also takes place in thymus.

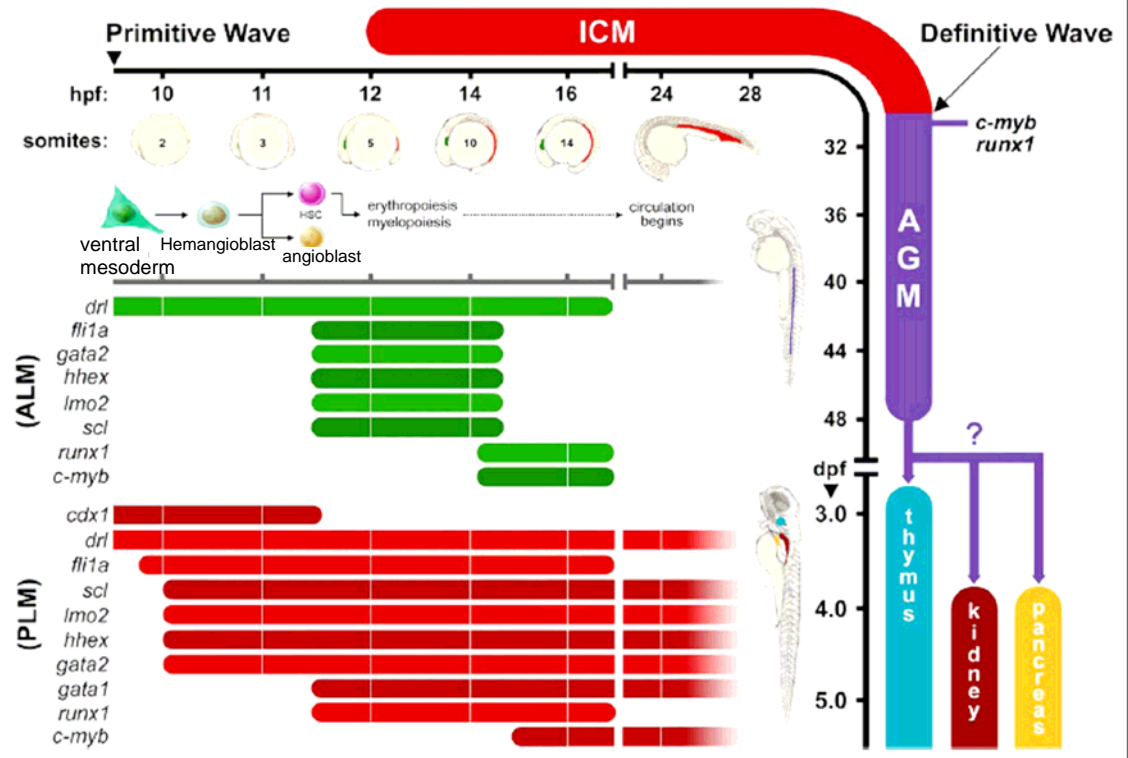


Figure 1.2 Hematopoietic program in zebrafish (Hsia and Zon, 2005)

Bilateral zebrafish thymi form as small outgrowths between the third and fourth pharyngeal pouches and firstly become populated by CLPs around 65hpf (Willett et al., 1999). Around 3-4dpf, expression of *gata3*, *ikaros*, the T cell receptor kinase *lck*, *rag1* and *rag2* are observed in the thymus (Trede et al., 2001; Willett et al., 1999; Willett et al., 1997). The thymi continue to develop and reach their adult size around 1 month postfertilization, contributing to T lymphopoiesis throughout the life (Lam et al., 2002; Willett et al., 1997). The origin of the CLPs that first colonize the thymi is not known. They are unlikely from the HSCs in kidney considering that the kidney hematopoiesis occurs several days later (Willett et al., 1999). It is postulated that a subset of *ikaros*-expressing cells in the ventral wall of the dorsal aorta at 48hpf may seed the thymi first (Willett et al., 2001; Willett et al., 1999).

1.2.4 Genetic methods to study hematopoiesis in zebrafish

1.2.4.1 Mutagenesis Screening

The first large-scale genetic screens in a vertebrate organism were carried out using zebrafish in Boston and Tuebingen (Driever and Fishman, 1996; Haffter et al., 1996). In these screens, ENU was used to mutagenize the DNA of the premeiotic germ cells in adult male fish. Then the mutagenized males (founder) were crossed with wild type female to produce F1 progenies, which contain heterozygotes for mutations within the zebrafish genome, at a rate of about 100-200 mutations per fish. The F1 fish were mated to wild type fish. The resulting F2 fish families were intercrossed and the mutant phenotypes were scored in the F3 generation (Figure 1.3). Over 2,000 mutants with abnormal embryonic development were isolated by visual inspection in the F3 generation (Driever and Fishman, 1996; Haffter et al., 1996). These mutants may affect the development of any aspect of zebrafish anatomy including blood

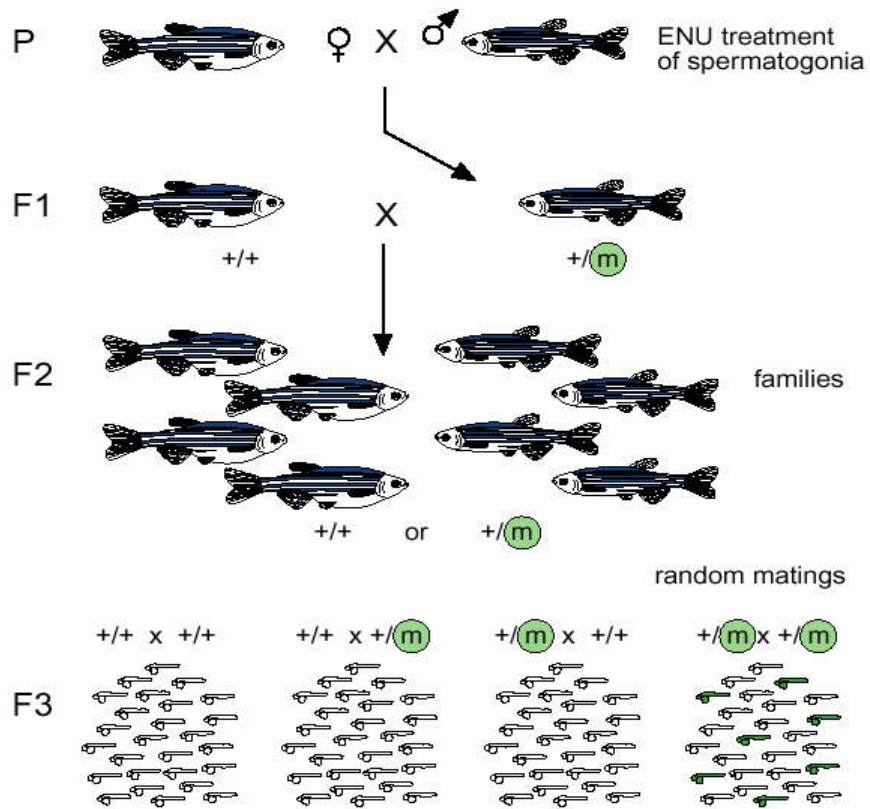


Figure 1.3 Outline of forward genetic screen in zebrafish (Haffter et al., 1996).

development (Weinstein et al., 1996; Ransom et al., 1996). Once the mutant is isolated, positional cloning is needed to perform to identify the responsible gene causing the phenotype. Some of the mutated genes have been cloned including those involved in hematopoiesis. For example, *weissherbst* mutant gene encodes Ferroportin 1, a novel iron exporter (Donovan et al., 2000; Fraenkel et al., 2005); *yquem* mutant gene encodes uroporphyrinogen decarboxylase (Wang et al., 1998). In the following ENU mutagenesis screens, whole-mount *in situ* hybridization (WISH) and fluorescent reporters were usually used to examine the expression of specific gene transcripts for mutants screening (de Jong and Zon, 2005).

In addition to chemical-induced mutations, insertional mutagenesis using a retroviral vector is also applied to cause genomic mutagenesis in zebrafish. This method allows rapid isolation of the disrupted genes by inverse PCR. However, the efficiency of insertional mutagenesis is low, only about 10% of the rate by ENU mutagenesis (Amsterdam et al., 1999; Amsterdam et al., 2004; Golling et al., 2002).

1.2.4.1.1 Zebrafish Genomics

The zebrafish genome is about 1700Mb, consisting of 25 chromosomes. The Sanger Institute started sequencing the genome of the zebrafish from February 2001 (http://www.sanger.ac.uk/Projects/D_erio/). The strategy being used is clone mapping and sequencing from BAC and PAC libraries, in combination with a whole genome shotgun (WGS) assembly. The clones are selected for sequencing based on their locations in the physical map, then manually annotated and accessible in Vega (http://vega.sanger.ac.uk/Danio_erio/index.html). Sequences released from Vega currently cover around 890Mb (Jun 2006) of the zebrafish genome, of which 280Mb

has been manually annotated. The assembly is generated based on the integration of the finished clone sequences and WGS sequences which are filled in the gaps between the clone contigs. The assembly is automatically annotated and can be browsed on the Ensembl site (http://www.ensembl.org/Danio_rerio/index.html). Currently the Sanger Institute has released the sixth assembly of the zebrafish genome (Zv6) in Ensembl, which includes 21,503 genes, 130 pseudogenes and 3,421 non-coding genes. The zebrafish genome project greatly simplifies the process of mapping the mutant genes.

1.2.4.1.2 Principles of Positional Cloning

In general, positional cloning consists of three steps (Detrich et al. 1999). The first step involves the identification of a DNA segment (marker) that is near the mutant locus by linkage analysis. The most commonly used approach is called Bulk Segregation Analysis (BSA) shown in figure 1.4.

In the second step of positional cloning, the closest marker is used to isolate clones from genomic libraries. If the marker and the mutant locus are closely linked, the first clones isolated may contain the gene. Otherwise, the process is repeated to carry out a genomic walk until linkage analysis demonstrates that the mutant locus is encompassed in a contiguous stretch of genomic DNA (contig). Based on the database of Zebrafish Genome Fingerprinting Project established by Sanger Institute (http://www.sanger.ac.uk/Projects/D_rerio/WebFPC/zebrafish/small.shtml), which provides over 2,500 FPC contigs including the clone sequences, it is easy now to identify the contig and even the clones containing the mutant gene.

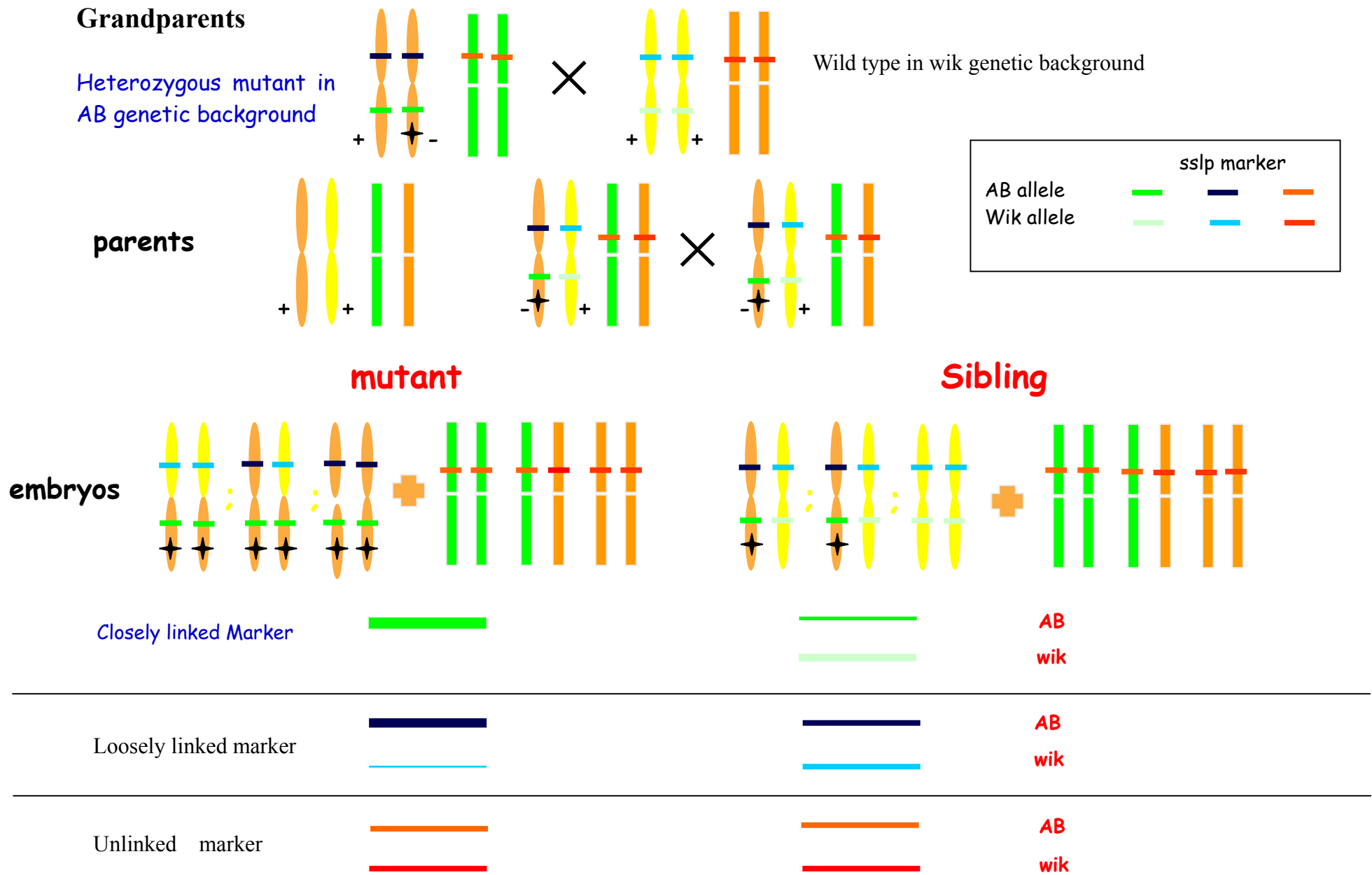


Figure 1.4 Bulk segregation analysis to isolate linked SSLP.

The third step is identification of the gene within the contig region. This may be accomplished in a number of ways, ranging from transgenic rescue of the mutation to sequence analysis of the genomic region.

1.2.4.2 Morpholinos

Antisense morpholino oligos (MOs), first developed for clinical therapeutic applications, were introduced into developmental biology early in 2000 and have been used in a range of model organisms, including zebrafish, frog, chick, and mouse to knockdown the mRNA of specific genes of interest (Nasevicius and Ekker, 2000; Heasman, 2002). As DNA analogs, they are not susceptible to enzymatic degradation and are stable in the cell. MOs work to block the translation initiation or interfere with normal splicing of the specific mRNA by targeting the translation initiation site or splicing sites. The advantages of MOs are high specificity and simple delivery method such as microinjection in zebrafish. However, they have limitations in that MOs only persist for 3-6 days and their injection can produce dose-dependent toxicity (Heasman, 2002). But, with cautious use and clear controls, MOs has proved to be the most generally used and useful reverse genetic method to study hematopoiesis in zebrafish.

1.2.4.3 Transgenic Reporters

Microinjection of DNA construct into 1-cell stage zebrafish embryos is successfully used to generate transgenic zebrafish carrying transgenic reporter such as GFP and DsRed under the control of the specific gene promoter. These transgenic fish express

the fluorescent proteins in the specific regions and the fluorescent positive cells are easily visible under the microscope in the transparent embryos (de Jong and Zon, 2005). Stable transgenic line can be generated with 1-5% efficiency of the germline transmission (de Jong and Zon, 2005). The fluorescent transgenic fish can be used in mutant screening, cellular defect analysis in mutants, cell fate mapping and hematopoietic cell transplantation experiments (Langenau et al., 2004; Traver et al., 2003).

1.2.4.4 Targeting Induced Local Lesions In Genomes (TILLING)

Although forward genetic studies are extremely valuable for hematopoiesis research in zebrafish, cloning of the responsible genes is still laborious. Reverse genetic techniques undoubtedly provide an alternative way to reveal gene functions. Morpholino knockdown is the most widely used reverse genetic method in zebrafish, but it has limitation that has been discussed above. Targeted gene knockout routinely done in mice, which requires homologous recombination in pluripotent ES cells, has not been established in zebrafish. Recently, target-selected mutagenesis, that is random mutagenesis followed by screening for mutations in specific target genes, has been used to complement reverse genetic analysis in zebrafish. This method, also called TILLING (targeting induced local lesions in genomes), has been successfully used in *Caenorhabditis elegans*, *Drosophila*, plants, mouse, rat and zebrafish (Wienholds et al., 2003; McCallum et al., 2000; Zan et al., 2003; Jansen et al., 1997; Beier, 2000; Bentley et al., 2000). In zebrafish, just like the forward genetic screens,

this strategy uses ENU to mutagenize the male fish, which are mated to wild type females to generate F1 populations. DNA from sacrificed F1 males or tail clip DNA from live F1 fish are screened for mutations in a specific gene of interest. The screening can be performed by direct sequencing of PCR products spanning the sequences of interest. Alternatively, an enzyme, CEL-I, which cleaves heteroduplex and is faster and cheaper, has also been proved successful (Wienholds et al., 2003). The mutant line is then recovered from cryopreserved sperm by in vitro fertilization or from the live F1 fish by mating. By this method, 15 different mutations in the *rag-1* gene have been identified (Wienholds et al., 2002; Wienholds et al., 2003).

1.2.5 Important zebrafish hematopoietic mutants

Over 50 blood mutants, consisting of 26 complementation groups, have been identified in large-scale zebrafish genetic screens (Weinstein et al., 1996; Ransom et al., 1996). Additionally, other hematopoietic mutants have been isolated as spontaneous mutations. These mutants, which were initially scored by observation of decreased blood circulation and then characterized by WISH analysis of the hematopoietic markers' expression, can be further subgrouped into the following 3 categories (Ransom et al., 1996).

1.2.5.1 HSC mutants

The HSC mutants, including *cloche* (*clo*), *spadetail* (*spt*) and *kugelig* (*kgg*), display defects in the development or maintenance of HSCs. The *clo* mutant has a severe

deficiency in endothelial and all lineages of blood cells, indicating *clo* is specific to hemangioblast formation (Stainier et al., 1995). The expressions of *scl*, *gata2*, *lmo2*, *gata1*, *hhex*, *runx1* and *runx3* are all downregulated in the *clo* mutant. And overexpression of *scl* or *hhex*, but not *bmp4*, can rescue the *clo* defects, suggesting *clo* may act after *bmp4* pathway but upstream of *scl* and *hhex* (Liao et al., 2002; Liao et al., 1998). Transient expression of *runx1* partially rescues *clo*, indicating its role is also downstream of *clo* (Kalev-Zylinska et al., 2002). However, none of them is a candidate for *clo* gene based on the mapping data.

spt mutant embryos display a defect in mesoderm cell migration, resulting in aberrant somite patterning and accumulation of mesoderm cells in the tail, which specifically disrupts the HSC formation in the ICM as indicated by reduced expression of hematopoietic markers *scl*, *gata1*, *gata2* and *runx1*. In contrast, coexpression of *scl* and *flk* at the 10-somite stage suggests that the angioblast formation is not disturbed in *spt*. ALM myelopoiesis and pronephronic duct formation are also normal in *spt* mutants (Amacher et al., 2002). Overexpression of *scl* in *spt* mutant successfully rescues erythroid development, suggesting that the *spt* works upstream of *scl* in HSC formation (Dooley et al., 2005). The *spt* mutant gene has been cloned and shown to be the *tbx16* gene, encoding a T-box transcription factor that regulates proper cell migration during gastrulation (Griffin et al., 1998).

The gene responsible for the *kcg* mutant, *cdx4*, is a member of the caudal-related

homeobox transcription factor family involved in Antero-Posterior patterning of the embryonic body axis by regulating *hox* genes (Davidson et al., 2003). *kgg* mutant has a severe reduction in the population of ICM-HSCs without disruption of the adjacent pronephronic duct precursors, indicating that the reduction of HSCs is due to a specific dysfunction of *hox* genes during HSC development rather than general posterior patterning defects. Consistent with this, overexpression of *hoxb7* or *hoxa9a*, but not *scl*, restores the erythroid production without correcting the morphological defects in *kgg* mutant. It is postulated that the *cdx4-hox* pathway acts upstream of *scl*, and perhaps other essential *scl* cofactors, to specify ICM-HSC fate (Davidson et al., 2003).

1.2.5.2 Erythroid progenitor mutants

Several mutants including *bloodless (bls)*, *moonshine (mon)* and *vlad tepes (vlt)* are defective in the development of the erythroid progenitor cells. *bls* has no circulating red blood cells until 5dpf when the definitive hematopoiesis initiates (Liao et al., 2002). First isolated as a spontaneous mutation, the *bls* mutation is inherited in a dominant manner with incomplete penetrance, where the bloodless phenotype varies from complete absence of circulating blood cells to severe anemia. *bls* mutants show that decreased number of primitive hematopoietic progenitors are formed from the PLM, but fail to differentiate and undergo apoptosis (Liao et al., 2002). Additionally *bls* mutants exhibit delayed initiation of lymphopoiesis, but normal primitive macrophage development. Overexpression of *scl*, but not *bmp4* and *gata1*, partially

rescues the *gata1*-expressing cells in the anterior ICM, suggesting that *bls* may regulate primitive hematopoietic cell differentiation or survival, potentially by regulating the expression of *scl*. Furthermore, cell transplantation experiments indicate that the *bls* gene is required in a non-cell autonomous manner for primitive hematopoiesis (Liao et al., 2002). But the *bls* gene has not been identified.

mon mutants display a severe anemia due to specific disruptions of both primitive and definitive erythropoiesis (Ransom et al., 2004). The hematopoietic progenitors are correctly specified early during the development of *mon* mutant embryos, but block in maturation at the proerythroblast stage and undergo apoptosis. In contrast, *mon* mutants have normal myeloid and lymphoid development. Positional cloning has revealed that *mon* encodes the zebrafish ortholog of mammalian transcriptional intermediary factor 1 γ (*TIF1 γ*), a transcription factor critical for the differentiation of erythroid precursors in a cell-autonomous manner (Ransom et al., 2004).

gata1 is identified to be the responsible gene for *vlt* mutant. *vlt* mutant exhibits an almost complete lack of circulating blood cells at the onset of circulation (Lyons et al., 2002). However, intact expression of *scl*, *lmo-2* and *cbfb* before 24hpf demonstrates the presence of normal hematopoietic progenitors. Myeloid and lymphoid lineage development is also normal in *vlt* mutant indicated by the intact expression of *pu.1*, *l-plastin* and *c/ebp1*, and *ikaros* and *rag-1*, respectively (Lyons et al., 2002). Therefore, consistent with the studies in mice, *gata-1* is essential for the

differentiation of the hematopoietic progenitors down the erythroid lineage.

1.2.5.3 Late stage erythrocyte mutants

This group of mutants initiates hematopoiesis normally with normal expression of *gatal*, typically pigmented blood, and staining with o-dianisidine. They begin to develop anemia around 2-4 dpf. This group of mutants is further divided into 3 subclasses: cytoskeletal protein mutants, hypochromic mutants and photosensitive mutants (Weinstein et al., 1996; Ransom et al., 1996).

Cytoskeletal protein mutants include *merlot (mot)*, *chablis (cha)*, *riesling (ris)* and *retsina (ret)*. *Mot* and *cha* encode erythrocyte protein 4.1, a structural membrane protein expressed in erythrocytes that anchors the spectrin-actin cytoskeleton to the cell membrane by binding to spectrin (Shafizadeh et al., 2002). *ris* encodes the erythroid β -spectrin protein (Liao et al., 2000). These three mutants all have normal onset of primitive hematopoiesis, but develop anemia by 4dpf due to the hemolysis of the abnormal red blood cells with membrane defects. Similar to *mot*, *cha* and *ris*, *ret* mutant also become anemic around 4dpf. But the circulating erythrocytes in *ret* display a defect in cytokinesis. *band 3*, which plays a critical role in chromosomal segmentation during anaphase, is revealed to be the gene affected in *ret* mutants (Paw, 2001; Paw et al., 2003).

Hypochromic mutants may have defects in any aspect of hemoglobin biosynthesis,

resulting in decreased level of hemoglobin in erythrocytes that show microcytic and hypochromia phenotype. This subgroup includes *sauternes (sau)* which encodes δ -aminolevulinate (ALAS2), an enzyme important in the heme biosynthetic pathway (Brownlie et al., 1998), *weiss Herbst (weh)* and *chardonnay (cdy)* that encode the iron transporter ferroportin 1 and divalent metal transporter 1 respectively (Donovan et al., 2000; Donovan et al., 2002), and *chianti (cia)* that encodes the transferrin receptor 1 critical for iron acquisition by erythrocytes (Wingert et al., 2004).

Photosensitive mutants display defective erythrocytes characterized by autofluorescence and lysis when exposed to ambient light. These mutants include *dracula (drc)*, *desmodius (dsm)*, *freixinet (frx)*, and *yquem (yqe)*. The *drc* mutant gene encodes ferrochelatase and provides a model for erythropoietic protoporphyria (Childs et al., 2000), whereas the porphyric phenotype of *yqe* is due to a mutation in the gene encoding uroporphyrinogen decarboxylase (UROD), homozygous deficiencies in which, cause hepatoerythropoietic porphyria (HEP) in humans (Wang et al., 1998).

All together, the zebrafish hematopoietic mutants not only enrich the knowledge of the conserved hematopoietic process, but also provide valuable models for human blood diseases.

1.3 Aims of the study

We use genetic methods to study hematopoiesis in zebrafish. Firstly, scored by WISH of *rag1* (Willett et al., 1997), we carried out a forward genetic screen to isolate the zebrafish mutants defective in hematopoiesis, especially T lymphocyte development. Secondly, among the isolated mutants, *wz260* proved to be a new allele of *ugly duckling* (*udu*) (Hammerschmidt et al., 1996), was selected for detailed characterization and positional cloning. Furthermore, functional study of *udu* gene in hematopoiesis was performed.

Chapter II Materials and Methods

2.1 Zebrafish maintenance and embryo culture

Zebrafish was maintained under the standard condition by the fish facility of IMCB. Zebrafish AB strain was used for mutagenesis, whereas WIK strain served as the mapping strain for positional cloning. *udu*^{tu24} mutant was kindly provided by Dr. Jiang Yun-Jin. And Tg(-5.0scl:EGFP)^{sq1} transgenic fish was generated by Jin Hao in our lab.

To obtain synchronized embryonic stages of zebrafish embryos, a pair of male and female fish was mated in the crossing tank separated by a transparent divider in the afternoon. The divider was pulled out next morning and the fertilized eggs were collected 15 min after the female fish started to spawn and raised in 0.03% sea salt egg water at 28.5°C. The stages of the embryos were determined according to Kimmel's description (Kimmel et al., 1995).

2.2 Whole-mount *in situ* hybridization (WISH) and *o*-dianisidine staining

2.2.1 Digoxigenin (DIG)-labeled RNA probe synthesis

Plasmid DNAs were linearized by the appropriate restriction enzyme (Table 2.1) and then purified using the PCR purification kit (QIAGEN). 1µg linearized plasmid DNA, 1µl RNA polymerase (SP6 or T7 or T3 from Stratagene), 1µl RNase inhibitor (Roche), 2µl 10X DIG RNA labeling mix (Roche), 4µl 5X reaction buffer (Stratagene), and nuclease free water was used for a 20µl-reaction of *in vitro* transcription. After

incubation in a 37°C water bath for 2 hr, 1µl RNase-free DNase I (Roche) was added to the reaction for further incubation at 37°C for 20 min. The reaction was stopped by 1µl 0.5M EDTA (pH 8) and the RNA products were precipitated with 2.5µl 4M LiCl and 75µl 100% ethanol at -80°C for 30 min followed by centrifugation at 4°C for 30min at 12,000 rpm. After washed with 70% cold ethanol, the RNA pellet was air-dried and resuspended in 20µl sterile DEPC water. 0.5µl of the RNA probe was loaded onto a 1% agarose gel to determine its quality and quantity. Finally, the probe was dissolved in WISH hybridization buffer (50% formamide, 5XSSC, 0.92mM citric acid, 0.1% Tween20, 50µg/ml heparin and 500µg/ml tRNA) at a final concentration of 0.5µg per ml and stored at -20°C.

2.2.2 WISH procedure for *rag1* screening

4dpf or 5dpf fish embryos were fixed in 4% paraformaldehyde dissolved in PBS (PFA) for 2 hr at room temperature (RT). All the following steps were carried out at RT unless specified. The fixed embryos were washed 2x5 min in PBST (PBS with 0.1% Tween 20), 1x5 min in 100% methanol, and then stored in fresh 100% methanol at -20°C for at least 20 min. For rehydration, the embryos were successively incubated in 50% and 30% methanol in PBST for 5 min each followed by 2x5 min washes in PBST. The embryos were further permeabilized by proteinase K (10µg/ml) (Finnzymes, Finland) digestion for 20 min. After a brief wash in PBST, the embryos were fixed in 4% PFA for 20 min followed by 3x10 min washes in PBST.

Subsequently the embryos were pre-hybridized in WISH hybridization buffer (Hb) for at least 2 hr at 60°C. Then the pre-Hb was removed and the embryos were hybridized with DIG-labeled *rag1* RNA probe (0.5µg/ml in WISH Hb) overnight (O/N) at 60°C. The RNA probe was removed and stored at -20°C for re-use. The embryos were successively washed in 2XSSCT at 60°C, 0.2XSSCT at 60°C, and PBST at RT for 10 min each. Then the embryos were blocked in 10% bovine calf serum (BCS)/PBST at RT for 1 hr followed by incubation with anti DIG-AP antibody (Roche) at 1:2000 dilution in 10% BCS/PBST for 2 hr at RT. After washed 2x10 min in PBST, 2x10 min in buffer 9.5T (100mM Tris, 5mM MgCl₂, 0.1% Tween20, pH adjusted to 9.5), the embryos were stained with NBT/BCIP color substrate solution (one NBT/BCIP tablet (Sigma) in 10 ml sterile water with 0.1% Tween20) in dark at RT. The *rag 1* signal could be detected after 1-2 hr of staining.

2.2.3 High-resolution WISH protocol

Except *rag1*, WISH was performed as follow. All of the steps were carried out at RT unless specified. Fish embryos were dechorionated by pronase (0.5mg in 1ml egg water) treatment or with forceps manually. The embryos were washed briefly in PBST to remove the chorions before fixed in 4% PFA at 4°C O/N. The fixed embryos were washed 2x5 min in PBST, 1x5 min in 100% methanol, and then stored in fresh 100% methanol at -20°C for at least 20 min. These embryos were then re-hydrated with a series of methanol/PBST solutions (3:1, 1:1, 1:3), 5 min each, and subsequently 2x5 min wash in PBST. The embryos were permeabilized by proteinase K digestion

(10 μ g/ml) for an appropriate time (Table 2.2). After a brief wash in PBST, the embryos were refixed in 4% PFA for 20 min followed by 5x5 min washes in PBST. The embryos were equilibrated in WISH pre-Hb for 5 min at 65°C, and then changed into fresh WISH pre-Hb and pre-hybridized for 2-5 hr at 65°C. Then the pre-Hb was replaced by the Hb with specific RNA probe (0.5 μ g/ml in Hb), which had been denatured at 68°C for 8 min followed by immediately cooling on ice, and the hybridization was performed O/N at 65°C. On the next morning, the Hb with the RNA probe was removed and stored at -20°C for recycling use. The embryos were then washed as following: 2x30 min in 2X50%formamide/2XSSCT at 65°C, 3x20 min in 2XSSCT at 65°C, 2x30 min in 0.2XSSCT at 65°C, and 2x 5min in PBST at RT. After the washes, the embryos were blocked by 2% lamb serum in PBST for at least 1 hr at RT, and followed by incubation with anti-DIG-AP antibody solution (1:5000 dilution in the blocking buffer) O/N at 4°C. Subsequently the embryos were washed with PBST 6x20 min, and then buffer 9.5T 2x10 min. The embryos were stained with NBT/BCIP substrate solution in dark from 1/2 hr to O/N at 4°C depending on the probe used. The color reaction was stopped by washing the embryos twice with PBST for 10 min each, followed by fixing with 4% PFA for 1 hr. After 1 hr washes with PBST, the embryos were equilibrated in 70% glycerol at 4°C O/N for taking images.

2.2.4 *o*-Dianisidine staining of hemoglobin

2dpf live embryos were dechorionated by pronase treatment or with forceps manually,

Table 2.1 List of Constructs for antisense RNA Probes

Gene	Vector	Linearizing enzyme	RNA polymerase	Sequence region of cDNA
<i>rag-1</i>	PBluescript KS+	BamHI	T7	1426-2944
<i>hoxa3a</i>	pGEM-Teasy	SacI	T7	Full length
<i>foxn1</i>	pGEM-Teasy	StyI	SP6	131-828
<i>scl</i>	pGEM-Teasy	PstI	T7	4-1125
<i>lmo2</i>	pGEM-Teasy	Sall	T7	872-1643
<i>gata-1</i>	-	XbaI	T7	-
<i>band3</i>	pGEM-Teasy	BamHI	SP6	1174-3378
<i>βe1-globin</i>	PBluescript SK+	XbaI	T7	30-584
<i>pu.1</i>	pGEM-Teasy	SacII	SP6	1-1005
<i>mpo</i>	pGEM-Teasy	ApaI	SP6	44-2325
<i>l-plastin</i>	PBluescript KS+	ApaI	T3	404-800
<i>lysozyme C</i>	PBluescript KS+	xhoI	T7	-
<i>gata2</i>	pDrive	xbaI	T7	931-2394
<i>udu</i>	pcDNA3.1(-)	Asp718	T7	30-6708
<i>p53</i>	pBluescript SK+	ClaI	T3	Full length
<i>gadd45al</i>	pGEM-Teasy	ApaI	SP6	83-903
<i>udu</i>	pGEM-Teasy	HincII	T7	5995-6716

Table 2.2 Duration of Proteinase K Permeabilization for Zebrafish WISH

Stage of Embryo (dpf)	Proteinase K Treatment (min)
<1	0
1-2	5
2-3	10-15
3-4	15-20

followed by a brief wash in PBST to remove the chorions. The embryos were then incubated with *o*-dianisidine staining buffer (*o*-dianisidine (0.6mg/ml), 0.01M sodium acetate (pH 4.5), 0.65% H₂O₂, and 40% (v/v) ethanol) in dark for 15 min (Detrich, III et al., 1995). The signals were then observed under the light microscope. For taking photos, the stained embryos were fixed by PFA and equilibrated in 70% glycerol.

2.3 Genetic Screen

2.3.1 ENU mutagenesis

The ENU mutagenesis was performed according to standard protocols with minor modifications (Mullins et al., 1994; Solnica-Krezel et al., 1994). Before mutagenesis, AB strain male fish were crossed with females to select the male fish that generated fertilized eggs. 6 to 10 of the selected males were placed in an 800ml plastic cylinder with fine mesh bottom, and then dunked in 300ml of ENU working solution (3mM ENU in 10mM sodium phosphate buffer) at 22.5°C. After one hour's treatment, the fish were transferred to the cylinder with fresh fish water and left for 6 hr, then transferred into a 5-liter container with 28°C fish water O/N. The treatment was repeated 3 times within 1 to 3 weeks. The ENU working solution was inactivated by incubating with equal amount of 2X inactivation solution (20% sodium thiosulfate, 1% NaOH) O/N before discarding.

2.3.2 Generation of F1 fish and F2 families

On the third day after the last mutagenesis treatment, the ENU treated male fish were

mated with wild type females. Initially, these male fish were unable to produce viable embryos due to severe defects in early embryogenesis. After the second or third cross, the mutagenized males (F0) produced relative normal F1 embryos. Each F0 male was used to generate about 100 to 150 F1 progeny. The surviving adult F1 fish were mated with each other to produce the F2 families.

2.3.3 *rag1* screen

The matured siblings in F2 families were intercrossed for F3 mutant screening. Ideally, each F2 family should have about 10 successful crosses. Approximately 400 crosses were set up a week. Embryos from successful crosses were collected and the F2 parents were maintained in individual tank with appropriate tracking number. Next morning the dead embryos were removed and the egg water was replaced with PTU water (0.003% 1-phenyl-2-thiourea in egg water) to prevent pigmentation. At 4 dpf, about 40 surviving embryos from each cross were subjected to WISH using *rag1* as a probe in specially designed boxes (section 2.2.2). When one quarter of the F3 embryos lost the *rag1* signal, the respective F2 parents (heterozygous) were scored as potential mutants and subjected to confirmation by repeating the WISH in their F3 embryos.

2.3.4 Outcrossing to generate F3, F4, and F5 progeny

The confirmed F2 heterozygous mutants were out-crossed with AB strain wild type to generate the F3 progeny to adulthood, and the mutant fish were identified by *rag1*

staining. The same process was repeated at least twice to clean the genetic background.

2.4 Positional cloning of *wz260*

2.4.1 Generation of mapping families and collection of the embryos

The AB background F4 or F5 heterozygous mutants were map-crossed with WIK wild type to generate the mapping families. The heterozygous hybrid mutants (as many as possible) were identified by *rag1* WISH staining. For each mapping family, AB F4 or F5 heterozygous mutant and WIK wild type were referred as AB grandparent and WIK grandparent respectively, whereas the identified heterozygous hybrid mutants were designated as parents. Each pair of parents were maintained in individual tank and mated weekly. The resulting embryos were segregated into mutant and sibling groups based on the *rag1* expression and stored in methanol at -20°C.

2.4.2 DNA preparation

Once the mapping family was successfully established and around 10 pairs of parents were identified, the AB and WIK grandparents were sacrificed and their genomic DNA were extracted by QIAgen Genomic-tip 100/G kit according to the manufacturer's instruction. To prepare the single embryo genomic DNA, embryos were placed into the wells of 96-well plate individually, incubating in 50µl 1X TE buffer (pH8.0) with 0.5mg/ml proteinase K at 55°C O/N. After incubation at 98°C for 10min, 1µl of embryo DNA sample was used as template for each PCR reaction.

2.4.3 Bulk segregation analysis (BSA)

BSA was used to determine the linkage between the mutation and molecular markers of simple sequence length polymorphisms (SSLP) that distribute throughout the genome (<http://134.174.23.167/zonrhmapper/positionCloningGuidenew/index.htm>). Genomic DNA from AB/WIK grandparents, 2 mutant pools (mixture of 24 single embryos each pool) and 2 sibling pools (mixture of 24 single embryos each pool) was subjected to PCR analysis with 300 pairs of SSLP markers covering the entire zebrafish genome (12 per chromosome, Table 2.3) as primers. PCR products were run on 3.5% MS agarose gels at two hundred volts for two hours to separate bands of different alleles. Linkage was assumed when a WIK band presented in the sibling pools but was absent in the mutant pools (Figure 1.4). In this case, z10036 and z1215 on chromosome 16 appeared to be linked with *wz260* mutant (Figure 4.6).

2.4.4 Linkage analysis with single mutant embryos

The potential linked markers isolated from BSA were tested on individual mutant embryo and the linkage was confirmed when most of the mutant embryos showed AB band only with a few recombinant mutant embryos containing both AB band and WIK band (Figure 4.7). The recombinants are important for determination of the positions between the linked SSLP markers and the mutation. If no recombinant embryos are shared by 2 linked SSLP markers, like z10036 and z1215, the mutation is localized between these 2 markers, one as the North, the other as the South. Otherwise,

Table 2.3 300 pairs of SSLP markers used for BSA

A.

Plate-1	1	2	3	4	5	6	7	8	9	10	11	12	
A	>z4593	>z9394	z3705	>z1705	>z1351	>Z9704	z5508	>Z6802	>Z22347	>z1781	z6974	z13296	LG1
B	>z4278	>z851	>Z7634	>z4662	z13620	>z1406	>z6617	z7358	>z1703	>Z20550	z22747	z13475	LG2
C	>z872	>Z7506	>Z8208	>z15457	>z9964	>Z11227	>z3725	>z20058	>Z7486	>z1191	>z6019	z1185	LG3
D	>z3275	>z984	>Z10164	>Z7490	>Z21636	z20450	>z5112	>z1366	z20533	z9920	z3439(L3)	z9257 (L3)	LG4
E	>z15414	>Z11496	>Z6727	z6614	>z1390	>z3804	>Z14143	>z4299	>z1677	>z1202	z1454	z8921	LG5
F	z15448	>z13275	>z880	>z6624	z10914	>z5294	>Z13614	z9230	>z4297	>z1680	z1701	gof2	LG6
G	>z3273	>Z10785	>z1206	>z4706	>z1182	z1059	>Z8156	z1239	>Z13880	>Z13936	>z5563	>z1313	LG7
H	>z1634	>z1068	>Z7819	z11001	z22270	>Z21115	>z789	>z4318	z8770	z8703	z6818(L2)	z20951(L5)	LG8

B.

Plate-2	1	2	3	4	5	6	7	8	9	10	11	12	
A	>Z20860	>z1777	>z562	>Z6268	>z4673	>z5080	>z1805	>z20031	>Z10789	>z4577	>z1270	z7564	LG9
B	>z9199	>Z6410	>Z8146	z3835	>z1145	z1191	z13219	>z9701	>z3260	z14193	z7262	z6427	LG10
C	>z1590	>z3527	>Z13666	>z4190	>z1393	>6909	>z13411	>z3362	>Z10919	z8032	z10727	z13395	LG11
D	>z1778	>z1225	>Z21911	>z1473	>z4188	>z4830	z1400	>z1358	z7576	z22103	z6920	z1312	LG12
E	>z1531	>z5643	>z6104	>Z13611	>z5395	>z1627	>Z7102	>z6657	>z1826	>z6007	z9951	z17223	LG13
F	z9366	>z5436	>z1536	>z5435	>z4203	>Z22107	>z1226	>z6666	>z3984	>z1801	z11837	z22144(L20)	LG14
G	>Z10289	>Z6312	>Z6712	>Z21982	>z4396	>Z11320	>Z13230	z7216	>Z7381	>z6024	>z5223	z21165	LG15
H	>z3741	>z1837	>Z21155	>z6365	z15453	>Z10036	>z1215	>z4670	>z1786	>z4175	z6921	z13202	LG16

C.

Plate-3	1	2	3	4	5	6	7	8	9	10	11	12	
A	>z9692	>z4268	>z1490	>Z22083	>Z22674	>z9847	z21703	>z4053	>z3491	>z1928	z3165	z6010	LG17
B	>z1136	>z1144	>Z13329	>Z8488	>Z10008	z8343	>z9154	>z5321	z11944	z7654	z11685	z20046(L20)	LG18
C	>z4009	>z160	>Z7450	>z3782	>z3816	>Z11403	>Z6661	>Z7926	>z1803	z5183	z7686	z4825	LG19
D	>z4329	>Z8554	>z3954	>Z22041	>Z7158	>z3964	>Z11841	>Z10056	>Z9334	>Z9708	>Z6804	z7171	LG20
E	>z3476	>z1274	z10508	>z4492	>Z10960	z6089	>z4425	>z1497	>z4074	z7925	z7405	z13719	LG21
F	>z1148	>Z10673	z11752	>z230	>Z10321	>Z21243	z9516	>Z9817	>z4682	z3093	z13223	z3286	LG22
G	>z5683	>Z8945	>z4003	>z15422	>z4421	>z3157	>z1773	>z176	z20039	z5141	z20133	z3211(L20)	LG23
H	>z5075	>z1584	>z5413	>Z23011	>z3399	z7627	>z5657	>z3901	>z157	z13229	z9325	z11862	LG24

D.

Plate-4	1	2	3	4	5	6	7	8	9	10	11	12	
A	>z1378	>z13232	>z3490	>z3528	>z5669	>z1462	>z9290	z11092	z8224	z1213	z8780	z1431	LG25

the mutation is localized on the same side of the markers. The marker with fewer recombinants is closer to the mutation. The genetic distance between a SSLP marker and a mutation can be calculated according to the following formula:

$$\begin{aligned} \text{Genetic distance (centimorgan(cM))} &= \text{recombinant number} / \text{total meiosis events} \times 100 \\ &= \text{recombinant number} / (\text{total embryo number} \times 2) \times 100 \end{aligned}$$

Based on the Zebrafish Genetic Maps such as MGH and T51 (http://zfin.org/cgi-bin/mapper_select.cgi), more SSLP markers between z10036 and z1215 were screened to narrow down the *wz260* interval (Table 2.4). Two closer SSLP markers z17246 and zk30O16-SSLP-S16 were then used to perform fine mapping by analyzing 5,864 meiosis events (Figure 4.9).

2.4.5 Searching for the contigs and clones containing the mutant gene

The closest North and South markers were used to blast the Ensembl (http://www.ensembl.org/Danio_rerio/index.html) or Vega database (http://vega.sanger.ac.uk/Danio_rerio/index.html), to define the North contig and South contig (www.sanger.ac.uk/Projects/D_rerio/WebFPC/zebrafish/small.shtml). If the North contig and South contig were not the same one, it would be necessary to link them together by their sharing markers or clones so that the genetic map embracing the mutant gene was linked with the physical map (Figure 4.10). Additional SSLP and Single nucleotide polymorphism (SNP) markers (Table 2.4)

were designed based on the BAC or BAC end sequences in the contig to further narrow down the mutant locus. *wz260* was mapped to a region covering by three overlapping BACs, zC196P10, zK7E18 and zC113G11 (Figure 4.10).

2.4.6 Identification of the mutant gene by sequencing analysis

Among the three BACs, zC196P10 was most likely to contain *wz260* mutant gene because it contained the nearest north marker SSLP-N6 with only 1 recombinant, corresponding to 0.02cM. Therefore I sequenced the RT-PCR products of the 4 Ensemble genes in BAC zC196P10 to search the point mutation site by comparing *wz260*^{-/-} and wild type. The DNA sequencing analysis found that *wz260*^{-/-} mutant zebrafish harbored a point mutation (T to A) in the Ensemble Gene ENSDARG00000005867. As complementary test revealed that *wz260* was a new allele of *ugly duckling (udu)* (Hammerschmidt et al., 1996), we designated it as *udu*^{sq1zl}. The other allele, *udu*^{tu24} also had a point mutation (T to A) in a different site of Ensemble Gene ENSDARG00000005867 (Figure 4.11 and 4.12).

2.5 Amplification of *udu* cDNA and the related plasmid construction

2.5.1 Total RNA extraction from embryos

Total RNA was extracted from 1dpf *udu*^{sq1zl} homozygous mutant and wild type embryos, respectively, using TRIzol (Gibco-BRL, USA), treated with DNase I and purified using RNeasy Mini kit (QIAGEN).

Table 2.4 The polymorphic SSLP/SNP markers used for *udu* mapping

Marker's name	Marker's type	Marker's direction	Primer sequence	Recombinants /total embryos
z10036	SSLP	North	5'-GGCCTGAGACACCATACTTTT C-3'/5'-GGCTGGGAGACATGAGG A-3'	14/172
z13946	SSLP	North	5'-CCAACCTCATCACTTCAGCA-3 '/5'-GCTTTCTAATTGCCTGTGGC- 3'	12/172
z17246	SSLP	North	5'-ATATCAGCAGGAGGGACGG-3' /5'-TGTCTGTCTTTCTGTGATGCT T-3'	20/2932
74za	SNP	North	5'-ACCAGTTACAAGCACAACAA G-3'/5'-GAGTCATCCTGAAGTAA AATG-3'	3/2932
232za	SNP	North	5'- ATGTGACTATTGCGAATGATC -3'/5'-TATGTTGGGACCGTTGTTT G -3'	2/2932
183ya	SNP	North	5'- ATAACAGCACAACCAGCGTA -3'/5'- TTAGCCTCCTGCATTAAGC -3'	2/2932
269za	SNP	North	5'-TAAAGTAACTTACAACACCAA CCC-3'/5'-CACCGTAAAACGCAA CAAT -3'	1/2932
183za	SNP	North	5'-TAGGTATTTGACATAAAAGAC AAC-3'/5'-GAAGTCAGTGTTTAGT AGTTCATC -3'	1/2932
SSLP-N6	SSLP	North	5'-AGTTAGAAATGATGATCTCAG TG-3'/5'-GCTTACTATCAAAGTGT ATGGGG -3'	1/2932
SSLP-S18	SSLP	South	5'-ACATGTGTATATGAGTACTTGC -3'/5'-ATGTGTTAAAATAATCTTC ACTCC -3'	27/2932
SSLP-S16	SSLP	South	5'-ATAGTGTCCAGCTGAGGGTC -3'/5'-GCTGAGATTAGGCAACTGT C -3'	29/2932
z1215	SSLP	South	5'-TCCTGTGATGTACAGCCTGG-3 '/5'-GAACCAAGCCCTCGCTTC-3'	33/172

2.5.2 5' and 3' Rapid Amplification of cDNA Ends (RACE)

5' and 3' RACE were performed using the BD SMART™ RACE cDNA Amplification Kit (Clontech, USA) according to the protocol provided by the manufacturer. RACE primers for *udu* gene were listed in Table 2.5. The RACE products were purified by gel-purification kit (QIAGEN) and cloned into pGEM®T-Easy Vector (Promega) for sequencing. Full-length sequence of *udu* was obtained by alignment of the end sequences and the middle fragments acquired from RT-PCR.

2.5.3 Cloning of *udu* cDNA constructs containing the wild type allele and the *udu*^{sq1zl} allele (pcDNA3.1-*udu*-wt, pcDNA3.1-*udu*-T2976A)

Total RNAs extracted from 1dpf *udu*^{sq1zl} homozygous mutant and wild type embryos were reversely transcribed using SuperScript™ III RNase H Reverse Transcriptase (Invitrogen) respectively. The synthesized cDNAs were used as templates to do PCR to amplify 2 fragments of *udu* cDNA (the primers were listed in Table 2.6). The first fragment (from 30bp to 2248bp) was subcloned into pcDNA3.1 vector (+) (Invitrogen) with Asp718 and BamHI. Then the second fragment (from 2248bp to 6708bp) was inserted into the pcDNA3.1 containing the first *udu* fragment construct with BamHI and XhoI. By this method, both the wild type and *udu*^{sq1zl} alleles of *udu* cDNA including all the coding region and most 5' and 3' UTR region were cloned into pcDNA3.1 vector (+) (Figure 2.1A).

2.5.4 Cloning of Flag-tagged and HA-tagged *udu* cDNA constructs (pcDNA3.1-N-Flag-*udu*-wt and pcDNA3.1-C-HA-*udu*-wt) and SANT-L domain deficient mutant construct (pcDNA3.1-*udu*- Δ SANT-L)

The Asp718 recognizing sequence joint with Flag tag sequence immediately followed by the initial part of *udu* coding sequence was designed as primers to amplify the N terminal Flag tagged *udu* fragments (Table 2.6). The XhoI recognizing sequence connective with C terminal HA tagged *udu* primers were also used to amplify the C terminal HA tagged *udu* fragments (Table 2.6). Then using the appropriate restriction enzymes, the N/C tagged *udu* fragments were subcloned into pcDNA3.1-*udu*-wt, replacing the corresponding untagged region (Table 2.6), to generate pcDNA3.1-N-Flag-*udu*-wt and pcDNA3.1-C-HA-*udu*-wt.

To make pcDNA3.1-*udu*- Δ SANT-L construct, SANT-L domain deficient C terminal fragment was also amplified using the specially designed primers and subcloned into pcDNA3.1-*udu*-wt, replacing the intact C terminal as the strategy in Figure 2.1B (Table 2.6 and Figure 2.1B).

2.6 *udu* cRNAs rescue experiments

2.6.1 Synthesis of *udu* cRNAs

Using *sma*I linearized pcDNA3.1- *udu*-wt, pcDNA3.1- *udu*-T2976A and pcDNA3.1-*udu*- Δ SANT-L as templates, the capped RNAs were synthesized and

Table 2.5 Primers for 5' and 3' RACE of *udu* gene

Name	Sequence
<i>udu</i> -3'-GSP	5'- CCTCTCAGTCCTGCTGGCATTGAAG -3'
<i>udu</i> -5'-GSP	5'- GCAATGGACGCTTAGACCGAGTTCG -3'
<i>udu</i> -3'-NGSP	5'- GCCACTCTTCTGAAGGGTCACACAC -3'
<i>udu</i> -5'-NGSP	5'- CTAGACTGTCGCTCTGGCTCCCCTGC -3'

Table 2.6 Primers for cloning of *udu* cDNA constructs

Construct's Name	Primer name	Primer sequence	Cloning enzyme
pcDNA3.1- <i>udu</i> -wt/ T2976A-first part	<i>udu</i> -30KpnIF	5'-GGGGTACCTTAATAGAAAG ATACCGATGGCTG -3'	Asp718 and BamHI
	<i>udu</i> -2397R	5'-ATGTCCTTCACTCGCATAC GC-3'	
pcDNA3.1- <i>udu</i> -wt/ T2976A-second part	<i>udu</i> -2118F	5'-TCTTCCTCCCAAACCCAAC C-3'	BamHI and XhoI
	<i>udu</i> -XhoI-L-2R	5'-CCGCTCGAGATTCTCAAAA CTAACATCTGAAGCAA-3'	
pcDNA3.1-N-Flag- <i>udu</i> -wt	<i>udu</i> -Asp718-AT G-flag-94F	5'-GGTACCATGGATTACAAGG ACGACGATGACAAGGGATGG AAACGCAAGTCTTCTTC -3'	Asp718 and BstEII
	<i>udu</i> -983-R	5'-AATGGGGAGGCGTTTGAG AAG-3'	
pcDNA3.1-C-HA- <i>udu</i> -wt	<i>udu</i> -5280-5353- XbaI-F	5'-CCAGTTTGAAGAGGCTGTT TG -3'	XbaI and ApaI
	<i>udu</i> -ApaI-HA- XhoI-C-R	5'-GGGCCCTTACAGACTAGCG TAGTCAGGTACGTCGTATGGG TAGCACTCGAGGTCCTGCTCT TCATCAGTGGC -3'	
PBluescriptSK- <i>udu</i> - ΔSANT-L-first part	<i>udu</i> -5280-5353- XbaI-F	5'-CCAGTTTGAAGAGGCTGTT TG -3'	XbaI and SpeI
	<i>udu</i> -5976+SpeI- R	5'-GACTAGTGTCTAAGGCTGG GCTCAGTGA -3'	
PBluescriptSK- <i>udu</i> - ΔSANT-L-second part	<i>udu</i> -6184-mo- SpeI-F	5'-GACTAGTGCTTCTCAGGCC AG -3'	SpeI and ApaI
	Pc3.1-ApaI- 1071R	5'-CCAGGGTCAAGGAAGGCA CG -3'	

polyadenylated using Ambion's mMessage mMachine High yield capped RNA Transcription kit and Ambion's Poly(A) Tailing Kit, respectively, according to the manufacturer's protocols (Ambion, USA). The concentration and the quality of the RNAs were determined by electrophoresis.

2.6.2 microinjection

For rescue experiment, about 1µg/µl cRNA was diluted 3 times with phenol red (0.1% in DPBS, Sigma) and 2nl was injected into each one-cell stage embryo derived from crosses of the adult *udu*^{sq1zl} heterozygous fish, by using gas microinjector (PLI-100, HARVARD APPARATUS).

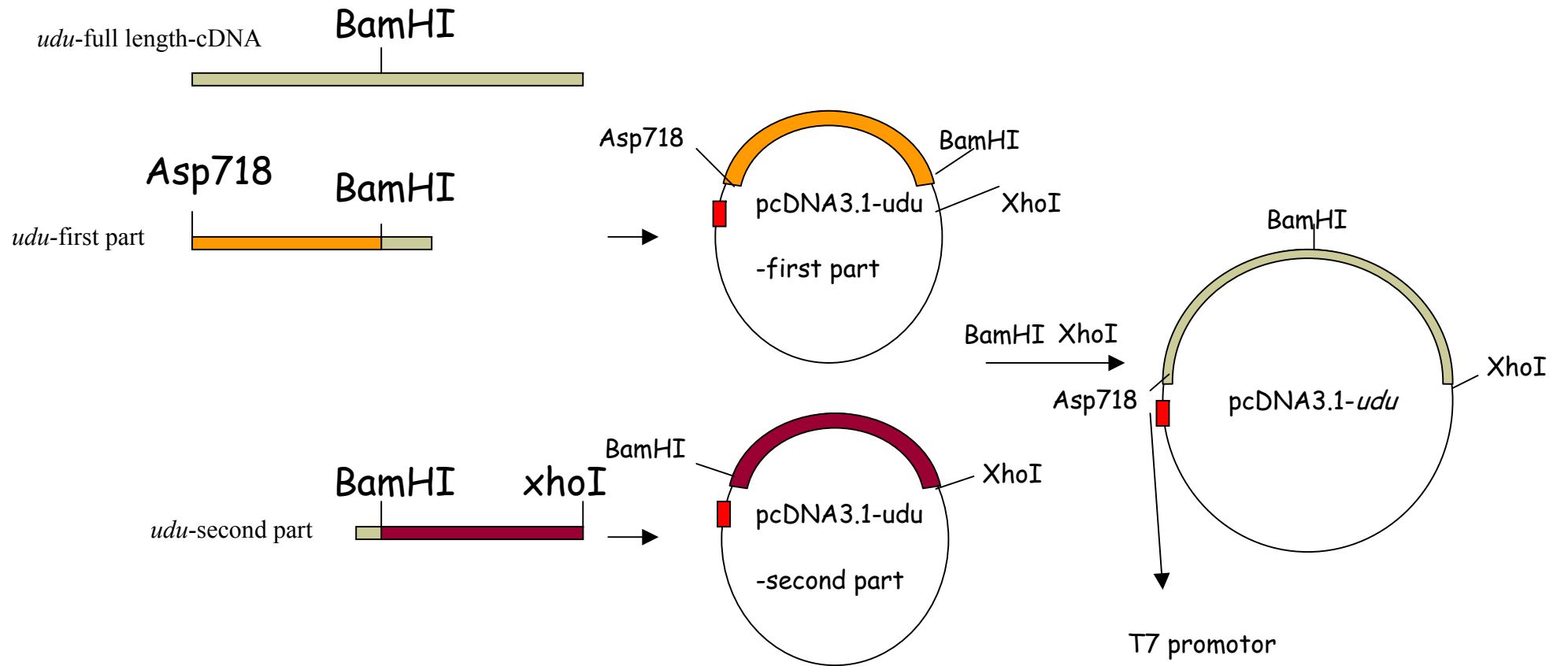
2.6.3 Evaluation of the rescue efficiency and genotyping analysis

WISH of *band3* at 22hpf stage, *o*-dianisidine staining of hemoglobin at 2dpf stage were used to evaluate the rescue efficiency. After scoring the phenotypes, the embryos' genomic DNA was extracted individually (section 2.4.2) and genotyped by sequencing the PCR products with the primers (5'-AAACACGCTACCCACAGTTCC-3'/5'-TTGTCTGATGTCTGTTGCTGC-3'). The rescue efficiency was calculated as division of the rescued mutant number by the total mutant number.

2.7 Morpholino knockdown

The *udu* MOs (Gene Tools, USA), MO-*udu*-1 (5'- TAACACTACACTCACCACCCC

A



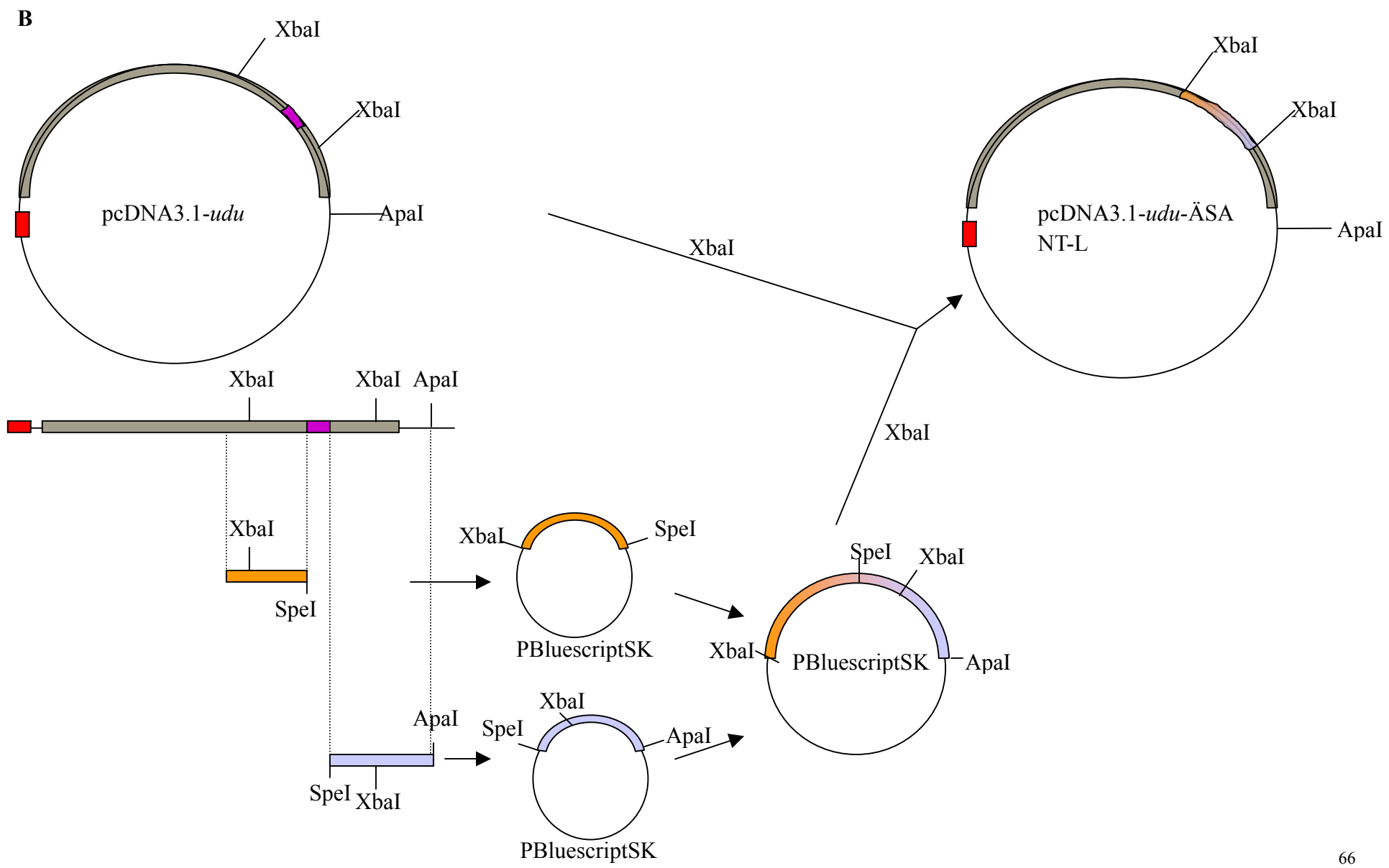


Figure 2.1 Cloning strategy of *udu* constructs. (A) To generate pcDNA3.1- *udu*-wt and pcDNA3.1- *udu*-T2976A, 2 overlapping fragments of *udu* cDNA that contain the BamHI cutting site were amplified from the cDNAs of 1dpf wild type or *udu*^{sq1zl} homozygous mutant embryos (the primers were listed in Table 2.6). The first fragment, joint with an Asp718 cutting sequence at beginning, was subcloned into pcDNA3.1 vector (+) with Asp718 and BamHI. The second fragment, with a XhoI cutting sequence in the end, was then subcloned into the pcDNA3.1-*udu*-first construct with the enzymes BamHI and XhoI. By this method, both the wild type and *udu*^{sq1zl} alleles of *udu* cDNA including all the coding region and most of the 5' and 3' UTR regions were cloned into pcDNA3.1 vector (+). (B) To make pcDNA3.1-*udu*-ΔSANT-L construct, SANT-L domain deficient C terminal fragment was amplified in two parts, subcloned into pBluescriptSK vector and then into pcDNA3.1-*udu*-wt, replacing the intact C terminal. The purple box demarcates the SANT-L domain.

TTTT-3') and MO-*udu-2* (5'-AAAAGGCTTGCTGACCGTCGTTGTC-3'), were designed to specifically block the RNA splicing of the *udu* gene, whereas the *p53* MO (5'-GCGCCATTGCTTTGCAAGAATTG-3') (Langheinrich et al., 2002) (Gene Tools, USA) was used to target the translational initiation site of the *p53* gene. The Standard Control MO provided by Gene Tools was used as control. ~0.5-1 pmol per embryo of each MO was injected into the one-cell stage embryos.

2.8 Acridine orange staining

Acridine orange (AO, acridinium chloride hemi- [zinc chloride], Sigma) was used to detect cell death. Embryos were dechorionated and placed in 5µg/ml of AO in egg water. After 30 minutes of staining, embryos were washed with egg water and viewed using the green filter with a fluorescence microscope.

2.9 FACS, cytology, and cell cycle analysis

The 24hpf *udu*^{-/-} mutant and sibling embryos (300-400/each pool) obtained from crosses of adult *udu*^{+/-}/Tg(-5.0scl:EGFP)^{sq1} and *udu*^{+/-} fish were separated based on the morphological phenotype and disaggregated in cold 0.9X PBS with 5% FBS. The cell suspensions were passed through a 70 µm-pore size filter and spun at 1000 rpm for 5 min. The pellets were re-suspended in 1ml Cell Dissociation Buffer-Free Hanks (Gibco, USA) and incubated at 37 °C for 20 min. After addition of 1ml washing buffer (Hanks buffered saline solution containing 20% calf serum, 5mM CaCl₂ and DNase (50µg/ml)), the cell suspensions were spun at 1000rpm for 5 min and

re-suspended in PBS. After passing through a 40 μm -pore size filter, 10^6 cells/ml samples were applied for FACS analysis (Beckton Dickinson).

For cytology analysis, about $1\text{-}2 \times 10^5$ sorted GFP⁺ cells were cytocentrifuged at 500rpm for 5 min onto glass slides and subjected to May-Grunwald and Giemsa staining. Images were captured by Olympus BX51 microscope equipped with Olympus DP70 digital camera.

For cell cycle analysis, cell suspensions (1×10^6 cells) were spun at 1000rpm for 5 min, re-suspended in 1ml warmed (37 °C) DMEM (Gibco, USA) supplemented with 2% Fetal Calf Serum, 10mM HEPES buffer (Gibco, USA), and 5 $\mu\text{g}/\text{ml}$ Hoechst 33342 (Sigma, USA), and incubated at 37 °C for 1hr. The cells were then put on ice immediately, spun down at 1000rpm for 5 min at 4 °C, re-suspended in ice-cold HBSS (Hanks Balanced Salt Solution from Gibco) with 2% Fetal Calf Serum and 10mM HEPES buffer (Gibco, USA), and finally subjected to cell cycle analysis by FACS.

2.10 Cell transplantation

Donor embryos derived from mating between adult *udu*^{+/-} fish were injected at the one-cell stage with rhodamine-dextran (Invitrogen). At around 3hpf, the injected donor embryos were dechorionated with forceps in an agarose- (2% agarose in 0.3X Danieau buffer) coated Petri-dish covered with 1X Danieau buffer and 15-30 donor

cells from each embryo were transplanted into dechorionated host embryos of the same stage. The manipulated donor embryos were saved for genotyping analysis. Contribution of the rhodamine-dextran-labeled donor cells to the circulating blood cells in the host embryos was scored at around 30hpf under fluorescent microscope.

2.11 Northern blot analysis of *udu* transcripts

2.11.1 RNA Preparation

Total RNA was prepared from different stages of zebrafish (1-8 cell stage, 6-8hpf, 12hpf, 24hpf, 3dpf, adult) using TRIzol (Gibco-BRL, USA). RNA concentration was double checked by UV-spectrometry and agarose gel. Then mRNA was isolated from the total RNA using QIAgen's oligotex mRNA kit.

2.11.2 Dig-labeled RNA Probe Preparation

Dig-labeled *udu*-3' (5995-6716bp of the cDNA) RNA probe was prepared and purified as described in section 2.2.1 (Table 2.1). Probe concentration was checked by UV-spectrometry and agarose gel. Probe aliquots were stored in -80°C.

2.11.3 Northern blot

4.5µl mRNA sample (1µg) was mixed with RNA loading buffer (2.0µl 10X MOPS, 10.0µl de-ionized formamide, 3.5µl 37% Formaldehyde, 2µl 0.4% bromophenyl blue) and denatured at 65°C for 15 min followed by immediately transferring on ice. Then the samples were loaded on a 0.7% agarose gel (0.7g agarose in 84.6ml RNase free

water, 10ml 10X MOPS, 5.4ml 37%Formaldehyde for 100ml gel) and run at 3-4V/cm with 1X MOPS running buffer for 6 hr. After running, the RNA gel was rinsed 4 times in de-ionized water and then soaked in water for 5 min. At the same time, a Nylon membrane (Hybond N⁺, Amersham Bioscience) was wetted and immersed in distilled water. Then both the gel and membrane were soaked in 20X SSC transfer buffer for 5 min. Subsequently, the membrane transfer system was set up to transfer RNA O/N. On the second day, the transferred membrane was cross-linked under the UV light and stained with Methylene blue solution followed by wash with water. Based on the marker position, the membrane was cut into two parts. The upper one was used for *udu* RNA probe, whereas the bottom one was used for *elf1 α* RNA probe. The membranes were pre-hybridized with hybridization buffer (Roche) at 68°C for 1 hour in the rotating incubator followed by adding the probe into hybridization buffer (20ng/ml) and further incubating at 68°C O/N. On the third day, the membranes were washed vigorously as following: 2X15min in 2XSSC/0.1%SDS at RT, 2X15min in 2XSSC/0.1%SDS at 68°C, 2X15min in 0.2XSSC/0.1%SDS at 68°C. After washed, the membranes were equilibrated in washing buffer (Roche) for 5min, incubated in blocking buffer (Roche) for 30min, and then in Anti-Digoxigenin-AP antibody solution (1:20,000 diluted in blocking buffer, Roche) for 30min. Finally the membranes were vigorously washed 2X15min in washing buffer. To detect the signals, the membranes were equilibrated first in detection buffer for 5min and then incubated in CDP-STAR (Roche) for 5 min followed by exposure with X-film in dark room.

2.12 Generation of rabbit anti-udu antibodies

2.12.1 GST-fusion protein expression and purification

Two DNA fragments corresponding to amino acids 4 to 91 (N-terminal) and 1818 to 1941 (C-terminal) of *udu* were PCR amplified with primers *udu*-N-F/R (5'-CGGGATCCAAACGCAAGTCTTCTTCTCCA-3'/5'-GGAATTCTCATGACCGCAAAGGGGATGAA-3') and *udu*-C-F/R (5'-CGGGATCCAAACATCGAAGGCATAAGAGA-3'/5'-GGAATTCTCACTCTTCATCTCGGCTGTGCTT-3') respectively using pcDNA3.1- *udu*-wt as the template. The DNA fragments were digested with restriction enzymes *Bam*HI and *Eco*RI and ligated into the same site of pGEX-6p-1 vector (Amersham) to generate pGEX-*udu*-N/C-Antigen. The constructs were verified by DNA sequencing and then transfected into *E. coli* strain BL21. BL21 harboring the pGEX-*udu*-N/C-Antigen was grown in 2 L of LB medium at 37 °C and induced with 0.1 mM IPTG at 30 °C for 3 h upon reaching log phase. The cells were harvested by centrifugation, resuspended and incubated in lysis buffer (20 mM Tris-HCl, pH 7.6, 500 mM NaCl, 0.1 mM PMSF, 2 mM benzamidine, 2 mM DTT) for 30min, and lysed by sonication. Clarified cell lysate was applied to a glutathione Sepharose 4B column (Amersham). GST-fusion protein was eluted by glutathione and half of them were subjected to PreScission protease (Amersham) digestion at 4°C O/N to cleave the GST tag. After desalting, the GST-*udu*-N/C-Antigen and untagged *udu*-N/C-Antigen were eluted with PBS and protein concentrations were determined with Coomassie staining. The concentrations were adjusted to 2mg/ml and the protein aliquots were

stored at -80°C .

2.12.2 Immunization of rabbits with GST-Udu-N/C-Antigen

For the priming immunization, 1ml 2mg/ml GST-udu-N/C-Antigen was mixed with 1ml Complete Freund's adjuvant (CFA; sigma) by two 3ml-syringes and a plastic 3-way stopcock on ice. Each GST fusion protein was used to inject 2 rabbits, with 1mg per rabbit. Then at two-week intervals, booster injections were performed with the same antigen (0.3-0.5mg) mixed with Incomplete Freund's adjuvant (IFA; Sigma). 50ml blood was collected from each rabbit from the 4th booster onwards. The blood sample was allowed to stand 4hr at RT and then O/N at 4°C until a clot formed. After removal of the clot and debris by centrifuging 10min at 4000rpm, 4°C , serum was collected and stored in aliquots at -80°C .

2.12.3 Antibody affinity purification

100 μg of untagged udu-N/C-Antigen was run on SDS-PAGE gel and then transferred to PVDF membrane. The PVDF membrane was stained with 0.1% (w/v) Ponceau S in 5% (v/v) acetic acid (Sigma) for a few seconds so that the protein could be visualized. Then the PVDF membrane corresponding to the untagged udu-N/C-Antigen protein was excised and destained with 0.1M sodium hydroxide for 10 seconds followed by several rinses with deionized water. The membrane was placed in a 15ml Falcon tube, ensuring that the side of the membrane containing the protein is facing up. After blocked with 5% (w/v) skim milk powder (Diploma) in PBS for more than 1 hr, the

membrane was treated successively with 0.2M glycine (pH 2.5) 3min, PBS 3X1min, 50mM Tris (pH 8.5) 1min, 100mM ethanolamine (Sigma) 3min and PBS 3X1min. These successive treatments were repeated for 2 more times. The membrane was then blocked with 5% milk in PBS for 1hr and incubated with 0.5ml of corresponding rabbit serum at 4°C O/N. After rinsed 3 times and further washed 3X1hr with PBS at 4°C, the antibody was eluted by incubating the membrane with 600µl 0.2 M glycine, pH 2.5 for 3 min and the 600µl of glycine containing the eluted antibody was collected into a 1.5ml tube containing 150µl 1 M Tris, pH 8.0, and 30µl BSA (10mg/mL) (NEB), mixed well and stored at 4°C. The membrane could be regenerated by repeating the successive treatments (skip the glycine treatment) and reused for more than 10 times to purify the same antibody.

2.13 Western blot analysis of Udu protein expression in transfected cells

2.13.1 Extraction of proteins from cultured cells transfected with udu constructs

293T cells were grown in 6-well plate and transfected with pcDNA3.1-*udu*-wt, pcDNA3.1-N-Flag-*udu*-wt and pcDNA3.1-C-HA-*udu*-wt respectively, using SuperFect Transfection Reagent (QIAGEN) according to the manufacturer's protocol. After 24hr of post-transfection, cells were washed twice with ice-cold PBS, and then harvested with 1ml ice-cold PBS by scraping with cell scraper followed by centrifugation at 4°C for 5min at 5,000rpm. The cell pellet was resuspended in 50µl whole cell lysis buffer (20mM HEPES, pH 7.9, 280mM KCl, 1mM EDTA, 0.1mM Na₃VO₃, 10% (v/v) Glycerol, 0.5% (v/v) NP40 (IGEPAL), 20mM NaF, 1mM DTT)

with Protease Inhibitor Cocktail (Roche) and incubated on ice for 10min to lyse the cells. After spun down at 4°C for 10min at 14,000rpm, the supernatant was saved as protein extraction at -80°C.

2.13.2 Western blot

5µl (about 30µg) protein extract was mixed with 2X SDS gel sample buffer (6% SDS, 0.25M Tris, pH 6.8, 10% glycerol, bromophenyl blue and 20mM DTT), boiling for 5 min, and then loaded on a 10% SDS polyacrylamide gel. For the western blot that tests the udu antibody using the untagged udu-N/C-Antigen, 20% SDS polyacrylamide gel was used. After 3 hr running at 30mA, the electrophoresed proteins were transferred onto methanol pretreated PVDF membrane. The membrane was blocked in 5% milk in PBS at 4°C O/N, then incubated with primary antibody (anti-flag/HA monoclonal antibody or anti-udu-C/N-Antigen rabbit serum) in blocking buffer for 2hr at RT. After washed in PBST 3X10min, the membrane was incubated with an appropriate secondary antibody (HRP conjugated) diluted in blocking buffer for 1 hr. The membrane was then washed in PBST 3X10min and the signals were detected with Amersham ECL kit.

2.14 Immunohistochemistry staining

COS-7 cells were grown on 22 x 22mm cover slips in 35-mm wells and transfected with pcDNA3.1-*udu*-wt using SuperFect Transfection Reagent (QIAGEN) according to the manufacturer's protocol. After 24hr of post-transfection, cells were washed with

PBS-CM (PBS with 1mM CaCl₂ and 1mM MgCl₂) and fixed with 3% paraformaldehyde (Fluka) in PBS-CM at 4 °C for 30 min. The fixed cells were washed with PBS-CM (2 times), 0.26% NH₄Cl in PBS-CM (2 times), PBS-CM (2 times), and permeabilized with 0.1% saponin (Sigma) in PBS-CM at room temperature for 15 min. The permeabilized cells were then incubated with rabbit anti-Udu-C-Antigen antibody (against aa 1818-1941) in FDB (PBS-CM with 5% normal goat serum, 2% fetal bovine serum, and 2% BSA) at 4 °C overnight. After rinsed with 0.1% saponin in PBS-CM (3 times), the cells were incubated with Alexa Fluor 488 donkey anti-rabbit IgG antibody (Molecular Probes, USA), washed with 0.1% saponin/PBS-CM (5 times), mounted with Vectashield mounting medium for fluorescence with propidium iodide (PI) (Vector, USA) and visualized on a Zeiss LSM 510 confocal system.

2.15 Affymetrix Array

Total RNA was extracted from the 1dpf *udu^{sq1z1}* homozygous mutant and sibling embryos, respectively, using TRIzol (Gibco-BRL, USA), treated with DNase I and purified using RNeasy Mini kit (QIAGEN). Hybridization was performed according to the manufacturer's instruction (Affymetrix). Data were analyzed using Microarray Suite 5.0 software (Affymetrix).

2.16 Real time PCR and Semi-quantitative RT-PCR

Total RNA was extracted as described above and reverse transcribed using

SuperScript™ III RNase H Reverse Transcriptase (Invitrogen). The amount of reverse transcribed cDNAs was normalized with the Realtime LightCycler (Roche) using elongation factor 1 α (*elf1 α*) as a reference. Semi-quantitative RT-PCR was performed for either 25 or 30 cycles at 94°C for 30 sec; 58°C for 10 sec; 72°C for 30 sec. Primer sequences are listed as follows: *p53* (5'-GCTTTTAGATTTAGTACAACCATTG-3'/5'-GCAAATGCGTGTAACAGTAATAAG-3'), *caspase8* (5'-GGAATGATCTGGAAGCCTGG-3'/5'-TAGCGTGGTTCTGGCATCTG-3'), *fos* (5'-CCAAAACAGAGAAAAGAGCAG-3'/5'-CAGTGTATCGGTGAGTTCACG-3'), *gadd45al* (5'-ATTGAAAGGATGGACTCGGTG-3'/5'-TTTCAGTTCTGCTCATCGCTC-3'), *tdag51* (5'-AAACAGCGACGATGCCTTACAA-3'/5'-CCAGGCAACAGCGGTCT-3'), *mdm2* (5'-CTCGCAGTGAGGGCAGTGAAG-3'/5'-TCTAGGCACGTAGCGGGAAGG-3'), *elf1 α* (5'-CTTCTCAGGCTGACTGTGC-3'/5'-CCGCTAGCATTACCCTCC-3').

Chapter III Genetic Screen for T lymphocyte deficient mutants

3.1 Results

3.1.1 Genetic screen for *rag1*-deficient mutants

After three rounds of ENU treatments (described in section 2.3.1), only 8 out of 40 male wild-type AB fish survived, one of which was sterile, possibly due to the high ENU concentration. The remaining 7 founder fish were used to generate about 700 F1 progeny by crossing with wild-type AB females, with the limit of 150 F1 fish from each founder (Table 3.1). The efficiency of mutagenesis was then determined by the frequency of induced mutations at the pigmentation locus, *albino*, by crossing the founder fish with *albino* homozygotes. It was found to be about 2×10^{-3} , within the normal mutagenesis rates of $0.9-3.3 \times 10^{-3}$ (van Eeden et al., 1999). The F1 fish derived from different founders were inter-crossed to generate 330 F2 families for genetic screen.

rag1 was used as a marker to score the mutants defective in T lymphocyte development or thymus organogenesis. As shown in figure 3.1, expression of *rag1* in thymus was clearly detected by WISH in the 4dpf wild-type fish (Figure 3.1). WISH of *rag1* was carried out with 4-5dpf F3 embryos from random sibling crossing within individual F2 family. When one quarter of the F3 embryos were negative for *rag1* expression, the corresponding F2 parents were scored as potential mutant carriers (Figure 3.2).



Figure 3.1 Expression of *rag1* in zebrafish. WISH of *rag1* in thymus of 4dpf fish.



Figure 3.2 Detection of *rag1* expression in wild type and mutant embryos. WISH of *rag1* (arrows) in 5dpf wild type (top) and mutant (bottom) larval.

Based on Mendelian segregation principle, half of the fish in each F2 family are heterozygous for a particular recessive mutation. The probability that both male and female are heterozygous can be calculated based on the formula $1 - 0.75^n$ where the n represents the number of successful crosses. We therefore set the criteria that 4 successful crosses should be the minimum number screened for each F2 family, which gave a 70% possibility of identifying the existed mutants. A total of 1551 successful crosses from 270 F2 families were screened and the average successful cross number achieved for each F2 family was 5.74, reaching 81% of the average probability to identify one mutation in our screen (Table 3.1). The other 60 F2 families were sex biased and could not produce enough successful crosses. Our primary screen resulted in isolation of 140 mutants from 110 families. These 140 F2 mutants were out-crossed with AB wild type to generate F3 families. During the F3 generation, 24 families were abandoned due to problems such as sterility, sex bias or absence of the mutant phenotype in the next generation. The remaining 86 mutant families were confirmed to be *rag1* expression deficient and were subjected to preliminary characterization (Table 3.1).

3.1.2 Data management

To organize the mutants efficiently, a fish-screen/mutant management database was established by using File Maker Pro 5.0 (Filemaker Inc.). As illustrated in Figure 3.3, the database consisted of three aspects of each mutant: I) basic information, which included the origin of founder, the family number, the number of screens and the time

Table 3.1 Summary of *rag1* genetic screen

	Number
Founder Fish	7
F1 Fish	~700
F2 Families	330
Screened F2 Families	270
Successful Crosses	1551
Successful Crosses per Family	5.74
Primary Identified Mutants	422
Identified Mutants Family	180
Rescreened Confirmed Mutants	140
Rescreened Confirmed Mutant Families	110
Identified F3 Mutant Families	86
Mutants retained and characterized	13

of out-cross; II) morphological phenotype under microscope; III) results of preliminary characterization. All the parameters were searchable, which made it easy to trace each pair of mutants during the screen.

3.1.3 Preliminary characterization of the *rag1*-deficient mutants

To investigate whether other hematopoietic lineage cells were defective in the 86 mutants we isolated, blood circulation was examined at the 3dpf and 5dpf embryos from crosses of the heterozygous F3 mutants. One mutant, *wz260*, lacked blood circulation. The decreased blood cell number was confirmed by *o*-dianisidine staining (Figure 3.4). This mutant was selected for further characterization and positional cloning, which would be discussed in detail in the next chapter.

WISH of *hoxa3* and *foxn1/whnb* was also performed at the 2dpf and 4dpf mutant embryos, respectively (Figure 3.5), to examine thymus organogenesis in these 86 *rag-1* expression-deficient mutants. None of the mutants lost the expression of *hoxa3* or *foxn1/whnb*, indicating that the thymus rudiment was generated normally in all of the mutants. However, in 6 of the mutants (*wz118*, *wz121*, *wz147*, *wz214*, *wz244* and *wz370*), the expression domains of *foxn1* corresponding to the thymic rudiments appeared to be smaller and more condensed (figure 3.6). At this moment, we were unable to determine whether loss of *rag1* expression in these 6 mutants was due to the thymus rudiment abnormality or lymphoid lineage deficiency. However, considering that other *rag1*-deficient mutants showed normal *foxn1* expression, I speculated that

A

Panel A shows a detailed data input screen for a mutant. At the top, there is a 'New Record' button and a 'Find' search bar. The main form includes fields for 'Mutant No.' (110-3), 'Mutant Name', 'Family No.' (110), and 'Origin of F1' (MH). Below these are fields for 'Rate', 'outcross date' (2001-12-28), and 'outcross strain'. A 'Notes' field is also present. The 'Mutant Confirmation' section contains checkboxes for various phenotypes: 'no circulation', 'small eyes', 'no RBC', 'curved body', 'relative normal', and 'Other...'. A note states 'All these screen are based on Rag1 in situ hybridization.' Below this are three 'Screen' sections (1st, 2nd, 3rd) with input fields for 'small eye', 'relative normal', and 'very abnormal'. There are also 'ratio' fields (ratio1: 1/4, ratio2: 1/4, ratio3:). The 'final phenotype' section has checkboxes for 'Not', 'short body', 'big yolk', 'pigmented eye', 'very abnormal', 'M', 'small eye', 'big heart', 'relative normal', 'all positive', 'curved body', and 'un-over'. A 'notes' field contains '4th-severe phenotype, 5th-curved body, small eye, big yolk'. The 'Mutant Characterization' section includes a 'Cross with other mutants' field with 'GATA3' entered.

B

Panel B shows a compact, summarized view of the database. It lists several mutant records, each with a header row containing 'Mutant No.', 'Family No.', 'Origin of F1', and 'out-cross'. Below each header is a row for 'Mutant/Total in this Family' and a 'Mutant Data' button. The 'final phenotype' section for each record contains checkboxes for various traits, with some checked. The records shown are: 40-13 (Family 40, Origin of F1 MJ, out-cross), 86-1 (Family 86, Origin of F1 MI, out-cross 2002-1-24), 86-3 (Family 86, Origin of F1 MI, out-cross 2002-1-24), 86-4 (Family 86, Origin of F1 mi, out-cross), and 107-4 (Family 107, Origin of F1 LG, out-cross).

Figure 3.3 Database management of *rag1* screen. A fish screen/mutant management database was established by using File maker Pro 5.0. Panel A shows an example of a full data input screen for a mutant. Panel B shows the summarized screen-shot of the database in a compact format.

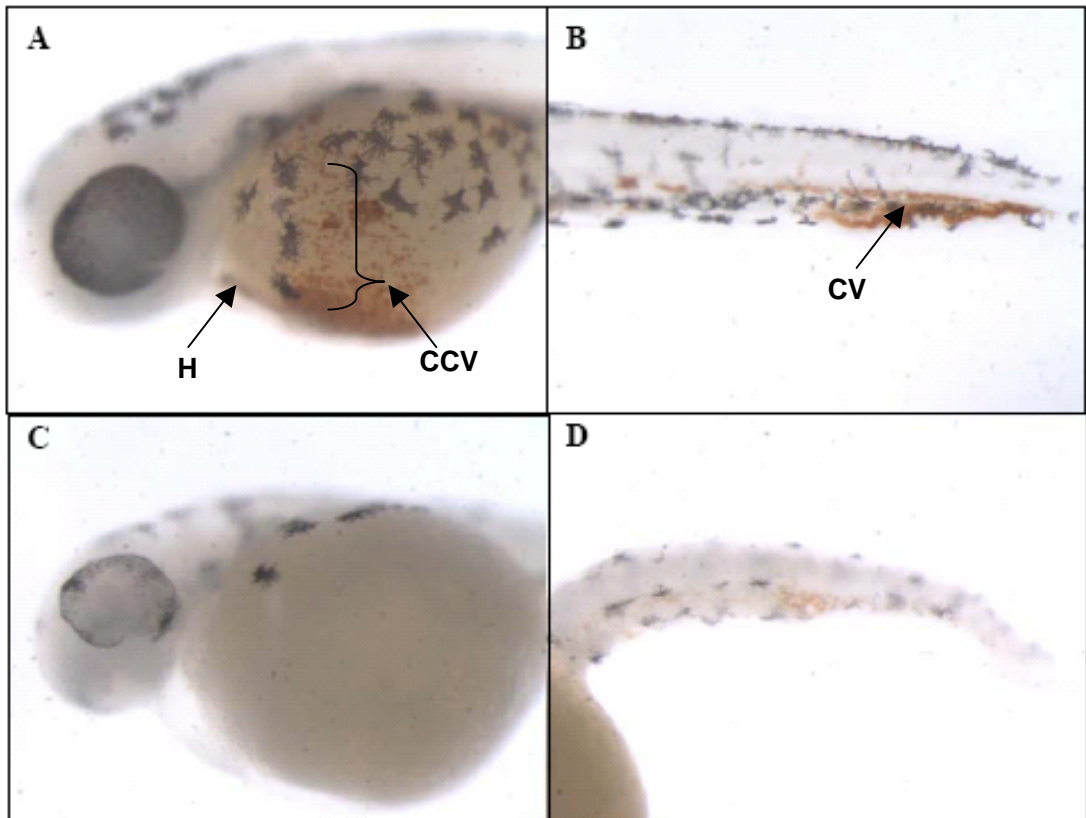


Figure 3.4 *o*-dianisidine staining of 2dpf wild type and mutant *wz260 (udu)* embryos. The *o*-dianisidine stains hemoglobin in the erythroid cells and develops brown coloration. (A and B) In wild type embryos, the stained erythroid cells were distributed in the heart (H), common cardinal vein (CCV) (A), and caudal vein (CV) (B). (C and D) In mutant *wz260 (udu)* embryo, the erythroid cells dramatically decreased.

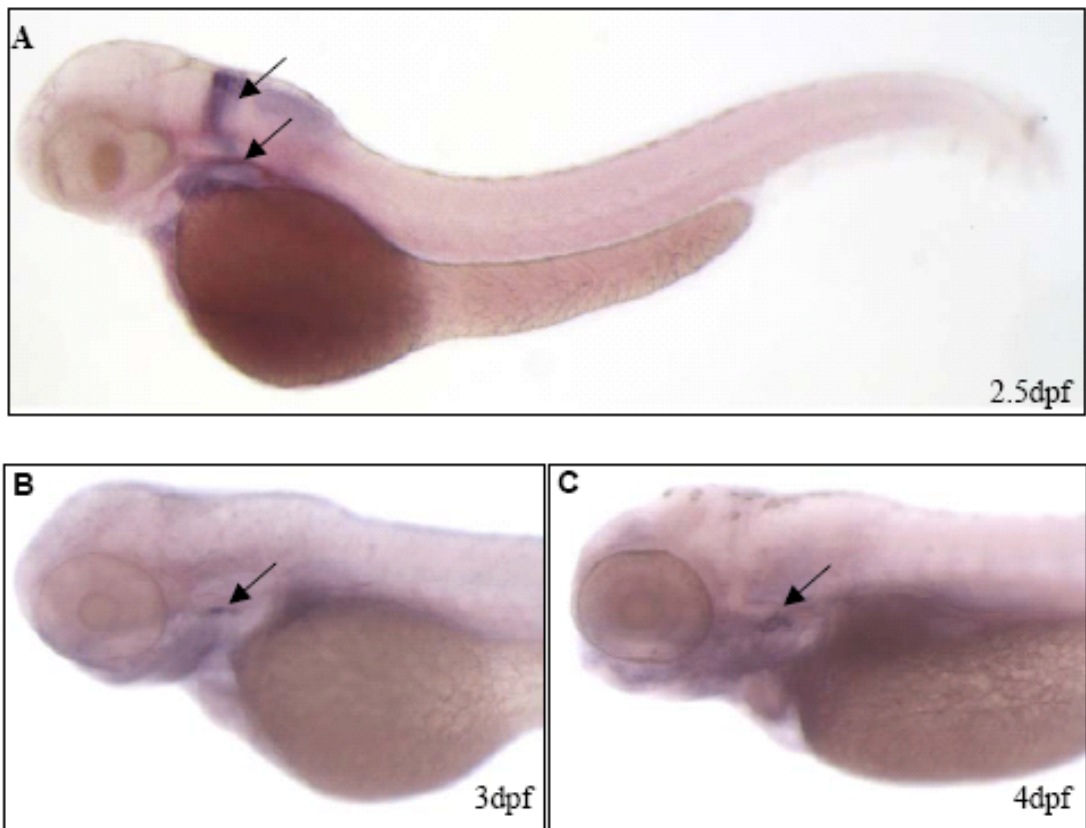


Figure 3.5 Expression of *hoxa3* and *foxn1* in zebrafish. WISH of *hoxa3* (arrows) in 2.5 dpf fish (A), *foxn1* (arrows) in 3 dpf (B) and 4 dpf fish (C).

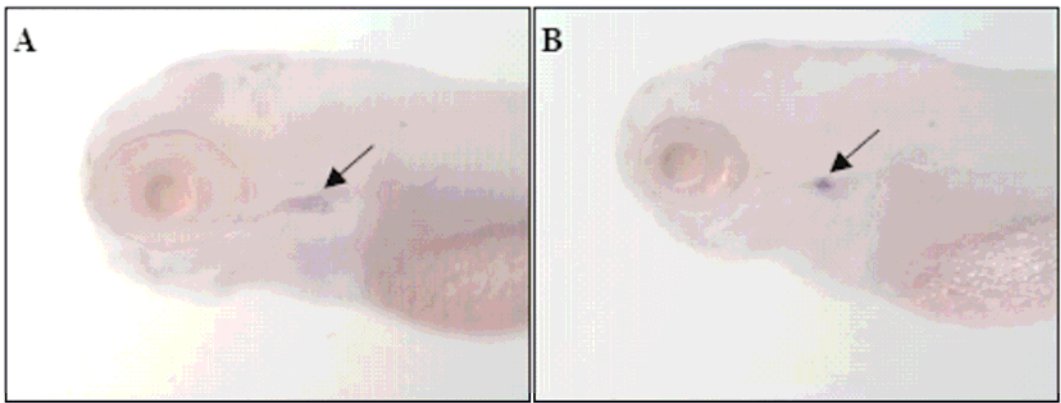


Figure 3.6 *foxn1* condensed expression domain in some mutant embryos. WISH of *foxn1* (arrows) in 5dpf wild type embryo (A) and mutant embryo (B).

the condensed *foxn1* expressions represented abnormal thymus development that might cause failure of recruitment of the CLPs.

Finally, morphology phenotype was also used to exclude mutants with general defects. At last, in addition to *wz260*, 12 morphologically relative normal mutants (*wz180*, *wz193*, *wz213*, *wz174*, *wz179*, *wz161*, *wz116*, *wz262*, *wz244*, *wz194*, *wz147* and *wz370*) were selected for maintenance and further study (figure 3.7).

3.2 Discussion

We carried out a forward genetic screen to isolate T lymphocyte deficient mutants based on WISH of *rag1*. With 2×10^{-3} mutagenesis efficiencies, 540 genomes were screened and 86 mutants were recovered from the F3 generation. The large number of the mutants isolated from our small-scale screen is possible because mutations in any genes affecting T cell development or thymus organogenesis could lead to loss of *rag-1* expression in thymus.

In principle, *rag1* expression-deficient mutants could be grouped into five different categories with deficiency in: I) Hemangioblast; II) HSC or multipotent progenitors; III) CLPs; IV) T cell lineage; V) Thymus organogenesis.

Based on results of preliminary characterization, none of the 86 *rag1*-deficient mutants belong to Category I. As *wz260* showed reduced primitive red blood cells, it

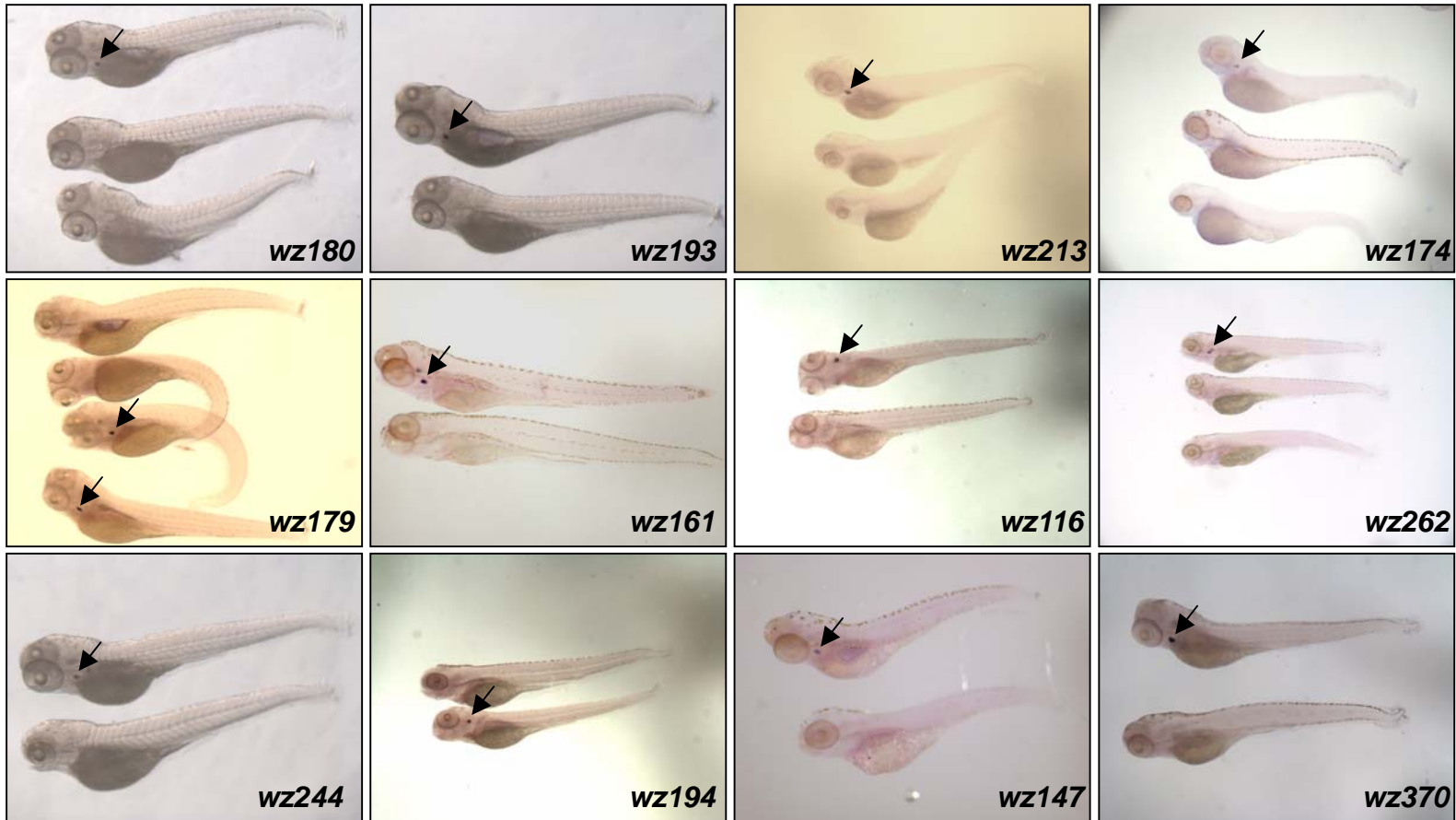


Figure 3.7 Twelve *rag1*-deficient mutants with relatively normal morphology. Each panel consists of 4dpf wild type (with thymic *rag1* staining indicated by arrows) and *rag1* deficient mutant fish.

raised the possibility that it might belong to Category II mutants, defective in HSC or multipotent progenitors. Other 85 mutants could not be excluded from this group based solely on the preliminary characterization. This was because most of our mutants die within 10dpf when the definitive red blood cells start to be dominant in circulation. Thus it was impossible to observe definitive blood circulation. Examination of *runx1* and *c-myb* (Burns et al., 2002; Thompson et al., 1998; Kalev-Zylinska et al., 2002) may provide clues to define mutants of this group. Category III mutants are defective in T and B lymphocyte development with intact erythroid and myeloid lineages. In zebrafish, B lymphocytes are first detected in kidney by *rag1* expression at 21dpf (Willett et al., 1999). The early lethal phenotypes of our *rag1*-deficient mutants make it impossible to examine B lymphocyte defects in this category. Finally, both Category IV (T cell lineage) and V (Thymus organogenesis) mutants lose only T lymphocyte but not the other blood cells. However, the causes of the T cell defect in these two categories are different. Category IV mutants have cell-autonomous defects in T cell development such as cell survival, differentiation, and migration, whereas Category V mutants are defective in thymus organogenesis, resulting in loss of T cells. *foxn1*, which is highly enriched in the thymus epithelial cells, is a well-known molecular marker important for thymus organogenesis, and serves as a thymus-specific marker that may distinguish these two types of mutants (Blackburn et al., 1996; Nehls et al., 1994). However, none of the 86 *rag1*-deficient mutants lost the *foxn1* expression, indicating that generation of the thymus rudiment occurs in these mutants. But we still could not exclude the possibility that the thymus

rudiment has other defects taking place before CLPs colonization, such as inability to provide the appropriate signals to attract or interact with CLPs. The condensed expression pattern of *foxn1* in some mutants may represent the defective thymus before the CLPs entry, or the thymus that failed to expand further due to the absence of CLPs.

Chapter IV Characterization of *udu* mutant embryo, positional cloning and functional study of *udu* gene

4.1 Results

4.1.1 Characterization of *udu* mutant

4.1.1.1 Morphological phenotype of *wz260* and complementary test between *wz260* and *ugly duckling* (*udu^{tu24}*)

From the *rag1*-deficient mutants we isolated, I selected *wz260* for further study including detailed characterization and positional cloning. *wz260* mutant began to show notable morphological abnormality at around 20hpf, such as short body axis, bent-down tail, irregular somites, small head, small eyes and no circulation with a cardiac edema. Later on, the general retarded phenotype became more severe and the fish died around 10dpf (Figure 4.1). These morphological phenotypes were similar to those of the zebrafish mutant *ugly duckling* (*udu^{tu24}*) isolated in the 1996 Tuebingen large scale screen (Hammerschmidt et al., 1996). I thus speculated that *wz260* mutant might be a new allele of *udu^{tu24}*. Complementation test was performed by mating the *wz260* heterozygous female with *udu^{tu24}* heterozygous male and vice versa. One quarter of the resulting embryos displayed the similar morphological phenotypes with *wz260* or *udu^{tu24}* mutant embryos and also lost *rag1* expression in thymus (Figure 4.1). These observations confirmed that *wz260* was indeed a new allele of *udu^{tu24}* and therefore was re-named as *udu^{sqlzl}*.

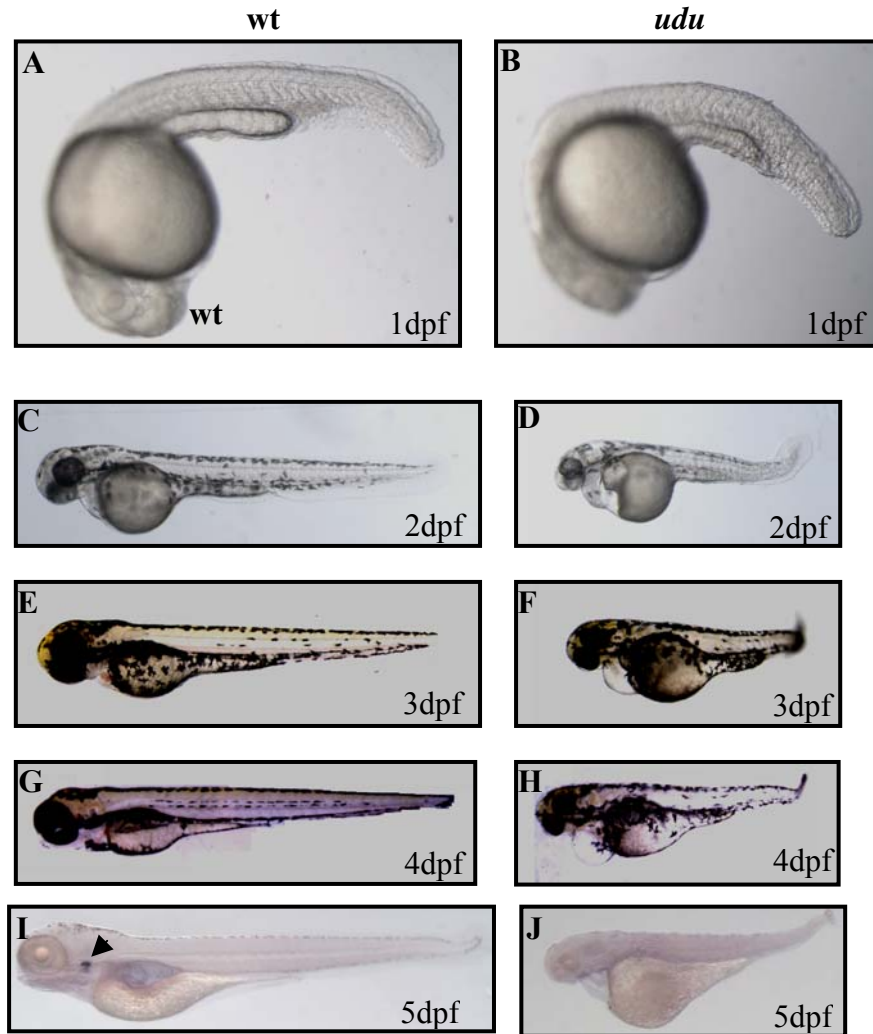


Figure 4.1 Morphological phenotype of *udu* (*wz260*) mutant. Live fish photos of wild type (A, C, E and G) and *udu* mutant fish (B, D, F and H) at 1 dpf (A and B), 2 dpf (C and D), 3 dpf (E and F) and 4 dpf (G and H). WISH of *rag1* (arrow) in 5 dpf wild type (I) and *udu* mutant fish (J). All embryos are in lateral views with anterior to the left.

4.1.1.2 Primitive hematopoietic hypoplasia in *udu*^{-/-} mutant

Observation under the microscope indicated that red blood cells significantly decreased in the *udu*^{-/-} mutant embryos. O-dianisidine staining of hemoglobin was then carried out. It showed that the stained erythrocytes were indeed markedly reduced in the 2dpf *udu*^{-/-} mutant embryos (Figure 3.4). To explore the hematopoietic defects in depth, I examined the expression of two critical early hematopoietic markers *lmo2* and *scl* (Liao et al., 1998; Gering et al., 1998). Whole-mount *in situ* hybridization (WISH) showed that neither *lmo2* (data not shown) nor *scl* exhibited apparent expression differences between the *udu*^{-/-} mutant and wild type embryos before 10-somite stage (Figure 4.2A and B), indicating that the *udu* gene is dispensable for the specification of hematopoietic progenitors. However, by the 18-somite stage, the level of *scl* and *lmo2* expression was reduced in the ICM region in *udu*^{-/-} mutant. Considering that at this stage the ICM region consists mainly of erythroblasts, I speculated that the erythropoiesis was affected in *udu*^{-/-} mutant. This was confirmed by the reduction of *gata1* expression from the 18-somite stage onwards (Figure 4.2C and D). Especially, by 22hpf, the expression of *band3*, an erythrocyte-specific membrane protein critical for erythrocyte maturation (Paw et al., 2003), was dramatically reduced in the *udu*^{-/-} mutant embryos (Figure 4.2E and F). And this remarkable decrease of *band3* expression at 22hpf could not be fully explained by the reduction of red blood cell number because expression of *βe1-globin* remained relative normal or only slightly reduced in these 22hpf *udu*^{-/-} mutant embryos (Figure 4.2G and H). Thus aberration in erythrocyte differentiation is very

likely the main reason for the decrease of *band3* expression in *udu* mutant, eventually leading to red blood cell hypoplasia as indicated by *βe3-globin* expression from 30hpf onwards (Figure 4.2 I-L).

Similar to erythropoiesis, initiation of myelopoiesis was normal as indicated by beginning of *pu.1* expression before the 10-somite stage (Figure 4.3 A and B). But further differentiation of primitive myeloid cells in *udu* mutant was impaired as it was shown by the decreased expression of *pu.1*, *mpo* and *lyc* by 24hpf in the ALM (Figure 4.3 C-H) where primitive myelopoiesis occurs. Notably, ectopic elevated expression of *pu.1* and *mpo* in the ICM region was detected in the *udu*^{-/-} mutant embryos between 24hpf and 30hpf (Figure 4.3 C-F). However, no ectopic elevated *l-plastin* (data not shown) or *lyc* expression was seen in the ICM region of these mutant embryos (Figure 4.3 G and H), suggesting that the ectopic *pu.1* and *mpo* expression in the ICM region was possibly caused by the increased number of the immature precursors rather than alteration of cell fate. This was further supported by the cytology analysis, which revealed that there was no obvious increase of myeloid lineage cells in the mutant embryos (data not shown).

4.1.1.3 Abnormal proliferation and differentiation of hematopoietic cells in *udu*^{-/-}

To further illustrate the cellular defect of the hematopoietic hypoplasia in *udu* mutant, we performed acridine orange staining on different stages of the *udu* mutant and wild type embryos and found that, while extensive cell death occurred in the central

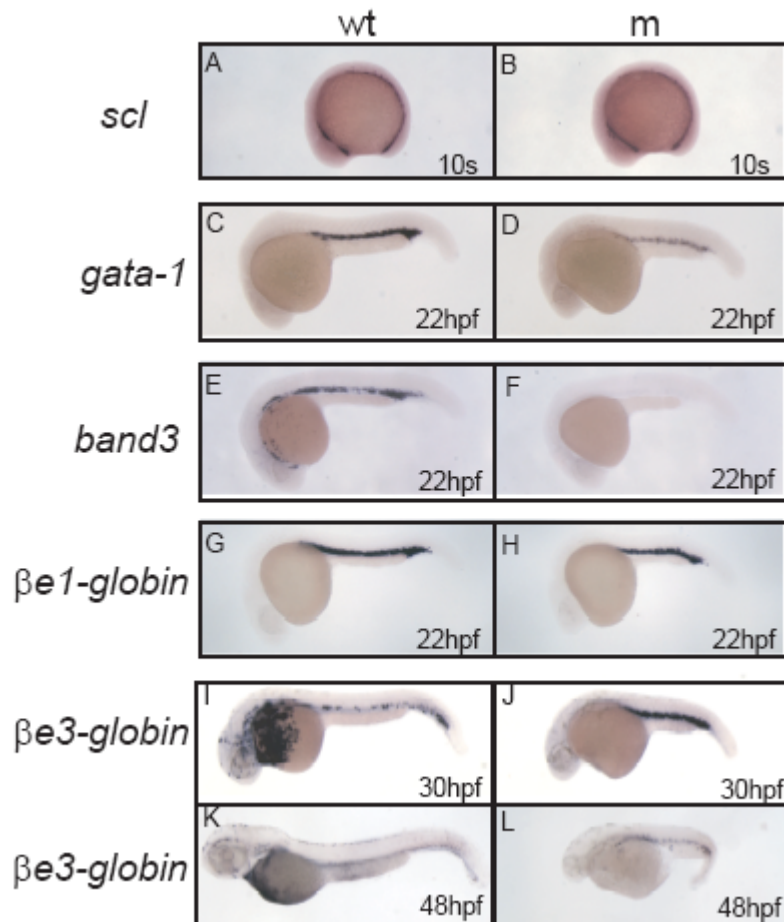


Figure 4.2 Primitive erythropoiesis is impaired in the *udu*^{-/-} mutant. (A-L) WISH of *scl* (A, B), *gata1* (C, D), *band3* (E, F), $\beta e1$ -globin (G, H), and $\beta e3$ -globin (I-L) in the wild type (A, C, E, G, I and K) and the *udu*^{-/-} mutant embryos (B, D, F, H, J and L). All embryos are in lateral views with anterior to the left.

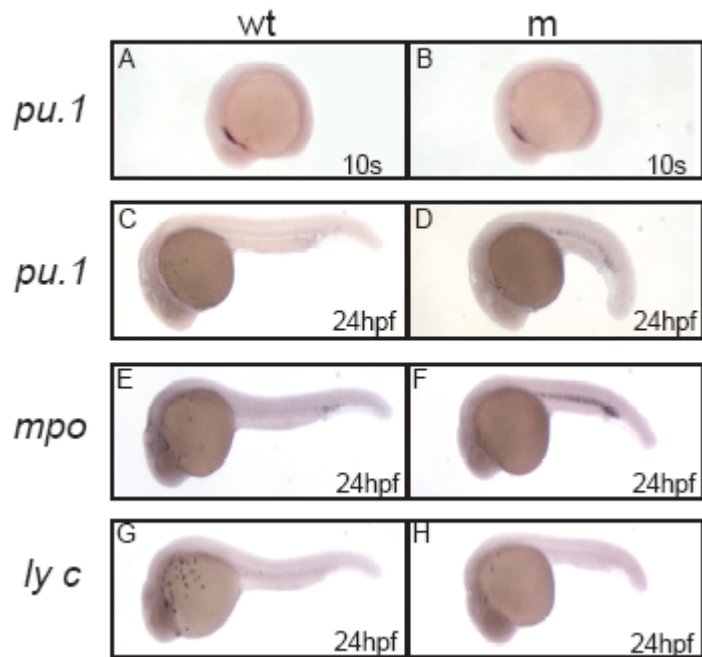


Figure 4.3 Myelopoiesis is defective in the *udu*^{-/-} mutant. (A-H) WISH of *pu.1* (A, B, C and D), *mpo* (E and F) and *ly c* (G and H) in the 10-somite (10s) (A and B) and 24hpf (C-H) wild type (A, C, E and G) and *udu*^{-/-} mutant embryos (B, D, F and H). All embryos are in lateral views with anterior to the left.

nervous system (CNS), no significant increase in apoptosis was observed in the ICM (Figure 4.4), suggesting that aberration in cell cycle rather than apoptosis may possibly contribute to the eventual absence of hematopoietic cells in *udu* mutant. To further clarify this issue, I out-crossed the *udu* heterozygous mutant fish with the Tg(-5.0scl:EGFP)^{sq1} (referred to as Tg(5'5kbscl:EGFP) in the original paper) transgenic line (Jin et al., 2006), in which the expression of the enhanced green fluorescent protein (EGFP) reporter gene is under control of *scl* promoter. The resulting *udu*^{+/-}/Tg(-5.0scl:EGFP)^{sq1} was then mated with *udu*^{+/-} fish. Finally, the GFP positive cells of the 24hpf *udu*^{-/-}/Tg(-5.0scl:EGFP)^{sq1} and sibling embryos were collected by the fluorescent activated cell sorting (FACS) (Figure 4.5A and D) and subjected to cell cycle analysis. DNA content examination using Hoechst 33342 staining revealed that, while wild type displayed 45.06%, 43.93% and 11.01% of cells in G1/G0, S and G2/M phases, respectively (Figure 4.5B), the *udu*^{-/-} mutant cells exhibited abnormal accumulation in G2/M (43.16%) and reduction in G1/G0 (32.13%) and S (24.71%) phases (Figure 4.5E). Besides, cytology analysis showed that the wild type GFP+ cells consisted of mainly erythroid cells in various levels of differentiation (more differentiated cells showed a round central nucleus, chromatin condensation and were smaller in size) and some myeloid cells (characterized by their irregular nucleus) (Figure 4.5C). In contrast, the *udu*^{-/-} mutant GFP+ cells were much larger, lacked chromatin condensation (Figure 4.5F), and similar to those found in the 16hpf wild type embryos (data not shown). It appeared that loss of *udu* gene leads to the block of erythrocyte maturation. Therefore, I conclude that the *udu*^{-/-} erythroid cells

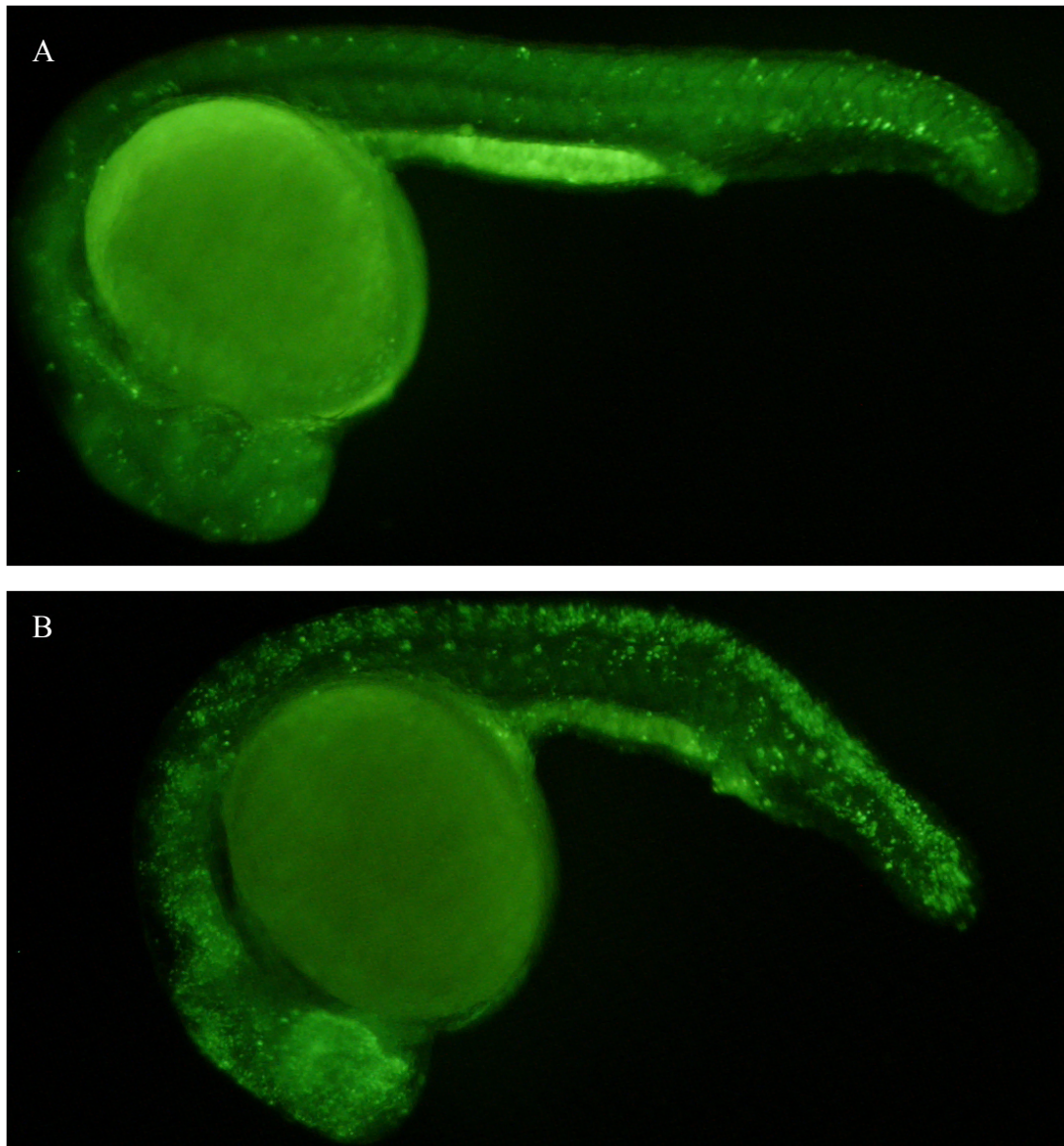


Figure 4.4 Extensive cell deaths in the CNS but not in the ICM in the *udu*^{-/-} mutant. (A and B) Acridine orange staining on 24hpf wild type (A) and *udu* mutant embryos (B).

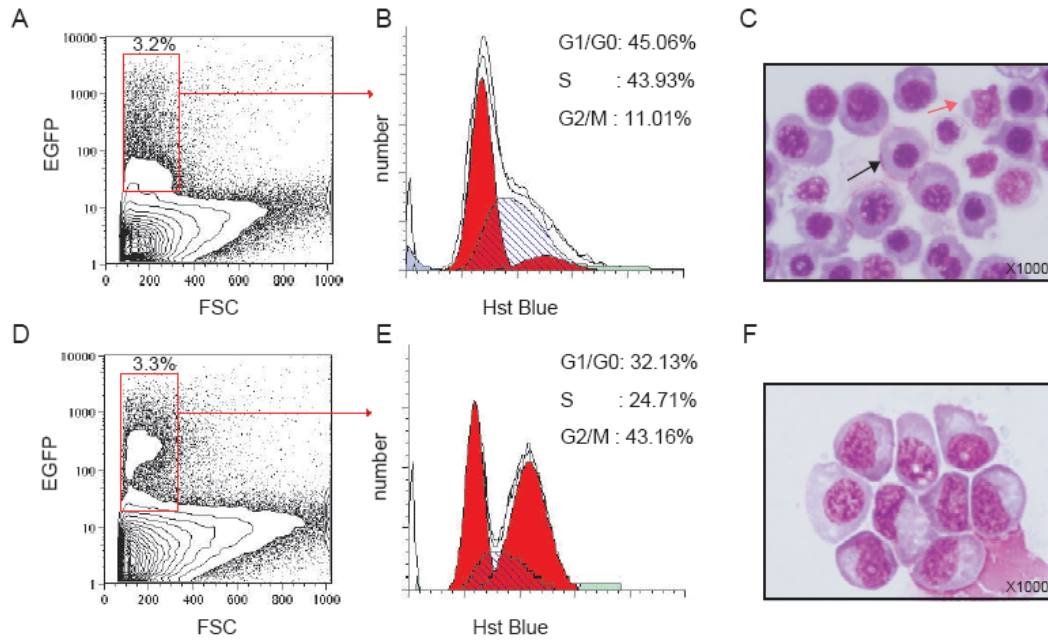


Figure 4.5 The *udu*^{-/-} erythroid cells are defective in proliferation and differentiation. (A and D) FACS profile of the cell suspensions from the 24hpf wild type (A) or *udu*^{-/-} mutant (D) embryos. The y axis indicates the intensity of the EGFP expression and the x axis represents the cell size. (B and E) The EGFP-positive hematopoietic cells in A and D (gated in the rectangle) are collected, respectively, and subjected to DNA content analysis by the Hoechst33342 staining. The y-axis indicates the cell number whereas the x-axis represents the DNA content. The percentages of each phase in cell cycle are given. (C and F) May-Grunwald and Giemsa staining analysis (magnification x1000) of the sorted EGFP-positive cells in A and D. Black and red arrows in C indicate erythroid and myeloid cell, respectively.

are actually defective in proliferation and differentiation.

4.1.2 Identification of the *udu* mutant gene

4.1.2.1 Positional cloning of *udu* gene

To unravel the molecular basis that underlies the phenotype of *udu*^{-/-} mutant, I next went on to clone the *udu* gene by positional cloning. By bulk segregation analysis (BSA), I found that the *udu* mutation was linked to SSLP (simple sequence length polymorphism) marker z10036 and z1215 on linkage group 16 (Figure 4.6). And the linkage was confirmed by 172 single embryo linkage analyses (Figure 4.7). Among the 172 embryos, there were 14 and 33 recombinants for marker z10036 and marker z1215 respectively. These recombinants of the two markers had no overlap, indicating that the *udu* gene was localized between z10036 and z1215. The z10036 direction was defined as North and the z1215 direction as South. The genetic distance between z10036 and *udu* gene was 4.1cM ($14/(172 \times 2)$), whereas the genetic distance between z1215 and *udu* gene was 9.6cM ($33/(172 \times 2)$).

Based on the genetic map provided by ZFIN (The Zebrafish Information Network), additional SSLP markers between z10036 and z1215 were screened for polymorphism first and then used to narrow down the *udu* interval (Figure 4.8). One polymorphic SSLP marker z17246 shared 2 recombinants with z10036 and was a closer north marker. To find a closer south marker, SSLP markers were designed based on the sequence of BAC zK30O16 that contained a BAC end marker zK30O16.sp6 mapped

between z10036 and z1215 (Figure 4.8). One marker SSLP-S16 on BAC zK30O16 was found to have 2 recombinants that were shared with z1215, indicating that it was a closer south marker. Then the fine mapping was carried out using z17246 and SSLP-S16. 2,932 mutant embryos were analyzed, 29 recombinants were found for SSLP-S16 and 20 recombinants for z17246 (Figure 4.9). Therefore, the genetic distance between *udu* gene and z17246 or SSLP-S16 was estimated to be 0.34cM and 0.49cM, respectively. The distance was close enough to carry out genome walking to link the genetic map with the physical map.

Based on Ensembl (http://www.ensembl.org/Danio_rerio/index.html) and Vega database (http://vega.sanger.ac.uk/Danio_rerio/index.html), as well as Zebrafish Genome Fingerprinting Project database provided by Sanger Center (www.sanger.ac.uk/Projects/D_rerio/WebFPC/zebrafish/small.shtml), blast search using z17246 and SSLP-16 found out the North Contig #9751 and the South Contig #10178 respectively. Due to the incomplete sequences and some mistakes in the shotgun assembly, these two contigs were mapped to two distinct regions at a long distance on Ensembl. It was not possible considering the real genetic distance. Therefore, I tried to link these two contigs together by blast searching using all the BAC end sequences within the two contigs. I found 7 BAC clones (zK7E18, zK181B14, zK185J5, zK254G19, zK31I15, zK288H24 and zK230G12) whose one end overlapped with North Contig #9751 and the other end overlapped with South Contig #10178, thereby bridging the North and South Contigs (Figure 4.10).

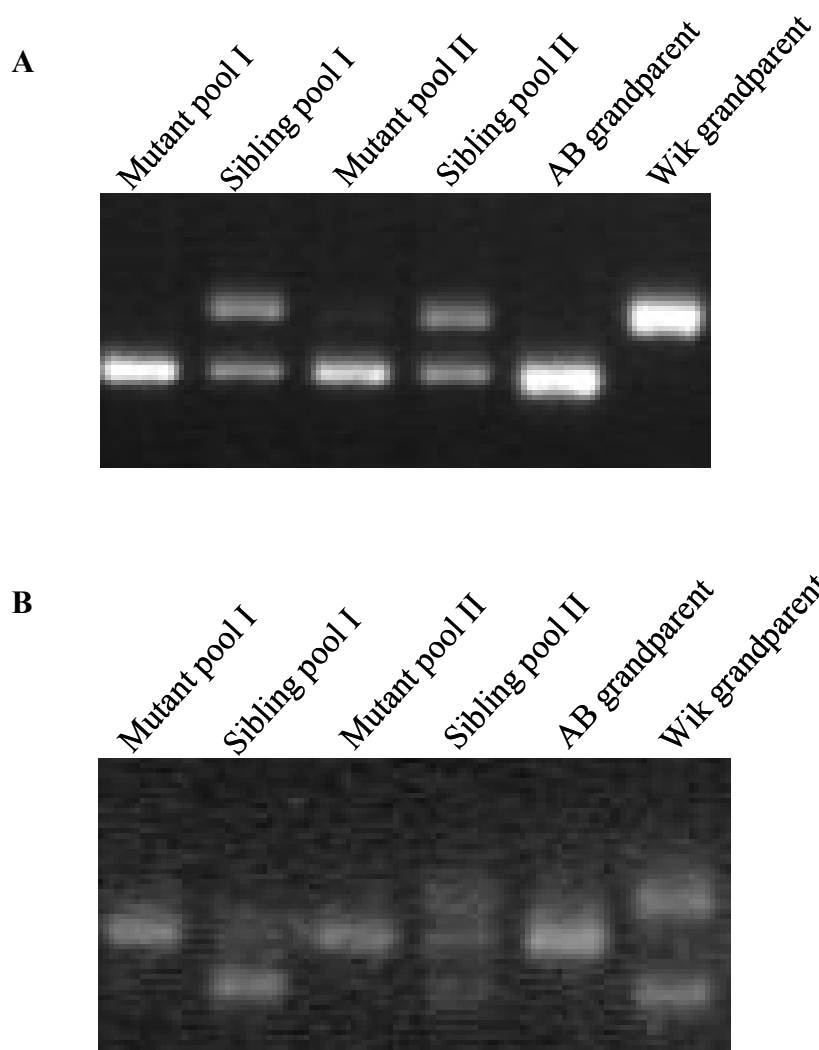


Figure 4.6 BSA identified that the *udu* mutation was linked to SSLP marker z10036 (A) and z1215 (B) on linkage group 16.

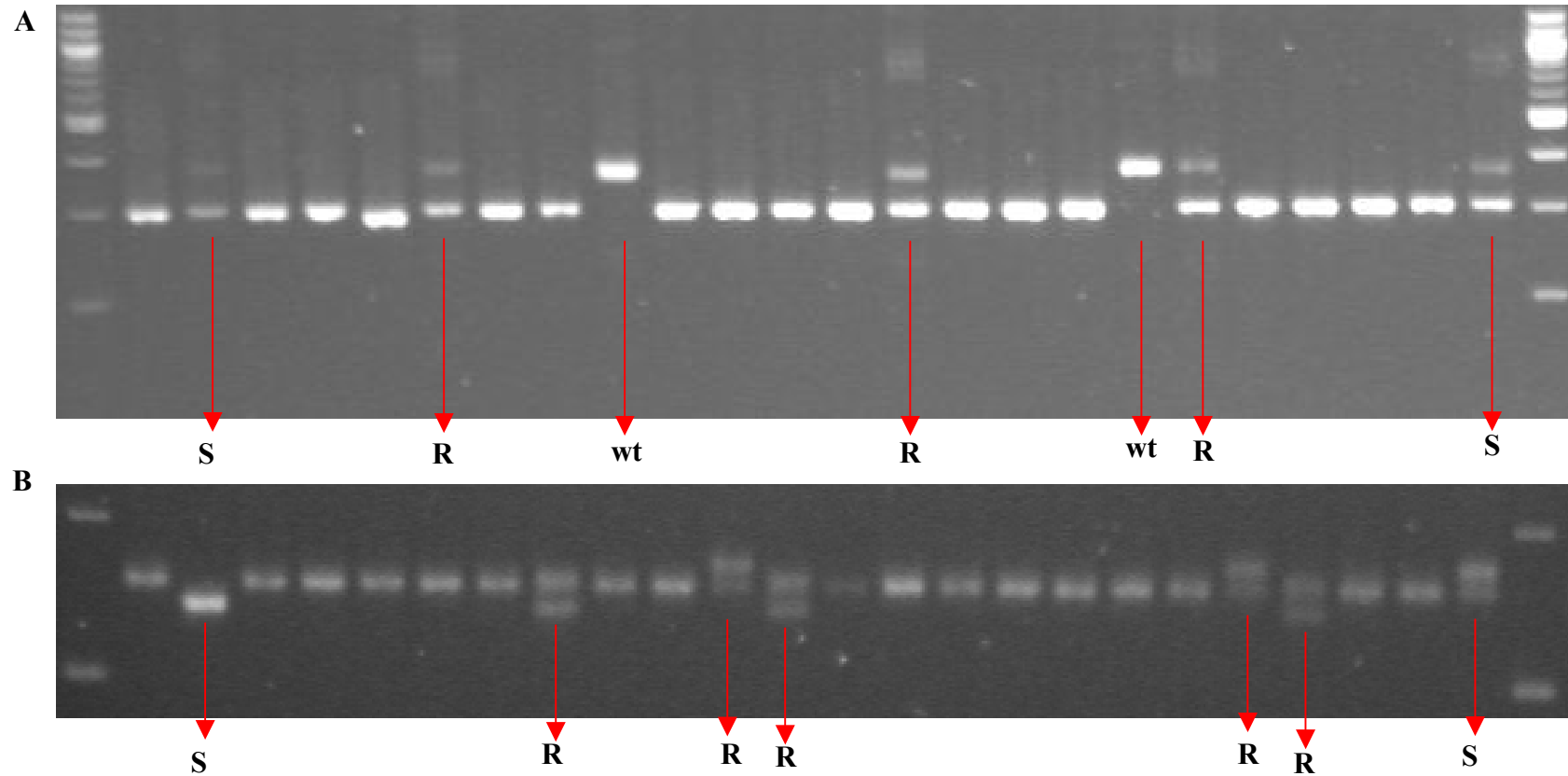


Figure 4.7 Single embryo linkage analyses of marker z10036 (A) and z1215 (B). In both of the panels, the first and last lanes are size standard markers. The lanes labeled with “S” and “wt” indicate the siblings and wild type embryos, respectively. The lanes labeled with “R” indicate the *udu*^{-/-} embryos in which recombination occurred between the *udu* gene and marker z10036 (A) or z1215 (B). The unlabeled lanes indicate the *udu*^{-/-} embryos without recombination.

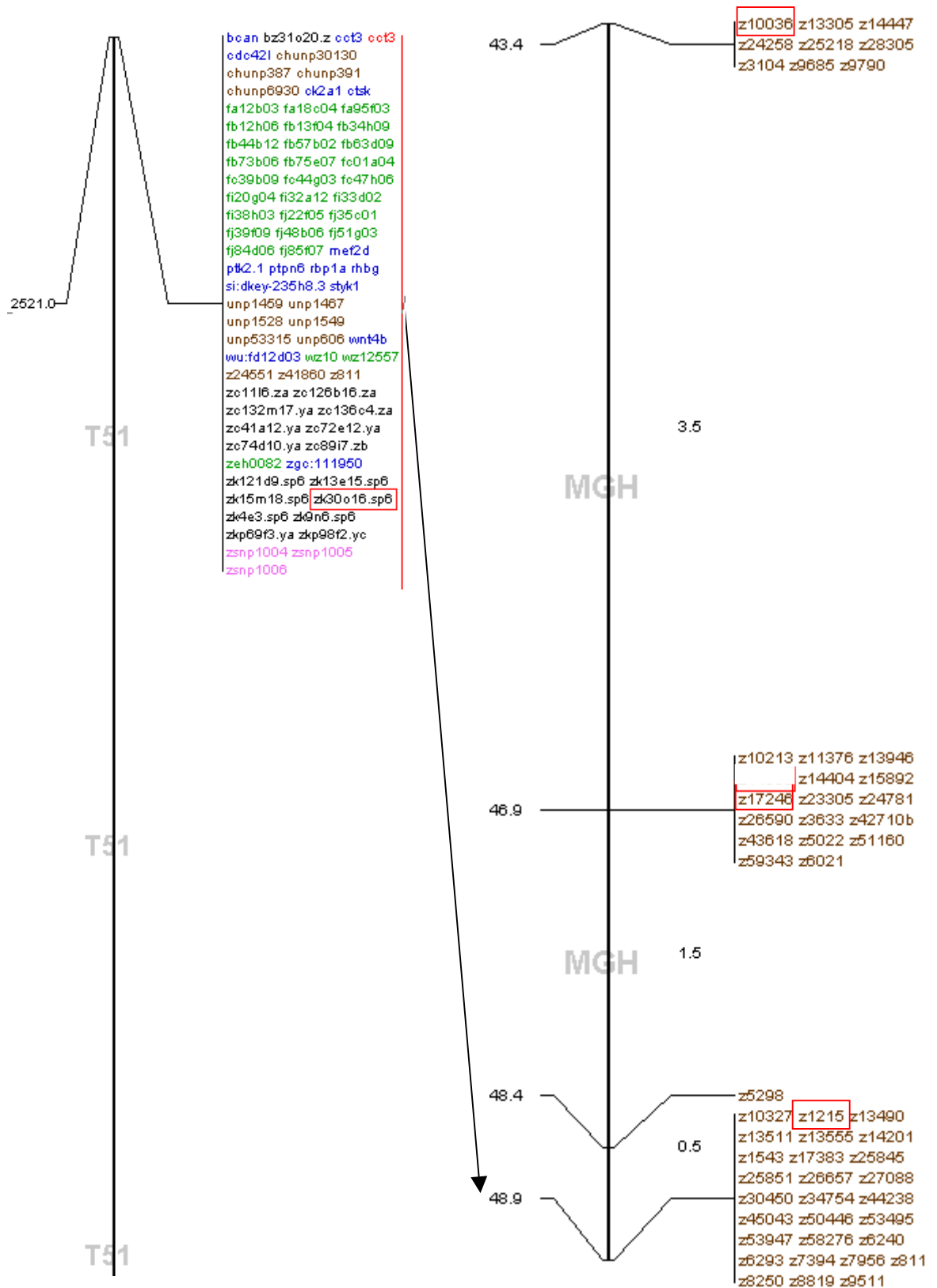


Figure 4.8 The genetic map T51 and MGH provided by ZFIN. Only the *udu* intervals are shown in the panel. The firstly identified linked markers by BSA (z10036 and z1215) as well as the markers used for fine mapping (z17246 and zK30O16.sp6) are highlighted with red boxes.

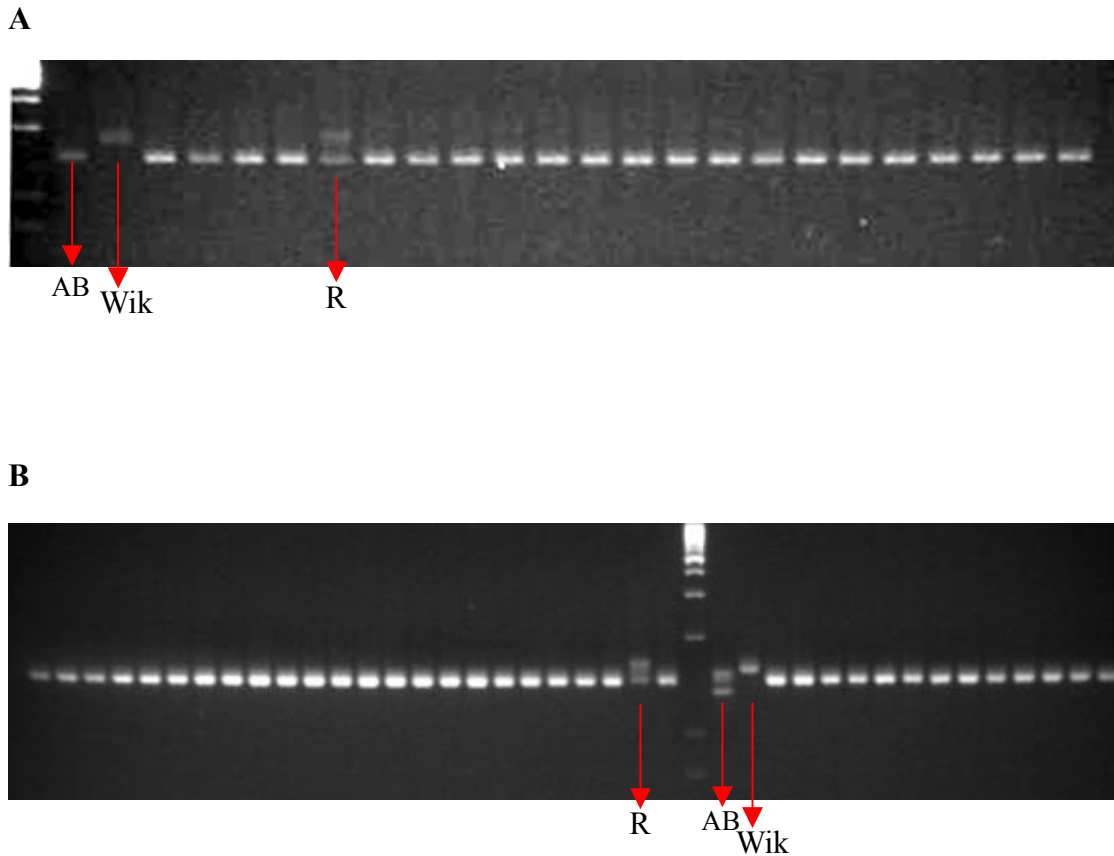


Figure 4.9 Fine mapping using z17246 and SSLP-S16. (A and B) Single mutant embryo linkage analysis with z17246 (A) and SSLP-S16 (B). The lanes labeled with “AB” and “Wik” represent the AB and Wik grandparents’ allele respectively. The lanes labeled with “R” indicate the recombinant *udu*^{-/-} embryos’ allele. The unlabeled lanes indicate the *udu*^{-/-} embryos without recombination.

To further narrow down the *udu* region, more markers were designed and screened for polymorphism based on the BAC clone sequences of the two contigs. Among the numerous markers I designed, only 2 SSLP and 5 Single Nucleotide Polymorphism (SNP) markers showed polymorphism between AB and WIK, and could be used for mapping (Table 2.4). The nearest north marker SSLP-N6 on BAC zC196P10 showed only 1 recombinant, corresponding to 0.02cM, whereas the nearest south marker SSLP-S18 located on BAC zC113G11 showed 27 recombinants. Thus, the *udu* gene was mapped within a 3-BAC overlapping region, zC196P10, zK7E18 and zC113G11 (Figure 4.11). To test if one of the 4 predicted genes in BAC zC196P10 was *udu* gene, I sequenced the RT-PCR products of these 4 genes to identify the mutation by comparing *udu*^{-/-} and wild type sequences. DNA sequencing analysis showed that a point mutation (T to A) of *udu*^{sq1zl} existed in Ensembl Predicted Gene ENSDARG00000005867, which appeared to be a novel gene. The other allele, *udu*^{tu24} also had a point mutation (T to A) in a different site of Ensembl Gene ENSDARG00000005867 (Figure 4.12). By using 5' and 3' RACE, I determined that the full-length cDNA sequence of ENSDARG00000005867 was 6,787 base pairs, comprising 31 exons, and 30.64 kb of genomic sequence (Figure 4.11 and 4.13). The open reading frame started from nucleotide 91 (on exon2) and ended at nucleotide 6258 (on exon31), encoding a 2,055 amino acid (aa) protein. The point mutation in *udu*^{tu24} and *udu*^{sq1zl} occurred at T1461 (exon12) and T2976 (exon21), respectively, both of which result in premature stop codons (Figure 4.11).

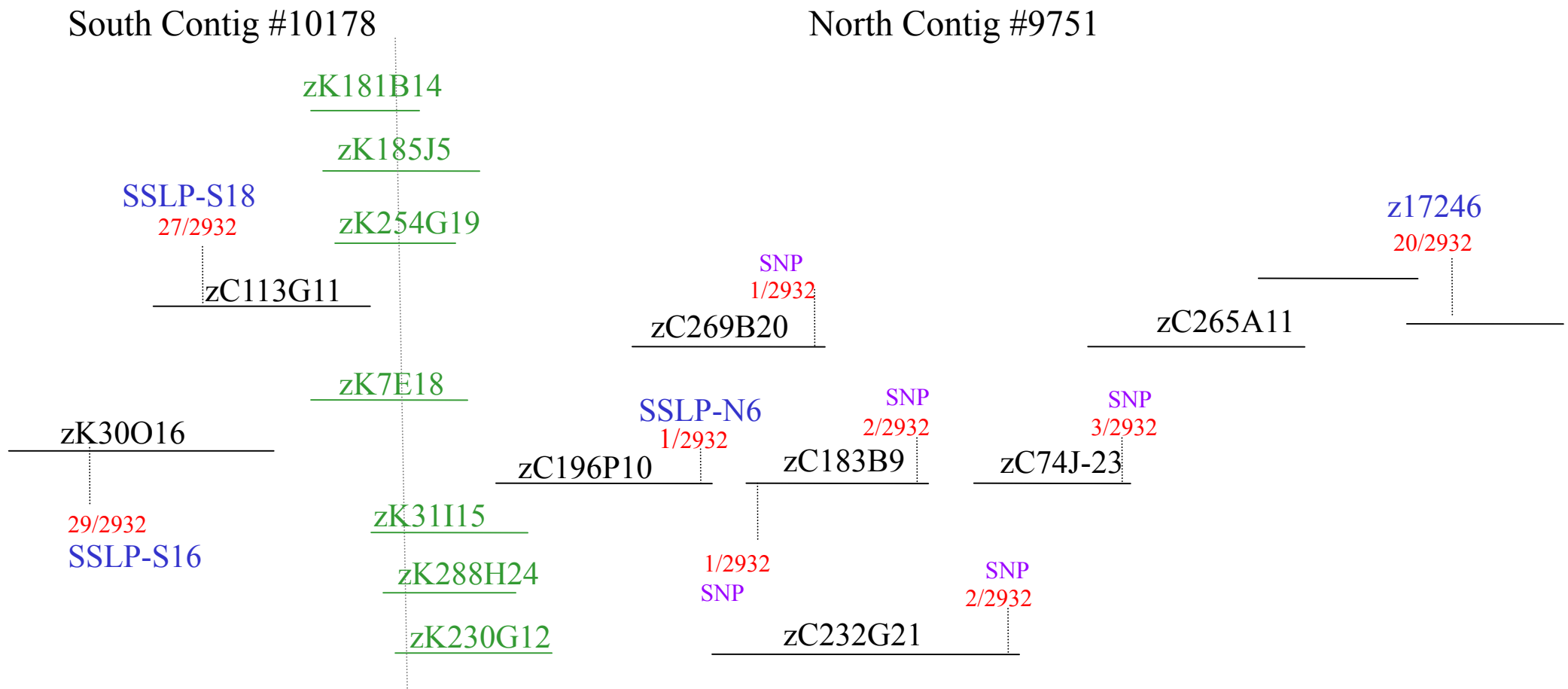


Figure 4.10 Alignment of North Contig #9751 and South Contig #10178. Each contig consists of a series of BAC clones aligned together. The seven green BAC clones, in which one end overlaps with North Contig #9751, and the other end overlaps with South Contig #10178, bridge the North and South Contigs. The SSLP and SNP markers as well as the corresponding recombinant numbers out of 2,932 embryos are labeled in the appropriate position of the BAC clones.

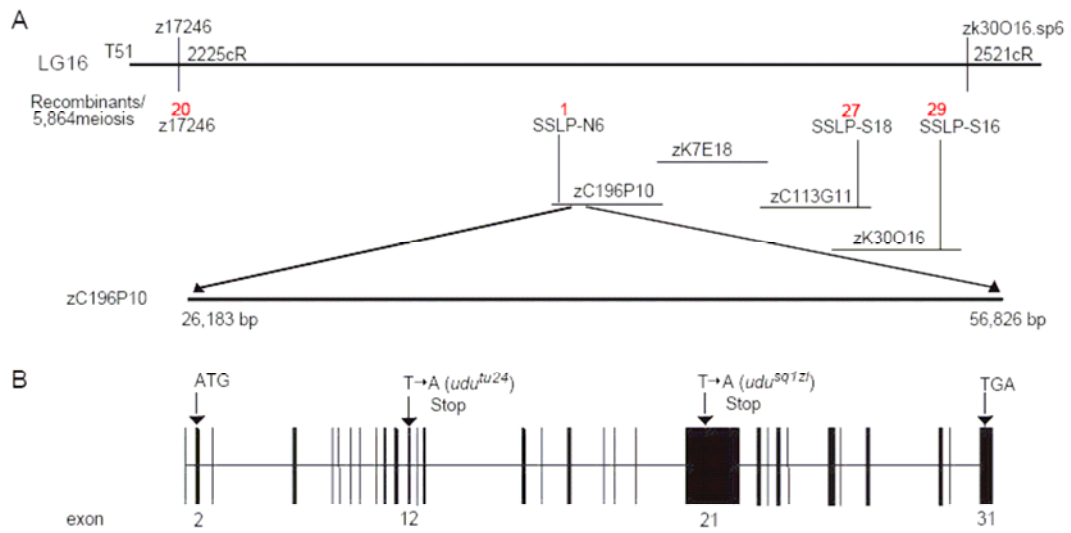


Figure 4.11 Positional cloning and gene structure of *udu* gene. (A) The *udu* gene is mapped to LG16 within the region covered by three BACs, zC196P10, zK7E18 and zC113G11. The number in red represents the number of the recombinants over 5,864 meiosis events for each SSLP marker. Sequence analysis confirms that the *udu* mutation is situated in the BAC zC196P10. (B) The *udu* gene consists of 31 exons (solid box) and encodes a protein of 2055 aa. Both *udu^{tu24}* and *udu^{sq1zl}* harbor a nonsense mutation in the exon 12 and 21, respectively.

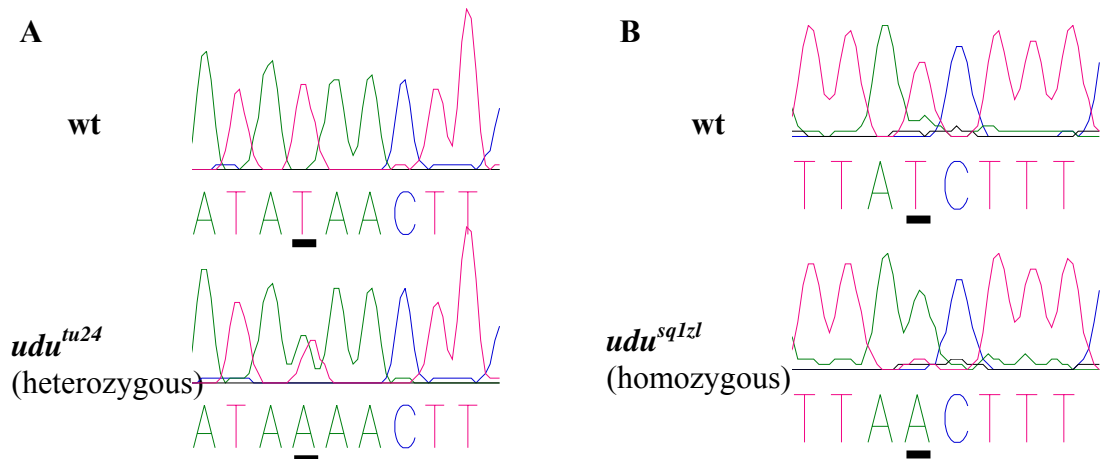


Figure 4.12 The nonsense mutation in Ensemble Gene ENSDARG00000005867 (*udu* gene) in *udu^{tu24}* and *udu^{sq1zl}* mutants. (A) Sequence comparison of Ensemble Gene ENSDARG00000005867 RT-PCR products from wild type and *udu^{tu24}* heterozygous mutant around the point mutation site. (B) Sequence comparison of Ensemble Gene ENSDARG00000005867 RT-PCR products from wild type and *udu^{sq1zl}* homozygous mutants around the point mutation site.

>udu cdna.seq

ACACCCGCGCTTTTGTGTGAAGCGGCGGGCTTAATAGAAAATACCGATGGCTGCAGACATACGTTCTGGGCTCAGAGA
CAGATTGAACATGGGATGGAAACGCAAGTCTTCTTCTCCAGAACCACAACCAAATCTTGTCAAATACCAAAGAGGGAAT
CCCTCAGCAGATCTCCTAGCTCATGGAAGAGGAAGGCCTTACACCCAGTAAAACAAAGAGCTGGACCTCCATTCAGTCC
CTTCTCCAGACAGGCATGTTGATCAGTGCAATGGCCAGGAGAAGATGTCCAGCGCAGGTGATGTTGAAGATGACAGTGA
CTGTATCCAGTCTCTACTCCAGTTTCATCCCTTTGCGGTGAGAAGAGGATGCGGAGCTGGGTCTGGTCACTGTTGG
ATGAGGACAGATGTAAGGGGAGGAATGGCTGAAGAAACGGAATGGAGTGAATATAAAGAAGAATGGAATAAATCAGACA
GAAGGAGAGATCCCTCAGAAAGAGGATGGAGATGTGGAGAAGACTATGGAACAGCTAAGTGAAGAAGATGAGAATGAGGA
AGAGCTCAGGAAGCTGGACAGAGATTTAACTCAAACTCAAAAACTCAACCTCTCTCTATCAATGTTGTAACATCA
TCCATGAGGTGGTAACCAATGAGCATGTTGTGGCCATGATGAAAGCTGCCATAAAAGAGACACAAGCATGCCATGTTT
GAGCTAAAATGACTCGTTCTAAGCTGAAGGAAGCTGTTGAAAAAGGGTGGGCATGGGAAAAGTGAACATCTCACC
AAAGAAGGCAAATGACATTAAGCCACCTCAATTTGTGGACATTCCACTGCAAGAAGAGGAGGACTCCTCAGATGAAGAGT
ATTGTCTGATGAAGACGAGGAAGATGAAACAGCTGAGGAGACGTTTTTGGAGAGTGTGTTGAAAGCACATCCTCCTCA
CCCCGCGGCATCAGACGTTTTCTTCTCAAACGCTCCCCATTGTGATGATGCCAGCAACAGCCCCAGACTGAAGCCAG
GCTGGCCCGCACTTGAGGGTTCGAGGCAGTGCCTATGGGTCCCTTGCCTCTCTCAATCTGTGGCCTTTCACGCT
CTCTTAAGACCTGGACCTTTCATCGAGAAACTCCATGTGTGGATAAAGAAGTGAACAAAGTCTCTCTGATGAGGAG
CCTTATCAGGCTCTCAGTAGTGGTGGAGCAGGGGAGCCAGACGACAGTCTAGTAGCTTGTGAACTCGGTCTAAGCGTCC
ATTGCGGGACGTCCTCTTGTATCAGCTGGAGGCTGAGCTCCGTGCGCCAGACATCAGCCAGATATGTATGATAATGTCT
CCACACCAGAGGACCGTGAATGGACCCAGTGGCTGCAAGGACTCATGACATCTCATCTGGACAACGACGAAGAAGCTGAT
GAAGATGACGACCCGAATATACTTCTTAGATGATTTAGATGAGCCAGATTTGGAGGATATCGAAATGATCGTGTGT
TCGTATTACAAAGAAGGAAGTCAATGAGCTCATGGAAGAGCTGTTTGGAGAGCTTTCATGATGAGTTGGCAGCCAATGAAC
CAGATGACGAAGGTCATGATGAAGATGAGGAGCGTGAAGAGGAGGCTAATGACACTCCACAATTCATATGTCCTCAAGCT
ATTAGGTTTGGAGGAGCCGCTGGCTCACATGTTGACAGCATGCAGGCGGACAGTTAGAGAGCAGCTGGATGCTTTACAGCA
GCGGCGAGAAAACAGGTCGACTACCCAGCATTCATCTGGGCTGGCATGGTTTTTGTGCAGCCAGCTGCCCTCTAG
TTGTACACCTGCACAGAGGATACAGCTGCAACAGCAAATACAGCAACATGTCCAGTTACTGACCAGGTCAGTATGCTG
TGTGACCACGTTGGGGCACTACAACTGAAGCTCAAACACCAAACATTTCTTGGGGGAGTTGCTGTCAATTTGCAGAGCG
GGCTGAGGATGAAAGATCAGCAGTGAATCTGGGTTTTAAAGTGTATTTAGGGTGTGTAATTTGCTTTCGTCATTA
TGTGGAGGAGGTTAAGCAAAGTCTTCTCTTTCGTGTCTTCTCCAAACCCAAACCGGCATCACTCAGTTCATTGCTAC
CCGTTGCTTCTGCTGGACTTGCATGGTTGTTGCGCACCCGCTCTGTCTTCTGTACCCAGAAGTCTTCCACATTGCAG
TCTGGATCCAGCCCTGCATCCTTCCCGCAGCAAACATTATACAGCAAAGGAGAAGACGGTTTGTAGTCTGGGTTTAA
AGCACTTCGCACAAAACAGAGTTCATATCAACTGATTAGCCGATATCTGATTCCGCCCCAAGCGTCAGGAGCAACTGCGT
ATGCGAGTGAAGGACATGGTATCCCCAAATACCCACACAATATCATCAAGTATTACTGCCAGAATCATGTGGTTCTCCTC
TTTGCCGGTGGTGTGCAACCTGTGGTGCATGGAGAGGAGCGCCCTCCTGTGGAGAGAGAACAGGAAGTCAATGCCAACT
GGCTAAAGAAAAGCTTACCATTGATCCAGAAGTCAATTTGCCAGAGCGATTTAACGATGACTTCCACCACGAAATCTGCT
AGCCTTCCCTTCCCTAAAGAAACAGCTACCCACAGTTCCTCCCTAAAGGTCTCTCTCTGCGTTTTGCACCCATCACAAGT
GGCAAGTCGCCCTTCCAGCCAAATCTCGAATCTGCGTGTCTTTACTAACCGTACACTCGCACCGTTAGCTAAAGCTC
CATCGTGTCCACAGGTACAGGACATTTACTGACCAATATCTCCACACCAGTACTATTACTAGCCAAAGCGCCTAGCACT
CCTATAAATGGGGTATTTCCATTAGTCCATCCCTCTTTGACCCAGCCATGGGACAGTCCCACTAAACGCTTCCATATC
TATTAATTCATATATCTTCTCCAGAATGGGTGCAAGTAATCCAGCACACCTTCTGCGAATTTACCCCTCTGTAG
TTCAGAAACCCCAATGTGACGCTCTCTACTTAGTACTGGACAGTCAAGACCCGTGGCGTGCAGCAACAGACATCAGAC
AAACACAAGAAGCGTACCATGGCTAGAAAAGTGGCCCTTTGAGACCAGCCCTCAGCTGCCCGACTGCTGCCCTTTC
TTCTGGGAGTATTGGAACATAAGCAACTCTGGCATAATTATAGATCAGCAAATATCCTTGAATGTCCACACAACCTTC
AATCAGATAATGTTATAGTTATCAAAGCCATGAAAATGTCAACACACACAGAACGGTCCCTTCTGTCTCCGGATCTG
GTTGTACAGTTAGTTCCTCAAACACAGGTTGCTGAAAACACCACAAGTCCCTCCCTAGAAAGACAACAACGAGATCAGA
CGTTTCACAACTGCAAAAGACATCCCTCAGTTCAATCTAGTGGCGAGAATGGTCAAAGGACTGATTTTTCTCCTCAGA
CCGAGCACCAGCTGCAGTGGACAGTTCTCAGTTTGTGCTGGTTGACTGTTTCTCTACTGGGCTCCTCAATTCCTA
CTTCTGCCCCAGGACTCCCTTGTCTGAAACCACTGCTTCACTTCTTCTGAAGGCACATTGCAAAATCTTTCGAGCA
GACCTCTCATTTAGACATTTCTACTACCTCAACAGCCCTGAAGAAGTCAAGAGACTGAGGTACATTTGAACAACCCAA
CCACATCATTTGCCAGTTAGCAGAGAGGAAGATGGAGAAAGACAGGAGGTGGATGAGGAAATGGTTGGAGACAGATGGGAA
GAGGAGATGGCCAGTGTCTTGTGTTGGTAGTCTCTTTGGCGCTTCTGAGTCTCTGAGTCTCTGACTCCAGCCAGCA
TGCAAGTATGGACAGTGGCAGTGTGCCATGGTGAGGTTGGAGATGGAAGATGGAGAGCTTCTTCTGTACTCAGCCT

CCGCAACACAGGAAACACCGGATGTGCACAAACACAGCAGCGGAGATGAGAAAGAGCAACAGTCCAGTGGAGGAGAGAAG
 CAGAACAGTGGGAATGAGGAGGGACGGGCTGAGGAGAGCGAGAGTAGGAAAAGATGAAGCGCAGGATGAAGATAAAGGAGG
 AGAAAAGAACGAGGATGGAGAAGGGGACGGAAATCGGGACGAGGGTGGAAGCGGTGATAAAGGAAGGGAGGAGAAGGATG
 GAGATGGAGAGAAAGATGGAGATGGAGAGCGAGATGAGGAAGAGGAGGATTTCCGATGACCTCACACAGGATGAAGATGAG
 GAGGAAGTGTATCGGCATCTGAGGAATCCGTGCTGTCTGTTCCAGAACTTCAGGAGACGATGGAGAAGTTGACCTG
 GCTGGCATCAGAGAGGAGACTGTGCAGAGAGGGTGACTCAGAGGAGGACAATTCACCCACGTCCCCAACATCCCCGACTT
 CCCCCAATCCCAGAACTCCCCAGCATCGCAGAATTTCTCAGGAAGAGAACTCGGAGGATGAGGATGATGGGGCGATGAAG
 GGTGATGAGCTGGAAGCAGGGGAGGGAGAAGGCCAAAAGCTTCTGAGGGGGACGCCACGCGGGTGATGATCCTCCACA
 GATCAGCGAGAAAGTAGGAGGCCGTGGAAGAGGTCGTGGTGCCTCTCTCCGCGCAGTTTAAAACGTGGGCGACGTCAGG
 AACGAGGCAGTAAAGATGCCTCAAAGCTGCTCCTGCTGTACGATGACCACATCTTGATAATGACCCAATGAGAGAAAGC
 AAAGACATGGCTTACGCACAGGCTTATCTCAACAGGGTACGTGAGGCTTTACAAGATGTCCAGGAAAAGTGGAGGAGTT
 TTTAGGCTGCTTTATGAGTTTGACCAAGCCGAGAGAGCCACAGTGTTATAGAGTTGTTTGCCAGCTTAAACAGCTGC
 TCAAGGACTGGCCGAGCTGCTCAAGGACTTTGCTGCTTTCCTTTTGCCGAACAAGCGCTGGAGTGTGGACTGTTTGAG
 GAGCAGCAGGCCCTTTGAGAGGAGTCGGCGGTTTCTGCGTCAGCTGGAGATCAGTTTTGGGGAAAATCCTTCTCATTATCA
 GAAGATTGTCAGAGCCCTGCAGAGTGGAAGTCTCTCAGTCTGCTGGCATTGAAGAGCTGAAAACACAGATGGCCACTC
 TTCTGAAGGGTCACACACACCTTACGGGAGAGTTTGGATGTTTTTTGATGAAATGCGTCCACCACCAGCAGCTCCAGGC
 CAGTTTGAAGAGGCTGTTTGGCCAGAGGATGTGGCCACTGGGACAGATGGAGAAGCAGGCGTGAGTGTGACCTCTAGAGG
 AGGTGTATGGGGAGGATTTGAGGAGGTCACGCTCCCCGATCTGGATGAGGATGAAGAGTACACAAGATCAGACAGATAA
 GCAGCAGAAGCAAGAGGAGAAAAGAAGTGCACACATACAAGGACTGTGATTTGGCCTGAGAAAAGATGTTCTGTTCTGT
 CATGACTCCGTTTCATGATGCCAAACATCGAAGGCATAAGAGAAAAGGATGCTTGCCTGTGAGAGCAACAAGGCTGCTAA
 TGGCTCAAAGGTGCTGAAGGGTCGTGATTACAGCATTTCATCTGCCGATGCACAGTCTGAAAGAGGAGGAGGAAAAGG
 AAGAGGAAAAGAGTGTGGGAGAGGATGGAGAGGCAGAGAAAGAGCTTAAAGACGAGACTTGCAGTGGAGCTAACAGTCCA
 CATCATGATGGGGAAGGGTCTGTGTGGGAGAGAGAAGAGAGGCCACTTCTCCATTCCAGAGGAGCAAAACACACATAA
 CCAAGATGATGAAGAAAAAATGAAGAGGAGAACCACCATGAAGAACCAGAGAAGCACAGCCGAGATGAAGAGGATTCAG
 CTGAATCTGGACAGACAGAAGCCGCTCAGCAGAGCTCACTGAGCCAGCCTTAGACGCACCCGTTGTGCAAAAAACATC
 TCCCTCACACCCACTGGAGAGAGAGTATCCTGTGGACCAGGGAGGCTGATCGAGTATCCTTACCACCTGTGAGCAGCA
 AGGAGCCAGTCTGAGCACATTCAGGCCGTGTCGAGCAGCTTGCAACAAAACAGCCAGCGAGGTTTCAAGGAGATTTT
 GGGATTTGATGCGTCTGTTCCACACGTCAGCTTCTCAGGCCAGTTCAGAGGACGAGGCTGCAGAGCAGCAGTCGGCCACT
 GATGAAGAGCAGGACTGAACCTGCCGTGACTGCTTCAATAAAAAATACTTATGCAGTTTTCTTACACTGACACCTGC
 CAAAGACGTGTTTAAAGCATGGTGGAAAAAAGGTTCTGTGGCCTCCTTTTAAACATGTGAAGTATAAATTCATTATATG
 AAGGTGCTATCCGTCACGTTCTAAACACAAAACCAACATAATTATGAAGAAATGTAGCACAAACTGCTCCATTTTATCC
 CTGATTATTGTATTGTAATGGACAAATGACAGGCTCTCACTTAGCACAAAATGAGATGTTTGATAGCAGAGAAATGTA
 GAGCACTAACAGCATATTTCTCACCTCCATGGTTTCTGACAGGTTGATTGTATATTTCTGTGAATATGTGAACATATGGCA
 TGTACAGTATTTTTATATCAGGGTGGTTTTGTTGTTTTTATTTTGCTTCAGATGTAGTTTTGAGAATGGCGCACAGTTG
 TTGGAAATCCAAATAATAAAAATGACTATTTATCCCCGAAAAAAAAAAAAAAAAAAAAAAAAAAAAAAAAA

Figure 4.13 *udu* cDNA sequence.

4.1.2.2 Confirmation of identity of the *udu* gene by cRNA rescue and morpholino knockdown

To investigate if the *udu* mutant phenotype was indeed caused by mutation in the Ensembl gene ENSDARG00000005867, *in vitro* synthesized wild type ENSDARG00000005867 cRNA was injected into one-cell stage *udu*^{-/-} mutant embryos. Examination of the *band3* expression by WISH and red blood cell number by O-dianisidine staining showed that primitive erythropoiesis was restored in 59 (92%) out of the 64 injected *udu*^{-/-} mutant embryos (Figure 4.14 and Table 4.1). In contrast, the mutant *udu-T2976A* cRNA which carries the point mutation in *udu*^{sq1zl} mutant failed to do so (Figure 4.14 and Table 4.1). I then carried out a second experiment, in which the Ensembl gene ENSDARG00000005867 expression was knocked down by the antisense morpholino oligonucleotides (MO) approach. Two *udu* MOs, MO-*udu*-1 and MO-*udu*-2, which specifically target the splice junction of the Ensembl gene ENSDARG00000005867, were synthesized and injected into the one-cell stage wild type embryos. WISH of *band3* and *βe1-globin* showed that the embryos injected with either MO-*udu*-1 or MO-*udu*-2 mimicked the *udu*^{-/-} mutant phenotype whereas the control MO had no effect (Figure 4.14). Taken together, these data demonstrate that the *udu* mutant phenotype is caused by loss-of-function of the ENSDARG00000005867 gene (herein referred as the *udu* gene).

4.1.3 Functional study of *udu* gene

4.1.3.1 Expression pattern of *udu*

WISH showed that the *udu* transcript was detected as early as the one-cell stage in wild type zebrafish embryos (Figure 4.15). The maternal *udu* mRNA retained robust

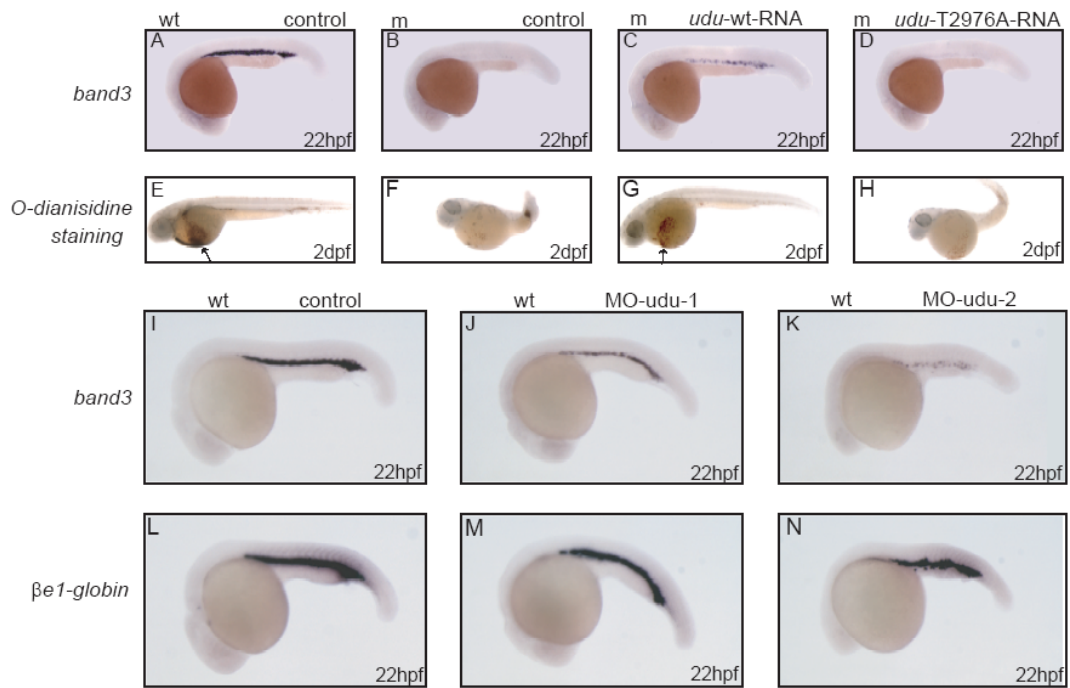


Figure 4.14 Confirmation of the *udu* gene by cRNA rescue and morpholino knockdown. (A-D) WISH of *band3* in the 22hpf wild type embryo (A), *udu*^{-/-} embryo (B), *udu*^{-/-} embryo injected with in vitro synthesized *udu*-wt RNA (C), and *udu*^{-/-} embryo injected with in vitro synthesized *udu*-T2976A RNA (D). (E-H) *o*-dianisidine staining of 2dpf wild type embryo (E), *udu*^{-/-} embryo (F), *udu*^{-/-} embryo injected with in vitro synthesized *udu*-wt RNA (G), and *udu*^{-/-} embryo injected with in vitro synthesized *udu*-T2976A RNA (H). (I-N) *band3* (I, J and K) and *βe1-globin* (L, M and N) expressions by WISH in the 22hpf control morphants (I and L), MO-*udu*-1 morphants (J and M) and MO-*udu*-2 morphants (K and N). In all the panels, embryos are in lateral views with anterior to the left.

Table 4.1. Rescue results

Injected RNA/ MO type		<i>udu</i> -wt	<i>udu</i> -T2976A	<i>udu</i> -ΔSANT-L	p53 MO	control MO
rescued mutant number/total mutant number	<i>o</i> -dianisidine staining	37/42	0/25	0/34	36/39	0/26
	<i>band3</i> expression	22/22	0/20	-	23/24	0/21
% Rescued		92%	0%	0%	94%	0%

expression during blastula stages and the expression was reduced at the onset of gastrulation (~6hpf). Around the time that segmentation started, the *udu* transcript, presumably the zygotic mRNA, began to re-appear in a ubiquitous manner, and was subsequently enriched in the CNS as well as the ICM from the 18-somite stage onwards. At 24hpf, *udu* mRNA was also detected in the anterior parts of kidney ducts.

Northern blot analysis showed that *udu* mRNA is expressed at all stages examined (1-8 cell stage, 6-8hpf, 12hpf, 24hpf, 3dpf, adult). *udu* mRNA was observed as a single transcript of approximately 7kb size, which corresponds to the size obtained by RACE (Figure 4.16).

To study the Udu protein expression, I generated anti-Udu-N and C-terminus rabbit serum. Western blotting analysis showed that the affinity purified antibodies were capable of recognizing untagged Udu-N-Antigen (residue 4-91aa) and Udu-C-Antigen (residue 1818-1941aa) respectively (Figure 4.17).

These anti-Udu polyclonal antibodies were also used to examine the *udu* protein expression in zebrafish by western blot as well as whole-mount immunohistochemistry staining. Unfortunately, the Udu antibodies did not work well with the whole fish embryos after many times of trying and protocols modification. This could be due to the low Udu protein expression in zebrafish and the relatively high background caused by ubiquitous expression. Therefore, I had to switch to detect the ectopically expressed Udu protein in 293T cells transfected with pcDNA3.1-*udu*-wt, pcDNA3.1-N-Flag-*udu*-wt and pcDNA3.1-C-HA-*udu*-wt respectively. Western blot results showed that both the Flag and HA monoclonal

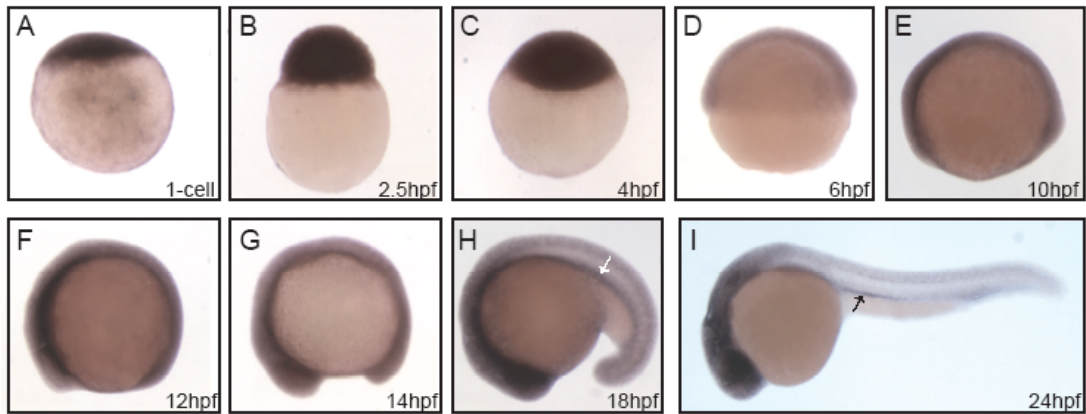


Figure 4.15 The temporal and spatial expressions of the *udu* gene during early zebrafish development. (A-I) Lateral views of WISH of *udu* in the one-cell (A), 2.5hpf (B), 4hpf (C), 6hpf (D), 10hpf (E), 12hpf (F), 14hpf (G), 18hpf (H), and 24hpf (I) embryos. White and black arrows indicate the ICM and the anterior region of kidney duct, respectively. Embryos in A to D are orientated with animal pole on top whereas embryos in E to I are orientated with anterior to the left.

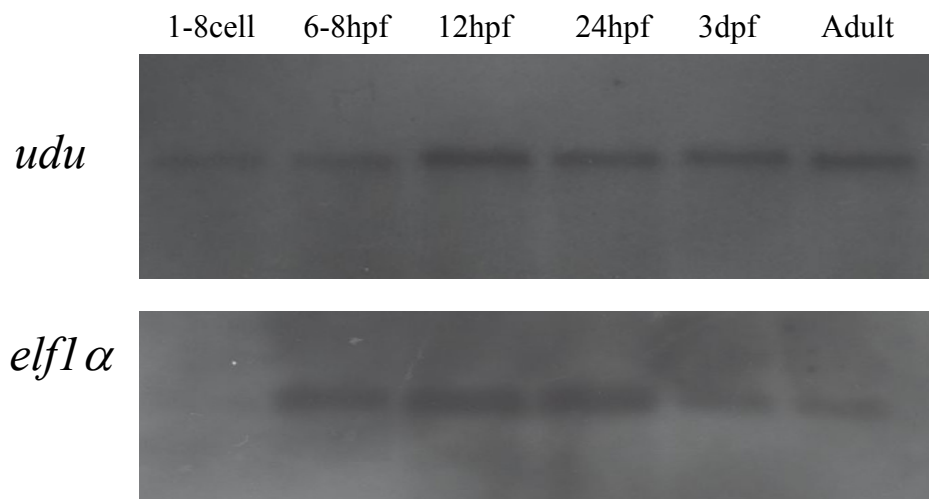


Figure 4.16 Northern blot analysis of *udu* mRNA expression at different stages of zebrafish (1-8 cell stage, 6-8hpf, 12hpf, 24hpf, 3dpf, adult). *udu* mRNA is observed as a single transcript approximately 7kb (upper panel). *elf1α* mRNA is detected as a loading control (lower panel).

antibodies could specifically detect the Flag or HA tagged Udu with a molecular weight ~250KD (Figure 4.18). Anti-Udu-C-Antigen antibodies not only detected the similar sized band of Udu, but also several smaller bands that may represent either degraded Udu protein or different isoforms of Udu (Figure 4.18). Further analysis is required to clarify this issue. The immunohistochemistry staining results of the transfected cells would be addressed in section 4.1.3.3.

4.1.3.2 Cell-autonomous erythroid defect in the *udu*^{-/-} mutant

From the temporal and spatial expressions of the *udu*, it is quite possible that Udu plays a cell-autonomous role during the primitive red blood cell development. To test this speculation, I performed cell transplantation experiment. Around 15-30 donor cells from the 3hpf *udu*^{-/-} mutant or sibling embryos pre-injected with rhodamine-dextran were transplanted into the same stage wild type host embryos. Contribution of the donor cells to the circulating blood cells in the host embryos was scored at around 30hpf by counting the number of the rhodamine-dextran labeled cells in the circulation under fluorescent microscope. As summarized in Table 4.2, when sibling donor cells were transplanted, about 42% (50/119) of the recipients had the rhodamine-dextran labeled donor cells in circulation, of which 20% (10/50) contained 10 to 30 circulating donor cells and 22% (11/50) had more than 30 circulating donor cells. In contrast, when the *udu*^{-/-} mutant cells were transplanted, only 26.7% (16/60) of the host embryos had the donor cells contributing to the blood circulation. More importantly, none of these embryos contained more than 10 circulating rhodamine-dextran labeled cells. Although non cell-autonomous effect is not excluded, the transplantation result strongly indicates that the *udu* gene can act cell-autonomously to affect development of the primitive red blood cell.

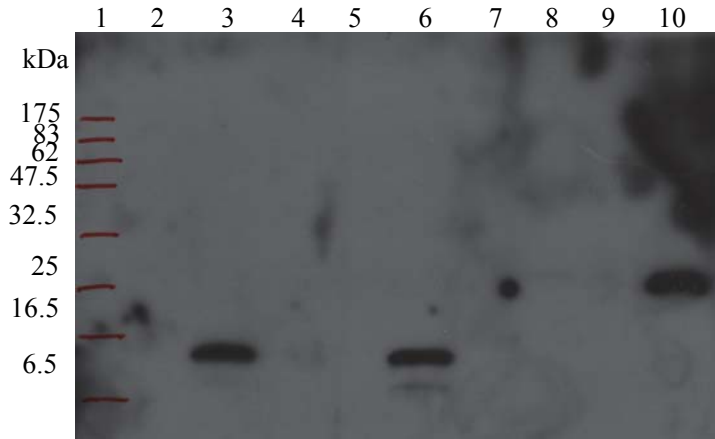


Figure 4.17 Western blot examination of purified anti-Udu-N and C-Antigen polyclonal antibodies by recognizing the untagged Udu-N-Antigen and Udu-C-Antigen. Lane 1 is the size standard marker; lane 2, 5 and 8 run GST protein; lane 3, 6 and 9 run untagged Udu-N-Antigen; lane 4, 7 and 10 run untagged Udu-C-Antigen. Lane 2-7 were detected by affinity purified anti-Udu-N-Antigen antibodies, whereas lane 8-10 were detected with purified anti-Udu-C-Antigen antibodies.

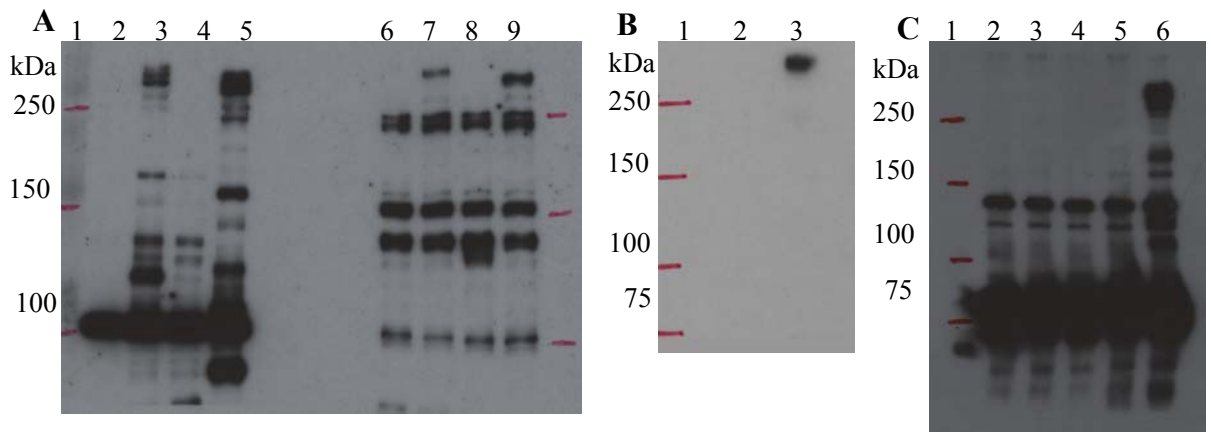


Figure 4.18 Western blot analysis of the ectopic expressed Udu protein in 293T cells. (A) anti-Udu-C-Antigen antibody (lane2-5) and anti-Udu-N-Antigen antibody (lane6-9) to detect Udu proteins in 293T cells transfected with pcDNA3.1(lane2,6), pcDNA3.1-*udu*-wt(lane3,7), pcDNA3.1-*udu*-T2976A(lane4,8) and pcDNA3.1-*udu*- Δ SANT-L(lane5,9). (B) anti-flag monoclonal antibody to detect Udu proteins in 293T cells transfected with pcDNA3.1(lane2), pcDNA3.1-N-Flag-*udu*-wt(lane3). (C) anti-HA monoclonal antibody to detect Udu proteins in 293T cells transfected with pcDNA3.1(lane2), pcDNA3.1-*udu*-wt(lane3), pcDNA3.1-*udu*-T2976A(lane4) and pcDNA3.1-C-HA-*udu*-wt(lane6). In A-C, lane1 is the size standard marker.

Table 4.2 Summary of cell transplantation analysis

Donor genotype	The total number of hosts	The number (percentage) of hosts with donor-derived tissue				
		Muscle	Blood			
			Total	>30 blood cells	11-30 blood cells	1-10 blood cells
sibling	119	86 (72.3%)	50 (42%)	11 (9.2%)	10 (8.4%)	29 (24.4%)
<i>udu</i> ^{-/-}	60	46 (76.7%)	16 (26.7%)	0 (0%)	0 (0%)	16 (26.7%)

4.1.3.3 The *udu* gene encodes a putative transcriptional modulator

Blast search of public databases revealed that the Udu protein had the highest homology to human and mouse GON4L (Kuryshv et al., 2006) (Figure 4.19). Sequence alignment showed that there were several highly conserved regions (Figure 4.19 and 4.20A). The first three conserved regions (CR-1, CR-2 and CR-3) shared no obvious similarity to any of the known domains. The fourth and fifth (from aa 1538 to 1740), either of which were predicted to consist of four α -helices, were similar to the PAH repeats found in SIN3 proteins, and thus were designated as PAH-like (PAH-L) 1 and 2 domain (Figure 4.20A). Finally, the solution structure (IUG2_A) of the last conserved region (SANT-L) of the mouse Udu homologue GON4L (www.ebi.ac.uk/thornton-srv/databases/cgi-bin/pdbsum/GetPage.pl?pdbcode=1ug2) revealed that this conserved region resembled the SANT domain found in several chromatin-remodeling molecules (Figure 4.20A and B), suggesting that the Udu protein may be involved in transcription regulation.

To test this possibility, I carried out rescue experiments with the truncated *udu*- Δ SANT-L RNA, in which the three α -helices (from aa 1963 to 2031) of the SANT-L domain of the Udu protein was deleted (Table 2.6 and Figure 2.1B). As shown in Figure 4.20, the red blood cell development was restored in the mutant embryos injected with the *udu*-wt RNA (Figure 4.20E). However, the truncated *udu*- Δ SANT-L RNA failed to do so (Figure 4.20F), demonstrating that the SANT-L domain is critical for the function of the Udu protein. I also transfected the *udu* cDNA (pcDNA3.1-*udu*-wt) into COS7 cells to examine the sub-cellular localization of the Udu protein. Immunohistochemistry staining showed that the Udu protein was

predominantly localized in the nucleus (Figure 4.20G-I). Taken together, these results strongly indicate that the Udu protein may function as a regulator of transcription.

4.1.3.4 The *udu*^{-/-} erythroid defect is mediated by a *p53*-dependent pathway

To identify potential target genes perturbed in *udu* mutant, I performed microarray analysis. Result from two sets of independent experiments showed that expressions of 87 and 57 genes were down- and up-regulated, respectively, with 2-fold and above differences in the *udu*^{-/-} mutant embryos (Table 4.3 and 4.4). Interestingly, several up-regulated genes, including *p53*, *fos*, *mdm2*, *gadd45a1*, *caspase 8*, and *tdag51*, are known to be involved in cell cycle control and apoptosis (Table 4.4). Their up-regulation in the *udu*^{-/-} mutant embryos was further confirmed by Semi-quantitative RT-PCR (Figure 4.21). Considering the G2/M cell cycle arrest of the *udu*^{-/-} erythroid cells, I focused on *p53* and its downstream target *gadd45a1*. WISH showed that in the 24hpf *udu*^{-/-} mutant embryos the expression levels of *p53* (Figure 4.22A and B) and *gadd45a1* (Figure 4.22I and J), especially *p53*, were significantly elevated in the CNS and the ICM, where the endogenous *udu* expression is normally enriched at this stage, suggesting that the G2/M cell cycle arrest of the *udu*^{-/-} erythroid cells is possibly caused by abnormal activation of the *p53* pathway. To test this possibility, I knocked down the p53 protein in the *udu*^{-/-} mutant embryos by the *p53* MO. The erythrocyte-deficient phenotype was rescued in the *udu*^{-/-} mutant embryos injected with the p53 MO but not control MO (Figure 4.22C-H). As anticipated, elevated *gadd45a1* expression was no longer detected in these p53 morphant mutants (Figure 4.22I-K). These data strongly suggest that loss-of-function mutation in the *udu* gene leads to activation of the *p53* pathway, resulting in red blood cell hypoplasia.

```

zebrafish Udu      1      10      20      30
..MGWKKK.....SSSPFPDNLVKLKRRLSRSP.....S..WKKKASTP.....
human_GON4L      M L P C K K R R T V T S L Q H K G N Q E N N V D L E S A V K P E D Q V K D L S S V S L S W D P H G R V A G F E V Q S L Q D A G N Q L G M E D T S L S S G M L Q T N T V N P I
mouse_GON4L      M L P C K K R R L S V T S S Q Q D D Q E G D D L D L E A A V K P E D Q V K D L S S V S L S W G Q Q D S A V C P E G L S M Q D G D D Q L R A E G L S L S N K M L A Q H V N L A V

          40      50      60      70      80      90      100     110
zebrafish Udu      . . . . . S K T K S W T I Q S L S P D R E V D Q C N G Q E K M S S A G . . . . . H V E D D S D C I Q S S T P V S S P L R S E D A E L G . L V I T V E D R C E G
human_GON4L      L E G V D V A I S Q G I T L P S L S F H P L N I H I G K G K L H A T C S K R K K M T L R P G P V T Q E D R C D H L T L K E P S G E P S E V K E B G K P Q M N S G G I P S L
mouse_GON4L      L E A V D V A V S Q E I P L P S L S S H S L P V H V D K G R L Q V S A S K K K R V V F T P G Q V T R E D R G D H P V P E E P S G E P A E A K T E G G E L E L R S G G V P L L

          120     130     140     150     160
zebrafish Udu      E E W L K K R G N V I K K N G I N Q T E G E I P K . . . . E D G V E K T M P Q . . . . . L S P E D N E E L R . . . . K
human_GON4L      P S G S Q A K P V S Q P R K S T O P D V C A S P Q E K P L R T L F H Q P E E I D G G L F I P M E Q D N R E S E K R R K K K K G T K R R K R D G R G Q E . G T L A Y D L K L D D M
mouse_GON4L      S S S S Q S A K P G A Q P R K S V O P D G S A F P Q D K P L G L V L R Q A E E M D G G L F I P T E Q D S E S D K K K K T K G T K R R K R D G K G L E Q G T M V Y D P K L D D M

          170     180     190     200     210     220     230     240     250
zebrafish Udu      L D R D T I L K S K L N I S S N V R N I T H E V V T N E H V V A M M K A A I K E T Q D M P F E P K M T R S K L K E V E K G V G M G N W N I S P I K K A N I K P P Q F V D I
human_GON4L      L D R T L E D G A Q H N I T A V N V R N I D H E V V T N E H V V A M M K A A I S E T E D M P F E P K M T R S K L K E V E K G V V I P T W N I S P I K K A S I K P P Q F V D I
mouse_GON4L      L D R T L E D G A Q H N I T A V N V R N I D H E V V T N E H V V A M M K A A I S E T E D M P L F E P K M T R S K L K E V E K G V V I P T W N I S P I K K A S I K P P Q F V D I

          260     270     280     290     300     310     320     330
zebrafish Udu      P L Q E E D S S D E E Y C P D E E E D E T A E E T F L E S D V E S T S S S P R C I R R . . . . . F P S Q T P P H C D D A S N S P R L K P R L A R H L R V A V P M G P P A P P
human_GON4L      H L E E D D S S D E E Y Q P D E E E D E T A E E S L L E S D V E S T A S S P R C A K K S R L R Q S S E M T E T D E E S G I L S E A E K V T P A I R H I S A V V P M G P P P P P
mouse_GON4L      H L E E D D S S D E E Y S P D E E E D E T A E E S L L E S D V E S T A S S P R C V K R S R L A L S S E V A E T D E E S G M L S E V E K A A T P A L R H I S A V V P M G P P P P P

          340     350     360     370     380     390     400     410     420
zebrafish Udu      P Q S C G L S R S L K T L D P E K H H A V D K E I E L S P L C M E Y Q A T S S G G A G E P D S L V A C R T R S K R P L R D V P I D Q L E A E L R A P D I T P D M Y D N V S P
human_GON4L      K P K Q T R D . . . . . S T M E K I H A V D E L A S S P V C M D S F O P M . . . . . D D S L I A F R T R S K M P L K D V P H G O L E A E L Q A P D I T P D M Y D . P N A
mouse_GON4L      K P K Q S R D . . . . . S V M E K I D A V D E L A S S P V C M D S F O P M . . . . . D D S L I A F R T R S K M P L K D V P H G O L E A E L Q A P D I T P D M Y D . P N A

          430     440     450     460     470     480     490     500
zebrafish Udu      D R E W T Q W L G L M T S H L D N E E A D D D D D P E Y N F L D L D E P D L D V R N D R A V R I T K K E V N G L M E E L F E E . . . . . H D S A A N E P D D G H
human_GON4L      D D E W K M H G C L M N D D V G N E E A D D D D D P E Y N F L D L D E P D E D R T D R A V R I T K K E V N G L M E E L F E E . . . . . Q D S G F S N M E D D G P
mouse_GON4L      D D E W K Q W L G L I N D D V E N E E A D D D D D P E Y N F L D L D E P D E D R T D R A V R I T K K E V N G L M E E L F E E V Q S V V P S K Q D E M G F S N M E D D G P

          510     520     530     540     550     560     570     580     590     600
zebrafish Udu      D E D E R E E E A N D T P Q F N V P Q A I R F E E P L A H M L T A C R T V R S Q L D A T Q Q R R E N Q V R T T Q H S S G P G M V F Q P S C P V V T P A Q Q I Q L Q Q Q I Q Q H
human_GON4L      E E E C V A E P R . . . . . P N F N T P Q A L R F E E P L A N L U N E Q H R T V K S L F E Q L K M K K S . A K Q L Q E V E K V P Q S E A H Q T L D L D P A Q R K R L Q Q Q M Q Q H
mouse_GON4L      E E E R A T E S R . . . . . P S F N T P Q A L R F E E P L A N L U N E R H R T V K S L L E Q L K M K K P S . V R Q Q P E V E K L K P Q S E A A H Q T L V L D P A Q R S R L Q Q Q M Q Q H

          610     620     630     640     650     660     670     680     690
zebrafish Udu      V O L L T Q S M I C D H V G A Q T L A Q T T K H I G I L L S F A R A E D E R S A V N L G K S V F R V C N L T S S I N L E E V K Q S P S L S L D P K P N R H S V H S V P
human_GON4L      V O L L T Q H L A T C N F N N P E A T T R I P L K L G T F A S S I A L H H Q Y N P K Q T L F O P C N L G A M Q L E E F S T H V S I D C S H K T V K K T A N E Y P
mouse_GON4L      V O L L T Q Y L L T T S N F N S S E A S T R V F L K I L G T F A S S I A L H Q Q N P R Q T L F O P C N W G A M R L E D F . T Q V S I D C S H K T . A K K T A S E P

          700     710     720     730     740     750     760     770     780
zebrafish Udu      L P A G L A W L F A T R S V F I Y F E L L E H C S I D P A L H S R S K H Y Y S G E D G L V L G L K H E A Q T E F F Y Q L I S R Y L I R P K R Q E Q R M R V K D M V S P K Y E
human_GON4L      C L E K Q V A W I L A S K V F M Y F E L L E V C S I K A K N E . Q D K I V F T A B D N L A L G L K H E E G T E F F N P L I S K Y L L T C N T A H Q T V R I R N L N M N R A S
mouse_GON4L      C L E K Q V A W I L A N K V F M Y F E L L E I C S I K A N N E . R D K I T T A B D N L A L G L K H E E G T E F F R P L I S K Y L V T C N T A H Q T V R I R N L N L N R A S

          790     800     810     820     830     840     850
zebrafish Udu      H N I I K V Y C Q N H V V P P P V V C K P V H G E E R P P V R E Q E V M P N W L K R S P L I O K S I C Q S . D L . T . M . S T . K S . . . . . A S L P F P K S T R
human_GON4L      D N I I K P Y K K T K Q L P V I G K C E E I Q P H Q W R P P I E R E H R P P F W L K A S L P S I O E E L R H M A D G A R E V G N M G T E I N S D R S L E K D N L E G S E S R
mouse_GON4L      N N V I K P Y K K T K Q L P V I V R C E E I Q P H Q W R P P I E R E H R P P F W L K A S L Q S I O E L R N I S E G A T E G S V T A E S S T Q H L Q A S P A L G D E R Q

          860     870     880     890     900     910     920     930     940
zebrafish Udu      Y P Q F L P K G L S T R H P S Q V A S P S Q P K S R I L R A F T N R T L A P I A K A P S C P T G T G H L L T N I S T P V L L L A Q A E S T P N G V F P L V H S . . . T P A H
human_GON4L      Y P L L L P K G V V L K K P . . V A T R F P R K A W R Q K R S S . . . V L P L L I Q P S P S L Q P S F N P G K T P A R S T H S E A P S K M V L R I P H I Q P A T V L Q T V P
mouse_GON4L      Y P L L L P K G V V L K K P . . G S K R F S R K A W R Q K R P L . . . V Q P L L I Q P S P S V Q P V F N P G K M A T W F T Q S E V P S N T V Q I P H I L Q P A A V L Q T L P

          950     960     970     980     990     1000    1010    1020    1030
zebrafish Udu      T V P L N A S Y P I N P H Y L S P E L G A S N P A H L P A N L P S V V Q K P Q C D V S L L S T G T V K T R G V Q Q Q T S D K H K R R T M A R K L A P L R P A P Q L P R L L S S G
human_GON4L      V P P L G V S G G E S P E S P A A L P A V P P . . E A R T S F L S E S C . . . . . T L L S A P V F K V M L P S L A P S K F R K P Y V R R P S K R R G V K A S P C M K A P V I
mouse_GON4L      F P S V G V R G E D G P E S P T S L P A M P C G S E A R T T F L S E T Q . . . . . S A P P S C S A P K L M L P S L A P S K F R K P Y V R R P S K R R G A K V S P C V K E A P I I

```

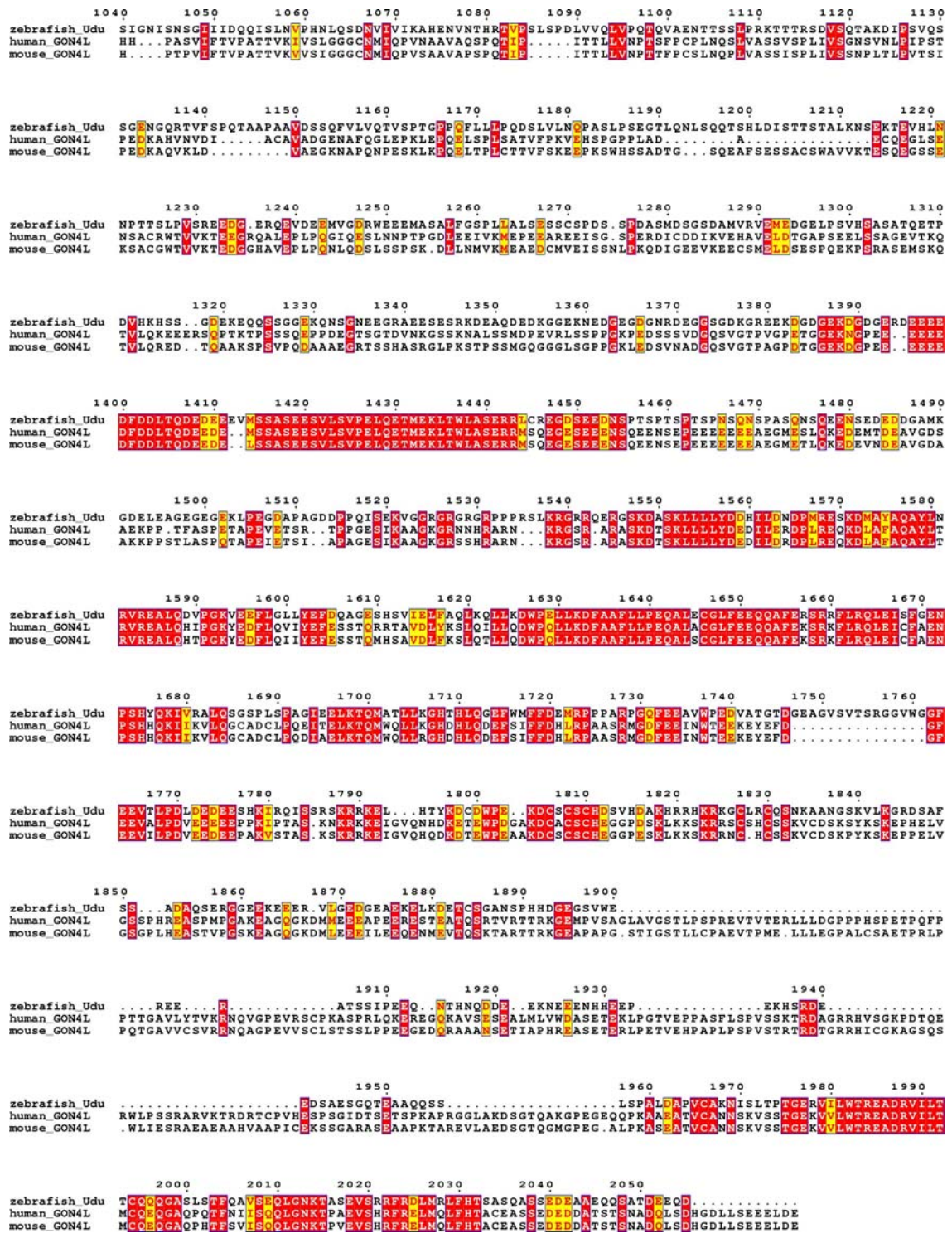


Figure 4.19 Sequence alignment of the zebrafish Udu, human and mouse GON4L proteins. Identical amino acids are labeled in red whereas homologous residues, which are scored if they are within a single group of neutral (A, C, G, P, S, T), hydrophobic (I, L, M, V), acidic (D, E, N, Q), basic (H, K, R), or aromatic (F, W, Y), are indicated in yellow.

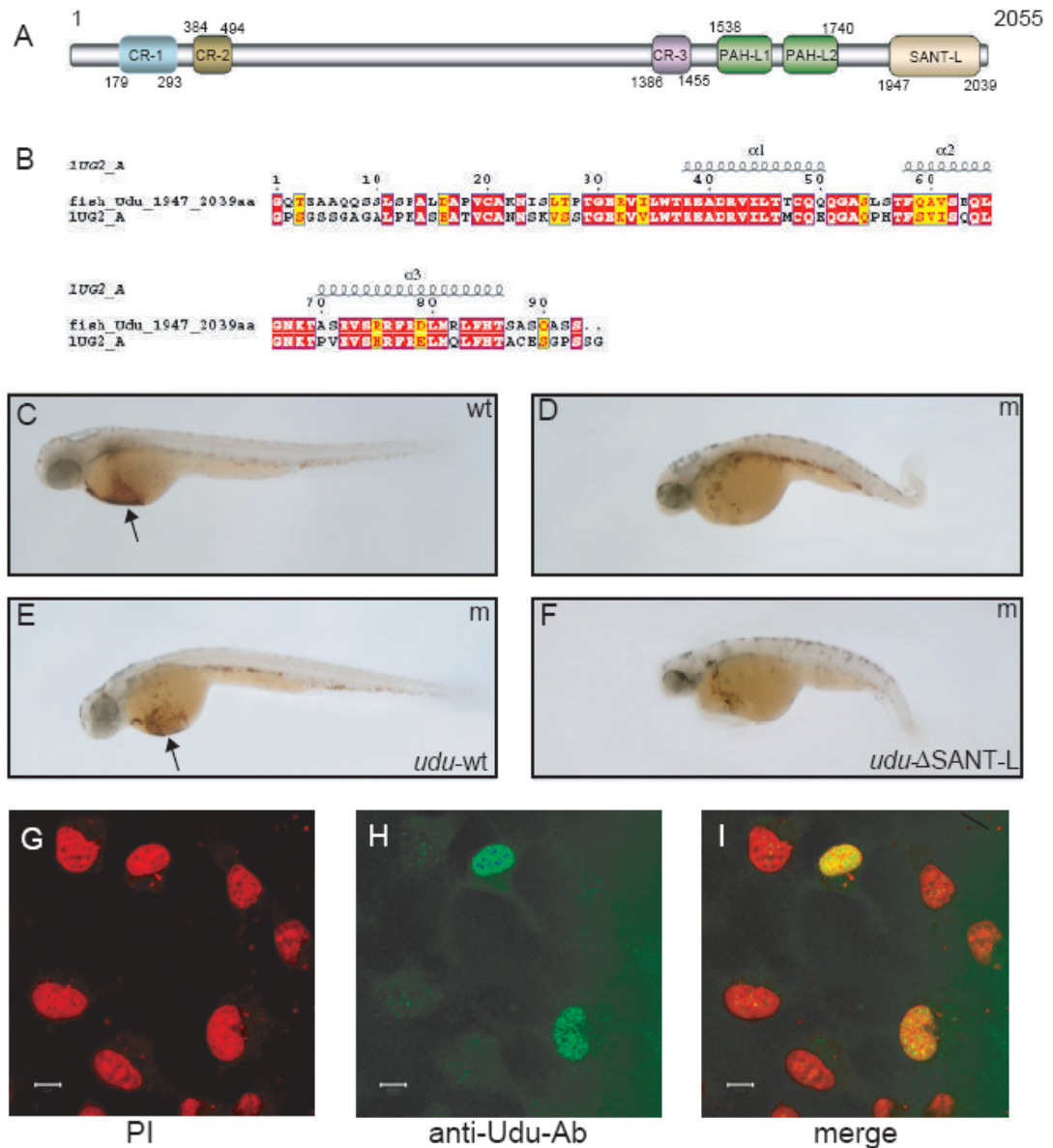


Figure 4.20 The Udu protein is a putative transcriptional modulator. (A) The Udu protein contains six conserved regions: CR-1, CR-2, CR-3, PAH-L1, PAH-L2 and SANT-L. (B) Protein sequence alignment of the SANT-L domain between zebrafish Udu (top, fish-Udu-1947-2039aa) and mouse Udu homologue GON4L (1UG2_A). (C-F) Lateral views of o-dianisidine staining of the 2dpf wild type (C), *udu*^{-/-} mutant embryos (D), the *udu*^{-/-} mutant embryo injected with *udu-wt* RNA (E), and the *udu*^{-/-} mutant embryo injected with *udu-ΔSANT-L* RNA (F). (G) Propidium Iodide (PI) staining of the pcDNA3.1-*udu-wt* transfected COS7 cells. (H). Immunohistochemistry staining of the pcDNA3.1-*udu-wt* transfected COS7 cells with the anti-Udu-C-Antigen polyclonal antibody. (I) Superimposed image of G and H. Arrows in C and E indicate o-dianisidine stained red blood cells. Scale bars in G-I represent 10μm.

Table 4.3 Summary of down-regulated genes in *udu*^{-/-} mutant

Affymetix gene ID	Gene name	Signal log ratio in 1st experiment	Signal log ratio in 2nd experiment
Dr.20971.1.S2_at	solute carrier family 4, anion exchanger, member 1	-6.6	-4.1
Dr.3027.1.S1_at	erythrocyte membrane protein band 4.1 (elliptocytosis 1, RH-linked)	-4.2	-2.1
Dr.16496.1.A1_at	---	-3.3	-1.1
Dr.10343.1.S1_at	ATPase, Na ⁺ /K ⁺ transporting, alpha 1a.2 polypeptide	-2.7	-2.9
Dr.450.1.S1_at	carbonic anhydrase	-2.4	-3.1
Dr.21393.1.A1_at	---	-2.2	-1.9
Dr.12602.1.S1_at	lysozyme	-2.1	-2.5
Dr.24764.1.S1_at	---	-2.1	-1.5
Dr.12386.2.S1_a_at	mesogenin 1	-1.9	-1.4
Dr.20010.14.S1_at	---	-1.8	-2.2
Dr.25422.1.S1_s_at	hemoglobin alpha embryonic-1	-1.8	-2.1
Dr.371.1.S1_at	zgc:85892	-1.8	-2
Dr.1450.1.S1_s_at	hemoglobin alpha embryonic-3	-1.8	-2
Dr.5372.1.S1_x_at	hairy-related 4	-1.8	-1.8
DrAffx.1.52.S1_at	ataxin 2-binding protein 1-like	-1.8	-1.7
Dr.5404.1.S1_at	calymmin	-1.7	-2
DrAffx.1.85.S1_s_at	hemoglobin beta embryonic-1	-1.7	-1.9
Dr.19402.1.A1_at	---	-1.7	-1.7
Dr.355.1.S1_at	GATA-binding protein 1	-1.7	-1.5
Dr.25683.10.S1_at	---	-1.6	-2.1
Dr.14667.1.S1_at	crystallin, beta B1	-1.6	-2.1
Dr.2166.1.S1_at	uroporphyrinogen decarboxylase	-1.6	-1.9
Dr.25729.1.S1_at	zgc:92724 /// zgc:86750	-1.6	-1.9
Dr.20143.1.S1_at	hairy-related 3	-1.6	-1.6
Dr.25060.3.A1_at	---	-1.6	-1.6
Dr.5434.1.S4_at	proteolipid protein 1a	-1.6	-1.5
Dr.4827.1.A1_at	leukocyte cell derived chemotaxin 1	-1.6	-1.4
Dr.12569.1.S1_at	Kruppel-like factor d	-1.5	-1.9
Dr.8180.1.S1_at	aminolevulinate, delta-, synthetase 2	-1.5	-1.9
Dr.24891.1.S1_at	---	-1.5	-1.6
Dr.14668.1.S1_at	GTP cyclohydrolase 1	-1.5	-1.6
Dr.8232.1.S1_at	hairy/enhancer-of-split related with YRPW motif 2	-1.5	-1.2
Dr.318.1.A1_at	achaete-scute complex-like 1b (Drosophila)	-1.4	-1.7
Dr.4160.1.A1_at	---	-1.4	-1.6
Dr.1837.1.A1_at	---	-1.4	-1.6
Dr.555.1.S1_at	neurogenin 1	-1.4	-1.6
Dr.10718.1.S1_at	neurogenic differentiation 4	-1.4	-1.6

Affymetix gene ID	Gene name	Signal log ratio in 1st experiment	Signal log ratio in 2nd experiment
Dr.7857.1.A1_at	---	-1.4	-1.2
Dr.3211.1.A1_at	---	-1.3	-1.9
Dr.4171.1.A1_at	phenylalanine hydroxylase	-1.3	-1.6
Dr.8072.1.S1_at	developing brain homeobox 1b	-1.3	-1.6
Dr.441.1.S1_at	sb:cb343	-1.3	-1.5
Dr.21808.1.A1_at	---	-1.3	-1.4
Dr.22360.1.A1_at	zgc:85890	-1.3	-1.3
Dr.11651.1.S1_at	MCM5 minichromosome maintenance deficient 5 (S. cerevisiae)	-1.3	-1.3
Dr.1050.1.S1_at	---	-1.3	-1.3
DrAffx.1.60.S1_at	pancreas specific transcription factor, 1a	-1.3	-1.3
DrAffx.2.19.S1_at	embryonic globin beta e3	-1.3	-1.1
Dr.15802.2.S1_a_at	---	-1.2	-2
Dr.5278.1.A1_at	Receptor PTP-like protein IA-2	-1.2	-1.7
Dr.3920.1.S1_at	oligodendrocyte lineage transcription factor 2	-1.2	-1.7
Dr.20958.1.S1_at	---	-1.2	-1.7
Dr.180.1.A1_at	cytochrome P450, family 26, subfamily b, polypeptide 1	-1.2	-1.6
Dr.10652.1.S1_at	spectrin, beta, erythrocytic	-1.2	-1.4
Dr.4833.6.S1_at	---	-1.2	-1.4
Dr.19463.1.S1_at	---	-1.2	-1.3
Dr.10336.1.S1_at	dopachrome tautomerase	-1.2	-1.2
Dr.2291.1.S1_at	MCM2 minichromosome maintenance deficient 2, mitotin (S. cerevisiae)	-1.2	-1.2
Dr.25187.1.S1_a_at	hairy-related 8a	-1.2	-1.2
Dr.3282.1.S1_at	endothelial differentiation, sphingolipid G-protein-coupled receptor, 1	-1.2	-1.1
Dr.9225.1.A1_at	---	-1.2	-1
Dr.518.1.A1_at	---	-1.1	-1.7
Dr.3407.1.A1_at	Transcribed locus, weakly similar to NP_034066.1 procollagen, type IX, alpha 3 [Mus musculus]	-1.1	-1.5
Dr.10492.1.S1_at	deltaA	-1.1	-1.4
Dr.18233.1.A1_at	metallothionein 2	-1.1	-1.2
Dr.19643.1.A1_at	---	-1.1	-1.2
Dr.21068.1.S1_s_at	POU domain gene 1 /// POU domain gene 23	-1.1	-1.2
Dr.4299.1.S1_at	---	-1.1	-1.2
Dr.23386.1.A1_at	---	-1.1	-1.1
Dr.1691.6.A1_at	---	-1.1	-1.1
Dr.18025.1.A1_at	---	-1.1	-1

Affymetix gene ID	Gene name	Signal log ratio in 1st experiment	Signal log ratio in 2nd experiment
DrAffx.2.105.S1_at	---	-1.1	-1
Dr.18151.1.S1_at	---	-1	-2.2
Dr.5112.1.S3_at	---	-1	-1.6
Dr.13772.1.A1_at	---	-1	-1.3
Dr.3967.1.A1_at	---	-1	-1.3
Dr.221.1.S1_at	POU domain gene 47	-1	-1.3
Dr.6932.3.S1_at	---	-1	-1.2
Dr.5091.1.S1_at	MCM4 minichromosome maintenance deficient 4, mitotin (<i>S. cerevisiae</i>)	-1	-1.2
Dr.3153.1.A1_at	---	-1	-1.1
Dr.26331.1.A1_at	---	-1	-1.1
Dr.18075.1.S1_at	---	-1	-1
Dr.12717.1.S1_at	zgc:55612	-1	-1
Dr.5345.1.S1_at	F-box protein 5	-1	-1
Dr.20896.1.S1_at	---	-1	-1

Table 4.4 Summary of up-regulated genes in *udu*^{-/-} mutant

Affymetix gene ID	Gene name	Signal log ratio in 1st experiment	Signal log ratio in 2nd experiment
Dr.12986.1.A1_a_at	v-fos FBJ murine osteosarcoma viral oncogene homolog	3.1	2.7
Dr.17659.1.S1_at	---	2.6	3.1
Dr.11242.1.A1_at	pleckstrin homology-like domain, family A, member 3	2.5	3.7
Dr.15033.1.S1_at	---	2.4	2.7
Dr.5925.1.A1_at	---	2.2	2
Dr.23587.1.A1_at	growth arrest and DNA-damage-inducible, alpha like	2	2.8
Dr.7532.1.A1_at	---	2	1.4
Dr.4083.1.A1_at	Transcribed locus	2	1.1
Dr.10914.1.A1_at	Wu:fc49d01	1.9	2
Dr.25767.1.S1_at	Transcribed locus	1.9	1.6
Dr.10334.1.S1_at	caspase 8	1.8	2.4
Dr.13121.1.A1_x_at	---	1.8	1.1
Dr.2953.1.S1_at	zgc:55750	1.7	2.3
Dr.14434.1.S1_a_at	piwi-like 1 (Drosophila)	1.7	2
Dr.12491.1.A1_at	---	1.6	2
Dr.15596.1.A1_at	---	1.6	1.4
Dr.13161.1.S1_at	Gadd45b1	1.5	2
Dr.26003.1.A1_at	Transcribed locus	1.5	2
Dr.11708.1.S1_at	zgc:55580	1.5	1
Dr.12833.1.A1_at	zgc:64213	1.4	2.3
Dr.18644.1.A1_at	---	1.4	1.7
Dr.15822.1.S1_at	zgc:64174	1.4	1.5
Dr.12724.1.A1_at	---	1.4	1.3
Dr.23385.1.A1_at	Transcribed locus, weakly similar to NP_508841.1 actin (act-4) [Caenorhabditis elegans]	1.3	2.2
Dr.17587.1.A1_at	Transcribed locus, weakly similar to NP_766602.1 hypothetical protein A330042H22 [Mus musculus]	1.3	2.1
Dr.7110.1.S1_at	zgc:77614	1.3	2.1
Dr.8209.1.S2_at	forkhead box O5	1.3	1.6
Dr.15781.1.S1_at	vaccinia related kinase 2	1.3	1.6
Dr.14673.2.S1_at	zgc:92830	1.3	1.5
Dr.681.1.A1_at	zgc:65909	1.3	1.4
Dr.8946.1.A1_x_at	Transcribed locus	1.3	1.2
Dr.7787.1.S1_at	---	1.2	1.7
Dr.16174.1.A1_at	Transcribed locus, moderately similar to NP_034768.2 basic transcription element binding protein 1 [Mus musculus]	1.2	3.4

Affymetix gene ID	Gene name	Signal log ratio in 1st experiment	Signal log ratio in 2nd experiment
Dr.2052.1.S1_at	tumor protein p53	1.2	1.5
Dr.6820.1.A1_at	GTP binding protein 1, like	1.2	1.4
Dr.6496.2.A1_at	---	1.2	1.3
Dr.3197.1.A1_a_at	Transcribed locus	1.2	1
Dr.25767.1.S1_x_at	Transcribed locus	1.1	2.2
Dr.11479.1.A1_at	---	1.1	1.7
Dr.6709.1.S1_at	---	1.1	1.6
Dr.8000.1.S1_at	zgc:101700	1.1	1.5
Dr.2067.1.A1_at	---	1.1	1.3
Dr.25536.1.A1_at	---	1.1	1.2
Dr.5129.1.S1_at	zgc:56722	1.1	1.2
Dr.24233.1.S1_at	Fibronectin 1-like	1.1	1.2
Dr.3197.3.A1_x_at	Transcribed locus	1.1	1.2
Dr.25376.1.A1_at	---	1.1	1
Dr.4048.1.S1_at	---	1.1	1
Dr.6242.1.A1_at	---	1	1.5
Dr.16273.1.S1_at	Transcribed locus	1	1.2
Dr.3197.1.A1_x_at	Transcribed locus	1	1.1
Dr.542.1.S1_at	murine double minute 2 homolog	1	1.1
Dr.12425.1.S1_at	zgc:92533	1	1.1
Dr.8145.1.S1_at	insulin-like growth factor 2 precursor	1	1.1
Dr.21979.1.A1_at	wu:fc92e10	1	1

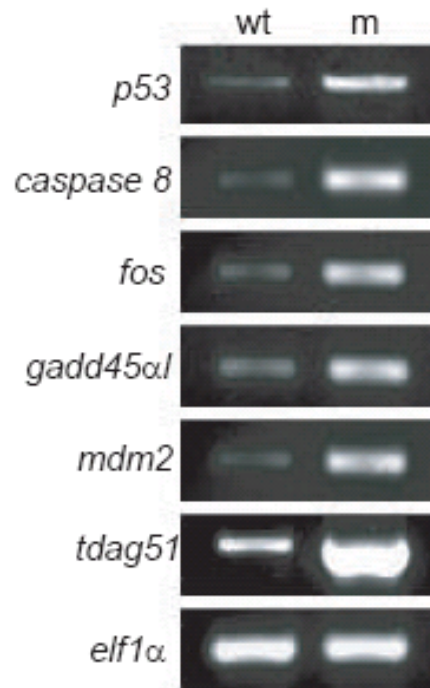


Figure 4.21 Verification of elevated *p53* and its target gene expressions in the *udu*^{-/-} mutant embryos by semi-quantitative RT-PCR. Left and right lanes represent the samples from 24hpf wild type (left) and mutant (right) embryos, respectively.

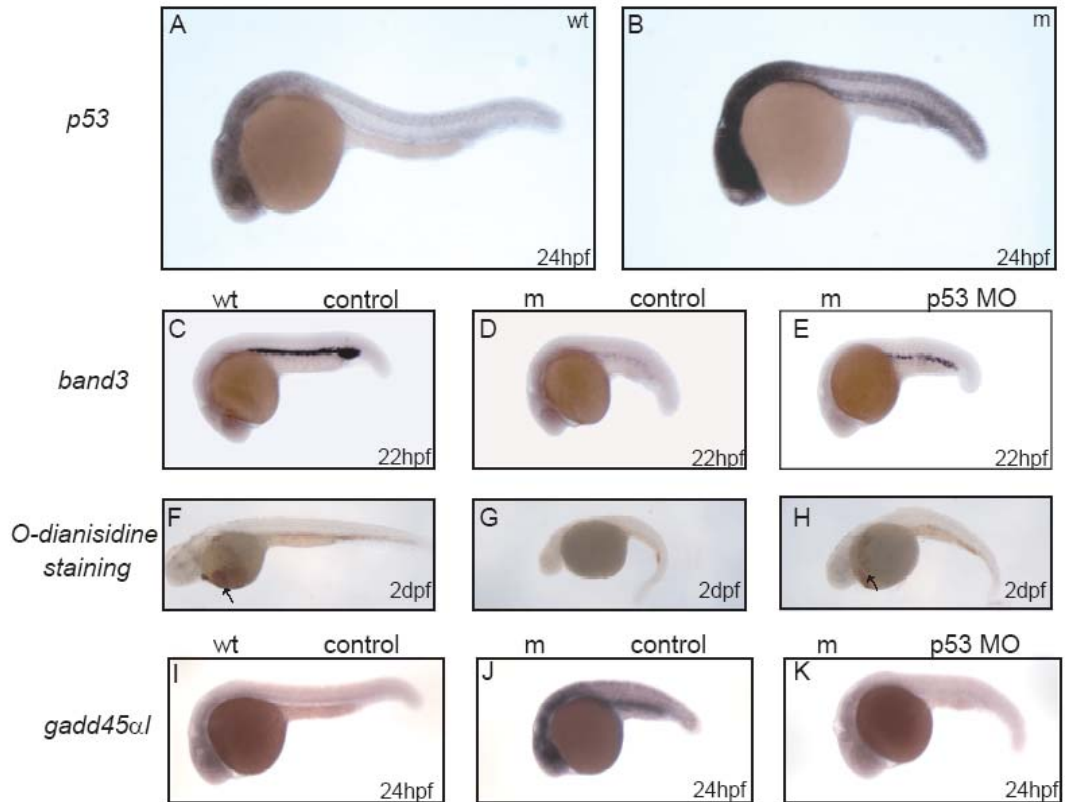


Figure 4.22 The hematopoietic phenotype of the *udu*^{-/-} mutant is mediated by a *p53*-dependent pathway. (A and B) WISH shows that *p53* expression is elevated in the 24hpf *udu*^{-/-} mutant embryo (B) compared to the wild type (A). (C-E) WISH of *band3* in the 22hpf wild type embryo (C) and *udu*^{-/-} mutant morphants injected with control MO (D) or *p53* MO (E). (F-H) O-dianisidine staining of the 2dpf wild type embryo (F) and *udu*^{-/-} mutant morphants injected with control MO (G) or *p53* MO (H). (I-K) WISH of *gadd45α* in the 24hpf wild type embryo (I) and the *udu*^{-/-} mutant morphants injected with control MO (J) or *p53* MO (K). Arrows in F and H indicate o-dianisidine stained red blood cells. All embryos are in lateral views with anterior to the left.

4.2 Discussion

4.2.1 Analysis of the hematopoietic phenotype of *udu* mutant

The zebrafish mutant *ugly duckling* (*udu^{tu24}*) was first isolated from the 1996 Tuebingen large scale screen as a mutant affecting morphogenesis during gastrulation and tail formation (Hammerschmidt et al., 1996). In this project, I reported the isolation and detailed study of a new *udu* allele, *udu^{sq1zl}*, as a mutant with defect in hematopoiesis. Cell cycle, cytology, and transplantation analyses showed that the primitive erythroid cells in the *udu^{sq1zl}* homozygous mutants were severely impaired in proliferation and differentiation in a cell-autonomous fashion. In addition to the primitive erythropoiesis, primitive myelopoiesis and definitive lymphopoiesis also had defects in *udu^{-/-}* mutant, indicated by decreased *lysozyme C* expression and absence of *rag1* expression respectively. But the myelopoiesis and lymphopoiesis abnormality in *udu^{-/-}* mutant was not studied extensively in this thesis. Thus it was not clear whether the defects in the myelopoiesis and lymphopoiesis of the *udu^{-/-}* mutant shared similar features or similar mechanisms with primitive erythropoiesis. *udu* RNA microinjection, as well as *p53* MO, could successfully correct the mutant erythropoiesis phenotype to a satisfactory degree, but failed to restore the myelopoiesis and lymphopoiesis (data not shown). One possibility was the limitation of the rescue assay: slight increment of *lysozyme C* positive cell number was difficult to judge, whereas, the *rag1* expression at 4dpf could not be rescued due to the short life span of the *udu* RNA and the *p53* MO. The other possibility was that the mechanism to cause myelopoietic and lymphopoietic defects was more complex than that to cause erythropoietic abnormality so that myelopoiesis and lymphopoiesis were harder to be restored. For example, cell migration that was required during

myelopoiesis and lymphopoiesis, could be impaired in *udu*^{-/-} mutant since morphogenesis was also affected in *udu*^{-/-} mutant during gastrulation and tail formation. Finally, definitive erythropoiesis was not established in *udu*^{-/-} mutant, but whether the initiation of the definitive hematopoiesis occurred and at which stage definitive hematopoiesis defects occurred remains not clear at this moment.

The comparable levels of expression of *lmo2* and *scl* in *udu*^{-/-} mutant and wild type before 10-somite stage indicate that the *udu* gene is dispensable for initiation of formation of primitive hematopoietic stem cell and early erythroid progenitor specification. However, presence of high level of maternal *udu* RNA raised a possibility that the lack of early hematopoietic phenotype in *udu* mutant is due to the function of the maternal *udu* RNA. Since both *udu* allele are homozygous lethal and die around 7-10dpf, it excludes the possibility to analyse the mutant progeny directly. The primordial germ cells replacement approach described by Ciruna et al. can be used to clarify this issue (Ciruna et al., 2002).

4.2.2 Cell-autonomous role of *udu* gene in erythropoiesis

The transplantation experiment was only performed in one direction: transplanting *udu*^{-/-} mutant or sibling donor cells into wild type host embryos. The results showed that donor cells from *udu*^{-/-} mutant could contribute to host circulating blood cells but with fewer number and lower ratio compared with wild type donor cells, indicating that the *udu*^{-/-} mutant donor cells could specify into erythrocytes but failed to further proliferate. Therefore, I concluded that the *udu* gene could act cell-autonomously to affect development of the primitive red blood cell. However, I did not carry out experiment to test non cell-autonomous effect because the *udu*^{-/-} mutant embryos have

no blood circulation but still have some erythrocytes expressing the hematopoietic markers, thereby preventing us from determining whether the wild type donor cells could contribute to normal erythrocytes in *udu*^{-/-} mutant host. So I could not exclude that the *udu* gene may also act non cell-autonomously in the regulation of primitive erythropoiesis.

4.2.3 The putative molecular mechanism involving Udu protein

In this part of my project, I cloned the *udu* gene, which encodes a novel nuclear protein that contains several evolutionary conserved regions, including two PAH-L repeats and a SANT-L or Myb-like DNA binding domain. The PAH domain, originally defined in the yeast SIN3 protein (Wang et al., 1990), is distantly related to the helix-loop-helix motif and has been shown to mediate protein-protein interactions (Spronk et al., 2000). The yeast SIN3 protein and its related mammalian homologues Sin3A and Sin3B interact, through the PAH domain, with numerous sequence-specific transcription factors and recruit the histone deacetylases (HDAC) to suppress downstream target gene transcription (Silverstein and Ekwall, 2005). The SANT and Myb-DNA binding (Myb-DB) domains have a similar overall structure but confer distinct functions (Boyer et al., 2004). The Myb-DB domain usually contains two to three tandem repeats and recognizes specific DNA sequence, whereas the SANT domain consists of one to two repeats and appears to play an important role in chromatin remodeling (Boyer et al., 2004). Considering the fact that the Udu protein contains only one repeat of this domain that appears to lack obvious patch of positive electrostatic surface, a notable feature of Myb-DB domain (Ogata et al., 1994), by structural modeling analysis (data not shown), we believe that this conserved region may resemble a SANT domain. Given the fact that the Udu protein has both PAH-L

and SANT-L domains, it is reasonable to speculate that Udu may function as a chromatin-remodeling molecule involved in transcription regulation of many target genes. However, further experiments are needed to confirm my hypothesis.

4.2.4 The possible relationship between Udu and p53

In this project, I found that there was robust elevation of the tumor suppressor *p53* expression as well as several *p53* downstream targets in the *udu*^{-/-} mutant embryos. Knockdown of the *p53* protein expression by *p53* MO could correct the mutant phenotype to a similar degree as the *udu* RNA complementation did. Thus, I concluded that the Udu protein plays a crucial role in regulating the proliferation and differentiation of erythroid cells through a *p53*-dependent pathway.

p53 is well recognized as one of the most important tumor suppressors in preventing cancer by modulating downstream target gene expression in response to various cell stresses, such as DNA damage and oncogene activation, resulting in cell cycle arrest or death of abnormal cells (Michael and Oren, 2002; Vogelstein et al., 2000). Although *p53*-deficient animals are viable and display no obvious developmental abnormality (Jin et al., 2000; Ollmann et al., 2000; Schumacher et al., 2005; Donehower et al., 1992), over-expression of *p53* during embryogenesis causes various developmental defects in mouse, fly and worm (Jin et al., 2000; Ollmann et al., 2000; Pan and Griep, 1994; Schumacher et al., 2005). In addition, the developmental defects caused by loss-of-function mutations in zebrafish DNA polymerase *delta1* and *def* have been shown to be associated with increased *p53* activity (Plaster et al., 2006; Chen et al., 2005). More recent studies in *p53*-null and Mdm2, a negative regulator of *p53* (Michael and Oren, 2002), conditional knockout mice have shown that *p53*

suppresses osteoblast differentiation and bone formation (Lengner et al., 2006; Wang et al., 2006). All these observations imply that p53 plays an important role in maintaining normal cell growth and differentiation during animal development. Our finding that the erythrocyte cell cycle and CNS apoptotic defects (data not shown) in the *udu*^{-/-} mutant are mediated through a *p53*-dependent fashion has provided another example to demonstrate that the p53 activity must be tightly controlled during embryogenesis in order to maintain normal cell growth and differentiation. Given the fact that Gadd45 is a well-known p53 downstream target gene involved in apoptosis and cell cycle regulation in mammals (Mak and Kultz, 2004; Michael and Oren, 2002; Vogelstein et al., 2000), we speculate that the G2/M cell cycle arrest of the *udu*^{-/-} red blood cells is likely mediated by the *p53-gadd45* pathway. At this moment it is not clear, however, how loss-of-function mutation in the *udu* gene leads to up-regulation of *p53* activity. One possible explanation is that the Udu protein may function as a general transcription regulator and its loss-of-function causes a global change in gene expression, which somehow leads to activation of *p53* pathway and up-regulation of *p53* expression. However, the fact that in the 24hpf wild type zebrafish embryos both *udu* and *p53* expressions are enriched in the CNS and the ICM, where rapid cell proliferation is taking place, raises the possibility that the Udu protein may act as a suppressor that directly regulates transcription or the protein activity of *p53*. Nonetheless, identifying the interaction partners or the direct target genes of Udu in the near future will help understand the relationship between Udu and p53.

In addition, it is worthy to mention that as a result of segmental duplication on human chromosome 1q22, a new gene next to the human GON4L is generated (Kuryshv et al., 2006). Surprisingly, this segmental duplication does not exist in rat, mouse,

chicken and zebrafish, suggesting that this duplication may be associated with more recent evolutionary events specific for the anthropoid primates (Kuryshv et al., 2006). This new gene, the Yin Yang (YY) 1-associated protein (YY1AP), encodes a protein highly similar (99% identity) to the region from aa residues 590 to 1337 of GON4L. YY1 is a multifunctional transcription factor involved in activation, repression and initiation of gene transcription (Shi et al., 1997; Thomas and Seto, 1999). Recent studies have shown that YY1 negatively regulates the p53 protein activity by disrupting the p53-p300 complex and enhancing the p53-Mdm2 interaction (Gronroos et al., 2004; Sui et al., 2004). YY1AP was isolated in a yeast two-hybrid screening as a YY1 interacting protein and was shown to be a co-activator of YY1 (Wang et al., 2004). Given the high degree of identity in their protein sequences between YY1AP and GON4L, it is conceivable to speculate that the Udu protein may play a role in down-regulation of the p53 activity through YY1.

4.2.5 The Udu homologue GON4L may be associated with tumor development

It has been known for sometime that human chromosome 1q22, where GON4L gene is localized, is amplified in several human cancer types, including ovarian and breast cancer (Cheng et al., 2004), sarcomas (Knuutila, 2004), and hepatocellular carcinoma (Wong et al., 1999; Marchio et al., 1997). A more detailed study has further confirmed that three loci covered by YAC955E11, YAC876B11 and YAC945D5 within 1q21-q22 have the highest amplified copy number in five out of the ten hepatocellular carcinoma cases examined (Wong et al., 2003). Intriguingly, the genomic fragment covered by the YAC876B11 contains a marker D1S2140 that is 30kb apart from the GON4L gene, suggesting that perhaps amplification of the GON4L gene is associated with tumor development that warrants future study.

4.2.6 Essential role of Udu in proliferation and differentiation of erythroid lineage

In this thesis I report the isolation and detailed study of a newly identified zebrafish *udu* mutant allele, *udu^{sq1zl}*. Loss-of-function mutation in the *udu* gene disrupts primitive erythroid cell proliferation and differentiation in a cell-autonomous manner, resulting in red blood cell hypoplasia. Positional cloning reveals that the *udu* gene encodes a novel nuclear factor that contains two PAH-L repeats and a SANT-L domain. Moreover, the expression of the tumor suppressor *p53* and several *p53* downstream targets is elevated in the *udu^{sq1zl}* mutant embryos. Knockdown of the p53 protein by *p53* MO could correct the mutant phenotype to the same extent as *udu* RNA injections in mutant embryos. Thus, these results indicate that the Udu protein is very likely to function as a transcription regulator essential for the proliferation and differentiation of erythroid lineage, probably through a *p53*-dependent pathway. However, it is not clear what is the molecular mechanism of Udu function in erythroid lineage proliferation and differentiation, two exclusive but interdependent processes coordinated elaborately during cell development. At this moment, I have not identified the relationship between Udu and the known factors involved in primitive erythropoiesis. Injection of *scl* or *gata1* RNA into *udu* homozygous mutant embryos failed to rescue erythropoiesis (data not shown), suggesting that the function of Udu in erythroid lineage development is not mediated by Scl or Gata1. Although the Udu pathway is not identified yet, *udu* mutant definitively provides a valuable model to study erythroid cell proliferation and differentiation.

Reference List

- Akashi,K., Traver,D., Miyamoto,T., and Weissman,I.L. (2000). A clonogenic common myeloid progenitor that gives rise to all myeloid lineages. *Nature* *404*, 193-197.
- Amacher,S.L., Draper,B.W., Summers,B.R., and Kimmel,C.B. (2002). The zebrafish T-box genes *no tail* and *spadetail* are required for development of trunk and tail mesoderm and medial floor plate. *Development* *129*, 3311-3323.
- Amatruda,J.F. and Zon,L.I. (1999). Dissecting hematopoiesis and disease using the zebrafish. *Dev Biol* *216*, 1-15.
- Amsterdam,A., Burgess,S., Golling,G., Chen,W., Sun,Z., Townsend,K., Farrington,S., Haldi,M., and Hopkins,N. (1999). A large-scale insertional mutagenesis screen in zebrafish. *Genes Dev* *13*, 2713-2724.
- Amsterdam,A., Nissen,R.M., Sun,Z., Swindell,E.C., Farrington,S., and Hopkins,N. (2004). Identification of 315 genes essential for early zebrafish development. *Proc Natl Acad Sci U S A* *101*, 12792-12797.
- Anguita,E., Hughes,J., Heyworth,C., Blobel,G.A., Wood,W.G., and Higgs,D.R. (2004). Globin gene activation during haemopoiesis is driven by protein complexes nucleated by GATA-1 and GATA-2. *EMBO J* *23*, 2841-2852.
- Antonchuk,J., Sauvageau,G., and Humphries,R.K. (2002). HOXB4-induced expansion of adult hematopoietic stem cells *ex vivo*. *Cell* *109*, 39-45.
- Barndt,R.J., Dai,M., and Zhuang,Y. (2000). Functions of E2A-HEB heterodimers in T-cell development revealed by a dominant negative mutation of HEB. *Mol. Cell Biol.* *20*, 6677-6685.
- Barreda,D.R., Hanington,P.C., and Belosevic,M. (2004). Regulation of myeloid development and function by colony stimulating factors. *Dev. Comp Immunol.* *28*, 509-554.
- Behre,G., Whitmarsh,A.J., Coghlan,M.P., Hoang,T., Carpenter,C.L., Zhang,D.E., Davis,R.J., and Tenen,D.G. (1999). c-Jun is a JNK-independent coactivator of the PU.1 transcription factor. *J. Biol. Chem.* *274*, 4939-4946.
- Beier,D.R. (2000). Sequence-based analysis of mutagenized mice. *Mamm. Genome* *11*, 594-597.
- Belaoussoff,M., Farrington,S.M., and Baron,M.H. (1998). Hematopoietic induction and respecification of A-P identity by visceral endoderm signaling in the mouse embryo. *Development* *125*, 5009-5018.
- Bennett,C.M., Kanki,J.P., Rhodes,J., Liu,T.X., Paw,B.H., Kieran,M.W., Langenau,D.M., Delahaye-Brown,A., Zon,L.I., Fleming,M.D., and Look,A.T. (2001). Myelopoiesis in the zebrafish, *Danio rerio*. *Blood* *98*, 643-651.
- Bentley,A., MacLennan,B., Calvo,J., and Dearolf,C.R. (2000). Targeted recovery of mutations in *Drosophila*. *Genetics* *156*, 1169-1173.
- Bhardwaj,G., Murdoch,B., Wu,D., Baker,D.P., Williams,K.P., Chadwick,K., Ling,L.E., Karanu,F.N., and Bhatia,M. (2001). Sonic hedgehog induces the proliferation of primitive human hematopoietic cells via BMP regulation. *Nat. Immunol.* *2*, 172-180.
- Bhatia,M., Bonnet,D., Wu,D., Murdoch,B., Wrana,J., Gallacher,L., and Dick,J.E. (1999). Bone morphogenetic proteins regulate the developmental program of human hematopoietic stem cells. *J. Exp. Med.* *189*, 1139-1148.
- Blackburn,C.C., Augustine,C.L., Li,R., Harvey,R.P., Malin,M.A., Boyd,R.L., Miller,J.F., and

- Morahan,G. (1996). The nu gene acts cell-autonomously and is required for differentiation of thymic epithelial progenitors. *Proc. Natl. Acad. Sci. U. S. A* *93*, 5742-5746.
- Boehm,T., Bleul,C.C., and Schorpp,M. (2003). Genetic dissection of thymus development in mouse and zebrafish. *Immunol Rev* *195*, 15-27.
- Boyer,L.A., Latek,R.R., and Peterson,C.L. (2004). The SANT domain: a unique histone-tail-binding module? *Nat Rev Mol Cell Biol* *5*, 158-163.
- Brown,L.A., Rodaway,A.R., Schilling,T.F., Jowett,T., Ingham,P.W., Patient,R.K., and Sharrocks,A.D. (2000). Insights into early vasculogenesis revealed by expression of the ETS-domain transcription factor Fli-1 in wild-type and mutant zebrafish embryos. *Mech Dev* *90*, 237-252.
- Brownlie,A., Donovan,A., Pratt,S.J., Paw,B.H., Oates,A.C., Brugnara,C., Witkowska,H.E., Sassa,S., and Zon,L.I. (1998). Positional cloning of the zebrafish sauternes gene: a model for congenital sideroblastic anaemia. *Nat Genet* *20*, 244-250.
- Brownlie,A., Hersey,C., Oates,A.C., Paw,B.H., Falick,A.M., Witkowska,H.E., Flint,J., Higgs,D., Jessen,J., Bahary,N., Zhu,H., Lin,S., and Zon,L. (2003). Characterization of embryonic globin genes of the zebrafish. *Dev Biol* *255*, 48-61.
- Burns,C.E., DeBlasio,T., Zhou,Y., Zhang,J., Zon,L., and Nimer,S.D. (2002). Isolation and characterization of runxa and runxb, zebrafish members of the runt family of transcriptional regulators. *Exp Hematol* *30*, 1381-1389.
- Buske,C., Feuring-Buske,M., Abramovich,C., Spiekermann,K., Eaves,C.J., Coulombel,L., Sauvageau,G., Hogge,D.E., and Humphries,R.K. (2002). Deregulated expression of HOXB4 enhances the primitive growth activity of human hematopoietic cells. *Blood* *100*, 862-868.
- Carver-Moore,K., Broxmeyer,H.E., Luoh,S.M., Cooper,S., Peng,J., Burstein,S.A., Moore,M.W., and de Sauvage,F.J. (1996). Low levels of erythroid and myeloid progenitors in thrombopoietin-and c-mpl-deficient mice. *Blood* *88*, 803-808.
- Chan,F.Y., Robinson,J., Brownlie,A., Shivdasani,R.A., Donovan,A., Brugnara,C., Kim,J., Lau,B.C., Witkowska,H.E., and Zon,L.I. (1997). Characterization of adult alpha- and beta-globin genes in the zebrafish. *Blood* *89*, 688-700.
- Chen,H., Ray-Gallet,D., Zhang,P., Hetherington,C.J., Gonzalez,D.A., Zhang,D.E., Moreau-Gachelin,F., and Tenen,D.G. (1995). PU.1 (Spi-1) autoregulates its expression in myeloid cells. *Oncogene* *11*, 1549-1560.
- Chen,J., Ruan,H., Ng,S.M., Gao,C., Soo,H.M., Wu,W., Zhang,Z., Wen,Z., Lane,D.P., and Peng,J. (2005). Loss of function of def selectively up-regulates Delta113p53 expression to arrest expansion growth of digestive organs in zebrafish. *Genes Dev* *19*, 2900-2911.
- Cheng,K.W., Lahad,J.P., Kuo,W.L., Lapuk,A., Yamada,K., Auersperg,N., Liu,J., Smith-McCune,K., Lu,K.H., Fishman,D., Gray,J.W., and Mills,G.B. (2004). The RAB25 small GTPase determines aggressiveness of ovarian and breast cancers. *Nat Med* *10*, 1251-1256.
- Childs,S., Weinstein,B.M., Mohideen,M.A., Donohue,S., Bonkovsky,H., and Fishman,M.C. (2000). Zebrafish dracula encodes ferrochelatase and its mutation provides a model for erythropoietic protoporphyria. *Curr Biol* *10*, 1001-1004.
- Choi,K., Kennedy,M., Kazarov,A., Papadimitriou,J.C., and Keller,G. (1998). A common precursor for hematopoietic and endothelial cells. *Development* *125*, 725-732.
- Ciruna,B., Weidinger,G., Knaut,H., Thisse,B., Thisse,C., Raz,E., and Schier,A.F. (2002). Production of maternal-zygotic mutant zebrafish by germ-line replacement. *Proc Natl Acad Sci U S A* *99*, 14919-14924.

- Crispino, J.D., Lodish, M.B., MacKay, J.P., and Orkin, S.H. (1999). Use of altered specificity mutants to probe a specific protein-protein interaction in differentiation: the GATA-1:FOG complex. *Mol Cell* *3*, 219-228.
- Cumano, A. and Godin, I. (2001). Pluripotent hematopoietic stem cell development during embryogenesis. *Curr Opin Immunol* *13*, 166-171.
- Dai, C.H., Krantz, S.B., and Zsebo, K.M. (1991). Human burst-forming units-erythroid need direct interaction with stem cell factor for further development. *Blood* *78*, 2493-2497.
- Danilova, N. and Steiner, L.A. (2002). B cells develop in the zebrafish pancreas. *Proc Natl Acad Sci U S A* *99*, 13711-13716.
- Davidson, A.J., Ernst, P., Wang, Y., Dekens, M.P., Kingsley, P.D., Palis, J., Korsmeyer, S.J., Daley, G.Q., and Zon, L.I. (2003). *cdx4* mutants fail to specify blood progenitors and can be rescued by multiple *hox* genes. *Nature* *425*, 300-306.
- Davidson, A.J. and Zon, L.I. (2000). Turning mesoderm into blood: the formation of hematopoietic stem cells during embryogenesis. *Curr. Top. Dev. Biol.* *50*, 45-60.
- Davidson, A.J. and Zon, L.I. (2004). The 'definitive' (and 'primitive') guide to zebrafish hematopoiesis. *Oncogene* *23*, 7233-7246.
- de Jong, J.L. and Zon, L.I. (2005). Use of the zebrafish system to study primitive and definitive hematopoiesis. *Annu Rev Genet* *39*, 481-501.
- De Robertis, E.M. and Kuroda, H. (2004). Dorsal-ventral patterning and neural induction in *Xenopus* embryos. *Annu. Rev. Cell Dev. Biol.* *20*, 285-308.
- DeKoter, R.P. and Singh, H. (2000). Regulation of B lymphocyte and macrophage development by graded expression of PU.1. *Science* *288*, 1439-1441.
- DeKoter, R.P., Walsh, J.C., and Singh, H. (1998). PU.1 regulates both cytokine-dependent proliferation and differentiation of granulocyte/macrophage progenitors. *EMBO J.* *17*, 4456-4468.
- Delassus, S. and Cumano, A. (1996). Circulation of hematopoietic progenitors in the mouse embryo. *Immunity* *4*, 97-106.
- Detrich, H.W., III, Kieran, M.W., Chan, F.Y., Barone, L.M., Yee, K., Rundstadler, J.A., Pratt, S., Ransom, D., and Zon, L.I. (1995). Intraembryonic hematopoietic cell migration during vertebrate development. *Proc. Natl. Acad. Sci. U. S. A* *92*, 10713-10717.
- Dickson, M.C., Martin, J.S., Cousins, F.M., Kulkarni, A.B., Karlsson, S., and Akhurst, R.J. (1995). Defective haematopoiesis and vasculogenesis in transforming growth factor-beta 1 knock out mice. *Development* *121*, 1845-1854.
- Dieterlen-Lievre, F. (1975). On the origin of haemopoietic stem cells in the avian embryo: an experimental approach. *J Embryol. Exp Morphol.* *33*, 607-619.
- Donehower, L.A., Harvey, M., Slagle, B.L., McArthur, M.J., Montgomery, C.A., Jr., Butel, J.S., and Bradley, A. (1992). Mice deficient for p53 are developmentally normal but susceptible to spontaneous tumours. *Nature* *356*, 215-221.
- Donovan, A., Brownlie, A., Dorschner, M.O., Zhou, Y., Pratt, S.J., Paw, B.H., Phillips, R.B., Thisse, C., Thisse, B., and Zon, L.I. (2002). The zebrafish mutant gene *chardonnay* (*cdy*) encodes divalent metal transporter 1 (DMT1). *Blood* *100*, 4655-4659.
- Donovan, A., Brownlie, A., Zhou, Y., Shepard, J., Pratt, S.J., Moynihan, J., Paw, B.H., Drejer, A., Barut, B., Zapata, A., Law, T.C., Brugnara, C., Lux, S.E., Pinkus, G.S., Pinkus, J.L., Kingsley, P.D., Palis, J.,

- Fleming,M.D., Andrews,N.C., and Zon,L.I. (2000). Positional cloning of zebrafish ferroportin1 identifies a conserved vertebrate iron exporter. *Nature* 403, 776-781.
- Dooley,K.A., Davidson,A.J., and Zon,L.I. (2005). Zebrafish scl functions independently in hematopoietic and endothelial development. *Dev Biol* 277, 522-536.
- Douagi,I., Vieira,P., and Cumano,A. (2002). Lymphocyte commitment during embryonic development, in the mouse. *Semin. Immunol* 14, 361-369.
- Driever,W. and Fishman,M.C. (1996). The zebrafish: heritable disorders in transparent embryos. *J Clin Invest* 97, 1788-1794.
- Dyer,M.A., Farrington,S.M., Mohn,D., Munday,J.R., and Baron,M.H. (2001). Indian hedgehog activates hematopoiesis and vasculogenesis and can respecify prospective neurectodermal cell fate in the mouse embryo. *Development* 128, 1717-1730.
- Evans,T., Reitman,M., and Felsenfeld,G. (1988). An erythrocyte-specific DNA-binding factor recognizes a regulatory sequence common to all chicken globin genes. *Proc. Natl. Acad. Sci. U. S. A* 85, 5976-5980.
- Fantoni,A., Bank,A., and Marks,P.A. (1967). Globin composition and synthesis of hemoglobins in developing fetal mice erythroid cells. *Science* 157, 1327-1329.
- Fassler,R. and Meyer,M. (1995). Consequences of lack of beta 1 integrin gene expression in mice. *Genes Dev.* 9, 1896-1908.
- Fong,I.C., Zarrin,A.A., Wu,G.E., and Berinstein,N.L. (2000). Functional analysis of the human RAG 2 promoter. *Mol. Immunol.* 37, 391-402.
- Fraenkel,P.G., Traver,D., Donovan,A., Zahrieh,D., and Zon,L.I. (2005). Ferroportin1 is required for normal iron cycling in zebrafish. *J Clin Invest* 115, 1532-1541.
- Fujiwara,Y., Browne,C.P., Cunniff,K., Goff,S.C., and Orkin,S.H. (1996). Arrested development of embryonic red cell precursors in mouse embryos lacking transcription factor GATA-1. *Proc Natl Acad Sci U S A* 93, 12355-12358.
- Fuller,K. and Storb,U. (1997). Identification and characterization of the murine Rag1 promoter. *Mol. Immunol.* 34, 939-954.
- Galloway,J.L. and Zon,L.I. (2003). Ontogeny of hematopoiesis: examining the emergence of hematopoietic cells in the vertebrate embryo. *Curr Top. Dev Biol* 53, 139-158.
- Garcia-Porrero,J.A., Godin,I.E., and Dieterlen-Lievre,F. (1995). Potential intraembryonic hemogenic sites at pre-liver stages in the mouse. *Anat. Embryol. (Berl)* 192, 425-435.
- Georgopoulos,K., Bigby,M., Wang,J.H., Molnar,A., Wu,P., Winandy,S., and Sharpe,A. (1994). The Ikaros gene is required for the development of all lymphoid lineages. *Cell* 79, 143-156.
- Gering,M., Rodaway,A.R., Gottgens,B., Patient,R.K., and Green,A.R. (1998). The SCL gene specifies haemangioblast development from early mesoderm. *EMBO J* 17, 4029-4045.
- Germain,R.N. (2002). T-cell development and the CD4-CD8 lineage decision. *Nat. Rev. Immunol.* 2, 309-322.
- Godin,I.E., Garcia-Porrero,J.A., Coutinho,A., Dieterlen-Lievre,F., and Marcos,M.A. (1993). Para-aortic splanchnopleura from early mouse embryos contains B1a cell progenitors. *Nature* 364, 67-70.
- Golling,G., Amsterdam,A., Sun,Z., Antonelli,M., Maldonado,E., Chen,W., Burgess,S., Haldi,M., Artzt,K., Farrington,S., Lin,S.Y., Nissen,R.M., and Hopkins,N. (2002). Insertional mutagenesis in

zebrafish rapidly identifies genes essential for early vertebrate development. *Nat Genet* 31, 135-140.

Griffin,K.J., Amacher,S.L., Kimmel,C.B., and Kimelman,D. (1998). Molecular identification of spadetail: regulation of zebrafish trunk and tail mesoderm formation by T-box genes
Development 125, 3379-3388.

Gronroos,E., Terentiev,A.A., Punga,T., and Ericsson,J. (2004). YY1 inhibits the activation of the p53 tumor suppressor in response to genotoxic stress. *Proc Natl Acad Sci U S A* 101, 12165-12170.

Haffter,P., Granato,M., Brand,M., Mullins,M.C., Hammerschmidt,M., Kane,D.A., Odenthal,J., van Eeden,F.J., Jiang,Y.J., Heisenberg,C.P., Kelsh,R.N., Furutani-Seiki,M., Vogelsang,E., Beuchle,D., Schach,U., Fabian,C., and Nusslein-Volhard,C. (1996). The identification of genes with unique and essential functions in the development of the zebrafish, *Danio rerio*. *Development* 123, 1-36.

Hamaguchi,I., Huang,X.L., Takakura,N., Tada,J., Yamaguchi,Y., Kodama,H., and Suda,T. (1999). In vitro hematopoietic and endothelial cell development from cells expressing TEK receptor in murine aorta-gonad-mesonephros region. *Blood* 93, 1549-1556.

Hammerschmidt,M., Pelegri,F., Mullins,M.C., Kane,D.A., Brand,M., van Eeden,F.J., Furutani-Seiki,M., Granato,M., Haffter,P., Heisenberg,C.P., Jiang,Y.J., Kelsh,R.N., Odenthal,J., Warga,R.M., and Nusslein-Volhard,C. (1996). Mutations affecting morphogenesis during gastrulation and tail formation in the zebrafish, *Danio rerio*. *Development* 123, 143-151.

Heasman,J. (2002). Morpholino oligos: making sense of antisense? *Dev Biol* 243, 209-214.

Heasman,J. (2006). Maternal determinants of embryonic cell fate. *Semin. Cell Dev. Biol.* 17, 93-98.

Herblot,S., Aplan,P.D., and Hoang,T. (2002). Gradient of E2A activity in B-cell development. *Mol Cell Biol* 22, 886-900.

Herbomel,P., Thisse,B., and Thisse,C. (1999). Ontogeny and behaviour of early macrophages in the zebrafish embryo. *Development* 126, 3735-3745.

Hoang,T. (2004). The origin of hematopoietic cell type diversity. *Oncogene* 23, 7188-7198.

Hong,W., Nakazawa,M., Chen,Y.Y., Kori,R., Vakoc,C.R., Rakowski,C., and Blobel,G.A. (2005). FOG-1 recruits the NuRD repressor complex to mediate transcriptional repression by GATA-1. *EMBO J.* 24, 2367-2378.

Hsia,N. and Zon,L.I. (2005). Transcriptional regulation of hematopoietic stem cell development in zebrafish. *Exp Hematol.* 33, 1007-1014.

Hu,M., Krause,D., Greaves,M., Sharkis,S., Dexter,M., Heyworth,C., and Enver,T. (1997). Multilineage gene expression precedes commitment in the hemopoietic system. *Genes Dev.* 11, 774-785.

Huber,T.L. and Zon,L.I. (1998). Transcriptional regulation of blood formation during *Xenopus* development. *Semin. Immunol.* 10, 103-109.

Ivanova,N.B., Dimos,J.T., Schaniel,C., Hackney,J.A., Moore,K.A., and Lemischka,I.R. (2002). A stem cell molecular signature. *Science* 298, 601-604.

Jansen,G., Hazendonk,E., Thijssen,K.L., and Plasterk,R.H. (1997). Reverse genetics by chemical mutagenesis in *Caenorhabditis elegans*. *Nat. Genet.* 17, 119-121.

Ji,R.P., Phoon,C.K., Aristizabal,O., McGrath,K.E., Palis,J., and Turnbull,D.H. (2003). Onset of cardiac function during early mouse embryogenesis coincides with entry of primitive erythroblasts into the embryo proper. *Circ. Res.* 92, 133-135.

Jin,H., Xu,J., Qian,F., Du,L., Tan,C.Y., Lin,Z., Peng,J., and Wen,Z. (2006). The 5' zebrafish scl

promoter targets transcription to the brain, spinal cord, and hematopoietic and endothelial progenitors. *Dev Dyn.* 235, 60-67.

Jin, S., Martinek, S., Joo, W.S., Wortman, J.R., Mirkovic, N., Sali, A., Yandell, M.D., Pavletich, N.P., Young, M.W., and Levine, A.J. (2000). Identification and characterization of a p53 homologue in *Drosophila melanogaster*. *Proc Natl Acad Sci U S A* 97, 7301-7306.

Johnson, G.R. and Moore, M.A. (1975). Role of stem cell migration in initiation of mouse foetal liver haemopoiesis. *Nature* 258, 726-728.

Kalev-Zylinska, M.L., Horsfield, J.A., Flores, M.V., Postlethwait, J.H., Vitas, M.R., Baas, A.M., Crosier, P.S., and Crosier, K.E. (2002). Runx1 is required for zebrafish blood and vessel development and expression of a human RUNX1-CBF2T1 transgene advances a model for studies of leukemogenesis. *Development* 129, 2015-2030.

Keller, G., Lacaud, G., and Robertson, S. (1999). Development of the hematopoietic system in the mouse. *Exp Hematol.* 27, 777-787.

Kennedy, M., Firpo, M., Choi, K., Wall, C., Robertson, S., Kabrun, N., and Keller, G. (1997). A common precursor for primitive erythropoiesis and definitive haematopoiesis. *Nature* 386, 488-493.

Kimmel, C.B., Ballard, W.W., Kimmel, S.R., Ullmann, B., and Schilling, T.F. (1995). Stages of embryonic development of the zebrafish. *Dev Dyn.* 203, 253-310.

Knuutila, S. (2004). Cytogenetics and molecular pathology in cancer diagnostics. *Ann Med* 36, 162-171.

Kondo, M., Wagers, A.J., Manz, M.G., Prohaska, S.S., Scherer, D.C., Beilhack, G.F., Shizuru, J.A., and Weissman, I.L. (2003). Biology of hematopoietic stem cells and progenitors: implications for clinical application. *Annu Rev Immunol* 21, 759-806.

Kondo, M., Weissman, I.L., and Akashi, K. (1997). Identification of clonogenic common lymphoid progenitors in mouse bone marrow. *Cell* 91, 661-672.

Kuryshv, V.Y., Vorobyov, E., Zink, D., Schmitz, J., Rozhdestvensky, T.S., Munstermann, E., Ernst, U., Wellenreuther, R., Moosmayer, P., Bechtel, S., Schupp, I., Horst, J., Korn, B., Poustka, A., and Wiemann, S. (2006). An anthropoid-specific segmental duplication on human chromosome 1q22. *Genomics*.

Kyba, M., Perlingeiro, R.C., and Daley, G.Q. (2002). HoxB4 confers definitive lymphoid-myeloid engraftment potential on embryonic stem cell and yolk sac hematopoietic progenitors. *Cell* 109, 29-37.

Labastie, M.C., Thiery, J.P., and Le Douarin, N.M. (1984). Mouse yolk sac and intraembryonic tissues produce factors able to elicit differentiation of erythroid burst-forming units and colony-forming units, respectively. *Proc. Natl. Acad. Sci. U. S. A* 81, 1453-1456.

Lahlil, R., Lecuyer, E., Herblot, S., and Hoang, T. (2004). SCL assembles a multifactorial complex that determines glycoprotein A expression. *Mol. Cell Biol.* 24, 1439-1452.

Lam, S.H., Chua, H.L., Gong, Z., Wen, Z., Lam, T.J., and Sin, Y.M. (2002). Morphologic transformation of the thymus in developing zebrafish. *Dev Dyn.* 225, 87-94.

Langenau, D.M., Ferrando, A.A., Traver, D., Kutok, J.L., Hezel, J.P., Kanki, J.P., Zon, L.I., Look, A.T., and Trede, N.S. (2004). In vivo tracking of T cell development, ablation, and engraftment in transgenic zebrafish. *Proc Natl Acad Sci U S A* 101, 7369-7374.

Langheinrich, U., Hennen, E., Stott, G., and Vacun, G. (2002). Zebrafish as a model organism for the identification and characterization of drugs and genes affecting p53 signaling. *Curr Biol* 12, 2023-2028.

- Lawrence,H.J., Christensen,J., Fong,S., Hu,Y.L., Weissman,I., Sauvageau,G., Humphries,R.K., and Largman,C. (2005). Loss of expression of the Hoxa-9 homeobox gene impairs the proliferation and repopulating ability of hematopoietic stem cells. *Blood* *106*, 3988-3994.
- Lawrence,H.J., Helgason,C.D., Sauvageau,G., Fong,S., Izon,D.J., Humphries,R.K., and Largman,C. (1997). Mice bearing a targeted interruption of the homeobox gene HOXA9 have defects in myeloid, erythroid, and lymphoid hematopoiesis. *Blood* *89*, 1922-1930.
- Leder,P., Hansen,J.N., Konkel,D., Leder,A., Nishioka,Y., and Talkington,C. (1980). Mouse globin system: a functional and evolutionary analysis. *Science* *209*, 1336-1342.
- Lekstrom-Himes,J. and Xanthopoulos,K.G. (1999). CCAAT/enhancer binding protein epsilon is critical for effective neutrophil-mediated response to inflammatory challenge. *Blood* *93*, 3096-3105.
- Lengner,C.J., Steinman,H.A., Gagnon,J., Smith,T.W., Henderson,J.E., Kream,B.E., Stein,G.S., Lian,J.B., and Jones,S.N. (2006). Osteoblast differentiation and skeletal development are regulated by Mdm2-p53 signaling. *J Cell Biol* *172*, 909-921.
- Lensch,M.W. and Daley,G.Q. (2004). Origins of mammalian hematopoiesis: in vivo paradigms and in vitro models. *Curr Top. Dev Biol* *60*, 127-196.
- Letting,D.L., Chen,Y.Y., Rakowski,C., Reedy,S., and Blobel,G.A. (2004). Context-dependent regulation of GATA-1 by friend of GATA-1. *Proc. Natl. Acad. Sci. U. S. A* *101*, 476-481.
- Liao,E.C., Paw,B.H., Oates,A.C., Pratt,S.J., Postlethwait,J.H., and Zon,L.I. (1998). SCL/Tal-1 transcription factor acts downstream of cloche to specify hematopoietic and vascular progenitors in zebrafish. *Genes Dev* *12*, 621-626.
- Liao,E.C., Paw,B.H., Peters,L.L., Zapata,A., Pratt,S.J., Do,C.P., Lieschke,G., and Zon,L.I. (2000). Hereditary spherocytosis in zebrafish riesling illustrates evolution of erythroid beta-spectrin structure, and function in red cell morphogenesis and membrane stability. *Development* *127*, 5123-5132.
- Liao,E.C., Trede,N.S., Ransom,D., Zapata,A., Kieran,M., and Zon,L.I. (2002). Non-cell autonomous requirement for the bloodless gene in primitive hematopoiesis of zebrafish. *Development* *129*, 649-659.
- Lieschke,G.J., Oates,A.C., Crowhurst,M.O., Ward,A.C., and Layton,J.E. (2001). Morphologic and functional characterization of granulocytes and macrophages in embryonic and adult zebrafish. *Blood* *98*, 3087-3096.
- Lieschke,G.J., Oates,A.C., Paw,B.H., Thompson,M.A., Hall,N.E., Ward,A.C., Ho,R.K., Zon,L.I., and Layton,J.E. (2002). Zebrafish SPI-1 (PU.1) marks a site of myeloid development independent of primitive erythropoiesis: implications for axial patterning. *Dev Biol* *246*, 274-295.
- Lin,C.S., Lim,S.K., D'Agati,V., and Costantini,F. (1996). Differential effects of an erythropoietin receptor gene disruption on primitive and definitive erythropoiesis. *Genes Dev.* *10*, 154-164.
- Liu,F. and Wen,Z. (2002). Cloning and expression pattern of the lysozyme C gene in zebrafish. *Mech Dev* *113*, 69-72.
- Long,Q., Meng,A., Wang,H., Jessen,J.R., Farrell,M.J., and Lin,S. (1997). GATA-1 expression pattern can be recapitulated in living transgenic zebrafish using GFP reporter gene. *Development* *124*, 4105-4111.
- Lyons,S.E., Lawson,N.D., Lei,L., Bennett,P.E., Weinstein,B.M., and Liu,P.P. (2002). A nonsense mutation in zebrafish gata1 causes the bloodless phenotype in vlad tepes. *Proc Natl Acad Sci U S A* *99*, 5454-5459.
- Mackaretschian,K., Hardin,J.D., Moore,K.A., Boast,S., Goff,S.P., and Lemischka,I.R. (1995). Targeted disruption of the flk2/flt3 gene leads to deficiencies in primitive hematopoietic progenitors. *Immunity.* *3*, 147-161.

- Mak,S.K. and Kultz,D. (2004). Gadd45 proteins induce G2/M arrest and modulate apoptosis in kidney cells exposed to hyperosmotic stress. *J Biol Chem* 279, 39075-39084.
- Manley,N.R. (2000). Thymus organogenesis and molecular mechanisms of thymic epithelial cell differentiation. *Semin. Immunol* 12, 421-428.
- Manley,N.R. and Capecchi,M.R. (1995). The role of Hoxa-3 in mouse thymus and thyroid development. *Development* 121, 1989-2003.
- Marchio,A., Meddeb,M., Pineau,P., Danglot,G., Tiollais,P., Bernheim,A., and Dejean,A. (1997). Recurrent chromosomal abnormalities in hepatocellular carcinoma detected by comparative genomic hybridization. *Genes Chromosomes Cancer* 18, 59-65.
- Matsuoka,S., Tsuji,K., Hisakawa,H., Xu,M., Ebihara,Y., Ishii,T., Sugiyama,D., Manabe,A., Tanaka,R., Ikeda,Y., Asano,S., and Nakahata,T. (2001). Generation of definitive hematopoietic stem cells from murine early yolk sac and paraaortic splanchnopleures by aorta-gonad-mesonephros region-derived stromal cells. *Blood* 98, 6-12.
- McCallum,C.M., Comai,L., Greene,E.A., and Henikoff,S. (2000). Targeted screening for induced mutations. *Nat. Biotechnol.* 18, 455-457.
- McKercher,S.R., Torbett,B.E., Anderson,K.L., Henkel,G.W., Vestal,D.J., Baribault,H., Klemsz,M., Feeney,A.J., Wu,G.E., Paige,C.J., and Maki,R.A. (1996). Targeted disruption of the PU.1 gene results in multiple hematopoietic abnormalities. *EMBO J.* 15, 5647-5658.
- Medvinsky,A. and Dzierzak,E. (1996). Definitive hematopoiesis is autonomously initiated by the AGM region. *Cell* 86, 897-906.
- Medvinsky,A.L., Samoylina,N.L., Muller,A.M., and Dzierzak,E.A. (1993). An early pre-liver intraembryonic source of CFU-S in the developing mouse. *Nature* 364, 64-67.
- Michael,D. and Oren,M. (2002). The p53 and Mdm2 families in cancer. *Curr Opin Genet Dev* 12, 53-59.
- Mombaerts,P., Iacomini,J., Johnson,R.S., Herrup,K., Tonegawa,S., and Papaioannou,V.E. (1992). RAG-1-deficient mice have no mature B and T lymphocytes. *Cell* 68, 869-877.
- Moore,M.A. and Metcalf,D. (1970). Ontogeny of the haemopoietic system: yolk sac origin of in vivo and in vitro colony forming cells in the developing mouse embryo. *Br. J Haematol.* 18, 279-296.
- Mucenski,M.L., McLain,K., Kier,A.B., Swerdlow,S.H., Schreiner,C.M., Miller,T.A., Pietryga,D.W., Scott,W.J., Jr., and Potter,S.S. (1991). A functional c-myc gene is required for normal murine fetal hepatic hematopoiesis. *Cell* 65, 677-689.
- Mukouyama,Y., Chiba,N., Mucenski,M.L., Satake,M., Miyajima,A., Hara,T., and Watanabe,T. (1999). Hematopoietic cells in cultures of the murine embryonic aorta-gonad-mesonephros region are induced by c-Myb. *Curr Biol* 9, 833-836.
- Muller,A.M., Medvinsky,A., Strouboulis,J., Grosveld,F., and Dzierzak,E. (1994). Development of hematopoietic stem cell activity in the mouse embryo. *Immunity.* 1, 291-301.
- Mullins,M.C., Hammerschmidt,M., Haffter,P., and Nusslein-Volhard,C. (1994). Large-scale mutagenesis in the zebrafish: in search of genes controlling development in a vertebrate. *Curr Biol* 4, 189-202.
- Nasevicius,A. and Ekker,S.C. (2000). Effective targeted gene 'knockdown' in zebrafish. *Nat Genet* 26, 216-220.
- Nehls,M., Kyewski,B., Messerle,M., Waldschutz,R., Schuddekopf,K., Smith,A.J., and Boehm,T. (1996).

- Two genetically separable steps in the differentiation of thymic epithelium. *Science* 272, 886-889.
- Nehls,M., Pfeifer,D., Schorpp,M., Hedrich,H., and Boehm,T. (1994). New member of the winged-helix protein family disrupted in mouse and rat nude mutations. *Nature* 372, 103-107.
- Nerlov,C., Querfurth,E., Kulesa,H., and Graf,T. (2000). GATA-1 interacts with the myeloid PU.1 transcription factor and represses PU.1-dependent transcription. *Blood* 95, 2543-2551.
- Neubauer,H., Cumano,A., Muller,M., Wu,H., Huffstadt,U., and Pfeffer,K. (1998). Jak2 deficiency defines an essential developmental checkpoint in definitive hematopoiesis. *Cell* 93, 397-409.
- Nichogiannopoulou,A., Trevisan,M., Neben,S., Friedrich,C., and Georgopoulos,K. (1999). Defects in hemopoietic stem cell activity in Ikaros mutant mice. *J Exp Med* 190, 1201-1214.
- Nishikawa,S.I., Nishikawa,S., Hirashima,M., Matsuyoshi,N., and Kodama,H. (1998). Progressive lineage analysis by cell sorting and culture identifies FLK1+VE-cadherin+ cells at a diverging point of endothelial and hemopoietic lineages. *Development* 125, 1747-1757.
- Nocka,K., Majumder,S., Chabot,B., Ray,P., Cervone,M., Bernstein,A., and Besmer,P. (1989). Expression of c-kit gene products in known cellular targets of W mutations in normal and W mutant mice--evidence for an impaired c-kit kinase in mutant mice. *Genes Dev.* 3, 816-826.
- North,T., Gu,T.L., Stacy,T., Wang,Q., Howard,L., Binder,M., Marin-Padilla,M., and Speck,N.A. (1999). Cbfa2 is required for the formation of intra-aortic hematopoietic clusters. *Development* 126, 2563-2575.
- Ogata,K., Morikawa,S., Nakamura,H., Sekikawa,A., Inoue,T., Kanai,H., Sarai,A., Ishii,S., and Nishimura,Y. (1994). Solution structure of a specific DNA complex of the Myb DNA-binding domain with cooperative recognition helices. *Cell* 79, 639-648.
- Ollmann,M., Young,L.M., Di Como,C.J., Karim,F., Belvin,M., Robertson,S., Whittaker,K., Demsky,M., Fisher,W.W., Buchman,A., Duyk,G., Friedman,L., Prives,C., and Kopczynski,C. (2000). Drosophila p53 is a structural and functional homolog of the tumor suppressor p53. *Cell* 101, 91-101.
- Orkin,S.H. and Zon,L.I. (1997). Genetics of erythropoiesis: induced mutations in mice and zebrafish. *Annu. Rev. Genet.* 31, 33-60.
- Pal,S., Cantor,A.B., Johnson,K.D., Moran,T.B., Boyer,M.E., Orkin,S.H., and Bresnick,E.H. (2004). Coregulator-dependent facilitation of chromatin occupancy by GATA-1. *Proc Natl Acad Sci U S A* 101, 980-985.
- Palis,J., Robertson,S., Kennedy,M., Wall,C., and Keller,G. (1999). Development of erythroid and myeloid progenitors in the yolk sac and embryo proper of the mouse. *Development* 126, 5073-5084.
- Palis,J. and Yoder,M.C. (2001). Yolk-sac hematopoiesis: the first blood cells of mouse and man. *Exp Hematol.* 29, 927-936.
- Pan,H. and Griep,A.E. (1994). Altered cell cycle regulation in the lens of HPV-16 E6 or E7 transgenic mice: implications for tumor suppressor gene function in development. *Genes Dev* 8, 1285-1299.
- Paw,B.H. (2001). Cloning of the zebrafish retsina blood mutation: a genetic model for dyserythropoiesis and erythroid cytokinesis. *Blood Cells Mol Dis.* 27, 62-64.
- Paw,B.H., Davidson,A.J., Zhou,Y., Li,R., Pratt,S.J., Lee,C., Trede,N.S., Brownlie,A., Donovan,A., Liao,E.C., Ziai,J.M., Drejer,A.H., Guo,W., Kim,C.H., Gwynn,B., Peters,L.L., Chernova,M.N., Alper,S.L., Zapata,A., Wickramasinghe,S.N., Lee,M.J., Lux,S.E., Fritz,A., Postlethwait,J.H., and Zon,L.I. (2003). Cell-specific mitotic defect and dyserythropoiesis associated with erythroid band 3 deficiency. *Nat Genet* 34, 59-64.

- Paw,B.H. and Zon,L.I. (2000). Zebrafish: a genetic approach in studying hematopoiesis. *Curr Opin Hematol.* 7, 79-84.
- Perkins,A.C., Sharpe,A.H., and Orkin,S.H. (1995). Lethal beta-thalassaemia in mice lacking the erythroid CACCC-transcription factor EKLF. *Nature* 375, 318-322.
- Peters,H., Neubuser,A., Kratochwil,K., and Balling,R. (1998). Pax9-deficient mice lack pharyngeal pouch derivatives and teeth and exhibit craniofacial and limb abnormalities. *Genes Dev.* 12, 2735-2747.
- Petrovick,M.S., Hiebert,S.W., Friedman,A.D., Hetherington,C.J., Tenen,D.G., and Zhang,D.E. (1998). Multiple functional domains of AML1: PU.1 and C/EBPalpha synergize with different regions of AML1. *Mol Cell Biol* 18, 3915-3925.
- Pevny,L., Lin,C.S., D'Agati,V., Simon,M.C., Orkin,S.H., and Costantini,F. (1995). Development of hematopoietic cells lacking transcription factor GATA-1. *Development* 121, 163-172.
- Pevny,L., Simon,M.C., Robertson,E., Klein,W.H., Tsai,S.F., D'Agati,V., Orkin,S.H., and Costantini,F. (1991). Erythroid differentiation in chimaeric mice blocked by a targeted mutation in the gene for transcription factor GATA-1. *Nature* 349, 257-260.
- Phillips,R.L., Ernst,R.E., Brunk,B., Ivanova,N., Mahan,M.A., Deanehan,J.K., Moore,K.A., Overton,G.C., and Lemischka,I.R. (2000). The genetic program of hematopoietic stem cells. *Science* 288, 1635-1640.
- Plaster,N., Sonntag,C., Busse,C.E., and Hammerschmidt,M. (2006). p53 deficiency rescues apoptosis and differentiation of multiple cell types in zebrafish flathead mutants deficient for zygotic DNA polymerase delta1. *Cell Death Differ* 13, 223-235.
- Porcher,C., Swat,W., Rockwell,K., Fujiwara,Y., Alt,F.W., and Orkin,S.H. (1996). The T cell leukemia oncogene SCL/tal-1 is essential for development of all hematopoietic lineages. *Cell* 86, 47-57.
- Pui,J.C., Allman,D., Xu,L., DeRocco,S., Karnell,F.G., Bakkour,S., Lee,J.Y., Kadesch,T., Hardy,R.R., Aster,J.C., and Pear,W.S. (1999). Notch1 expression in early lymphopoiesis influences B versus T lineage determination. *Immunity* 11, 299-308.
- Radomska,H.S., Huettner,C.S., Zhang,P., Cheng,T., Scadden,D.T., and Tenen,D.G. (1998). CCAAT/enhancer binding protein alpha is a regulatory switch sufficient for induction of granulocytic development from bipotential myeloid progenitors. *Mol Cell Biol* 18, 4301-4314.
- Radtke,F., Wilson,A., and MacDonald,H.R. (2004). Notch signaling in T- and B-cell development. *Curr Opin Immunol.* 16, 174-179.
- Radtke,F., Wilson,A., Stark,G., Bauer,M., van,M.J., MacDonald,H.R., and Aguet,M. (1999). Deficient T cell fate specification in mice with an induced inactivation of Notch1. *Immunity* 10, 547-558.
- Ransom,D.G., Bahary,N., Niss,K., Traver,D., Burns,C., Trede,N.S., Paffett-Lugassy,N., Saganic,W.J., Lim,C.A., Hersey,C., Zhou,Y., Barut,B.A., Lin,S., Kingsley,P.D., Palis,J., Orkin,S.H., and Zon,L.I. (2004). The zebrafish moonshine gene encodes transcriptional intermediary factor 1gamma, an essential regulator of hematopoiesis. *PLoS Biol* 2, E237.
- Ransom,D.G., Haffter,P., Odenthal,J., Brownlie,A., Vogelsang,E., Kelsh,R.N., Brand,M., van Eeden,F.J., Furutani-Seiki,M., Granato,M., Hammerschmidt,M., Heisenberg,C.P., Jiang,Y.J., Kane,D.A., Mullins,M.C., and Nusslein-Volhard,C. (1996). Characterization of zebrafish mutants with defects in embryonic hematopoiesis. *Development* 123, 311-319.
- Ratajczak,J., Marlicz,W., Machalinski,B., Pertusini,E., Czajka,R., and Ratajczak,M.Z. (1998). An improved serum free system for cloning human "pure" erythroid colonies. The role of different growth factors and cytokines on BFU-E formation by the bone marrow and cord blood CD34+ cells. *Folia Histochem. Cytobiol.* 36, 55-60.

- Rebollo,A. and Schmitt,C. (2003). Ikaros, Aiolos and Helios: transcription regulators and lymphoid malignancies. *Immunol. Cell Biol.* *81*, 171-175.
- Rekhtman,N., Radparvar,F., Evans,T., and Skoultschi,A.I. (1999). Direct interaction of hematopoietic transcription factors PU.1 and GATA-1: functional antagonism in erythroid cells. *Genes Dev* *13*, 1398-1411.
- Reya,T., Duncan,A.W., Ailles,L., Domen,J., Scherer,D.C., Willert,K., Hintz,L., Nusse,R., and Weissman,I.L. (2003). A role for Wnt signalling in self-renewal of haematopoietic stem cells. *Nature* *423*, 409-414.
- Robb,L., Elwood,N.J., Elefanty,A.G., Kontgen,F., Li,R., Barnett,L.D., and Begley,C.G. (1996). The scl gene product is required for the generation of all hematopoietic lineages in the adult mouse. *EMBO J* *15*, 4123-4129.
- Rodriguez,P., Bonte,E., Krijgsveld,J., Kolodziej,K.E., Guyot,B., Heck,A.J., Vyas,P., de,B.E., Grosveld,F., and Strouboulis,J. (2005). GATA-1 forms distinct activating and repressive complexes in erythroid cells. *EMBO J.* *24*, 2354-2366.
- Rylski,M., Welch,J.J., Chen,Y.Y., Letting,D.L., Diehl,J.A., Chodosh,L.A., Blobel,G.A., and Weiss,M.J. (2003). GATA-1-mediated proliferation arrest during erythroid maturation. *Mol. Cell Biol.* *23*, 5031-5042.
- Sasaki,K. and Matsumura,G. (1988). Spleen lymphocytes and haemopoiesis in the mouse embryo. *J Anat.* *160*, 27-37.
- Sasaki,K. and Sonoda,Y. (2000). Histometrical and three-dimensional analyses of liver hematopoiesis in the mouse embryo. *Arch. Histol. Cytol.* *63*, 137-146.
- Sauvageau,G., Thorsteinsdottir,U., Eaves,C.J., Lawrence,H.J., Largman,C., Lansdorp,P.M., and Humphries,R.K. (1995). Overexpression of HOXB4 in hematopoietic cells causes the selective expansion of more primitive populations in vitro and in vivo. *Genes Dev.* *9*, 1753-1765.
- Sawada,K., Krantz,S.B., Dessypris,E.N., Koury,S.T., and Sawyer,S.T. (1989). Human colony-forming units-erythroid do not require accessory cells, but do require direct interaction with insulin-like growth factor I and/or insulin for erythroid development. *J. Clin. Invest* *83*, 1701-1709.
- Sawada,S. and Littman,D.R. (1993). A heterodimer of HEB and an E12-related protein interacts with the CD4 enhancer and regulates its activity in T-cell lines. *Mol. Cell Biol.* *13*, 5620-5628.
- Schumacher,B., Hanazawa,M., Lee,M.H., Nayak,S., Volkmann,K., Hofmann,E.R., Hengartner,M., Schedl,T., and Gartner,A. (2005). Translational repression of *C. elegans* p53 by GLD-1 regulates DNA damage-induced apoptosis. *Cell* *120*, 357-368.
- Scott,E.W., Fisher,R.C., Olson,M.C., Kehrl,E.W., Simon,M.C., and Singh,H. (1997). PU.1 functions in a cell-autonomous manner to control the differentiation of multipotential lymphoid-myeloid progenitors. *Immunity.* *6*, 437-447.
- Scott,E.W., Simon,M.C., Anastasi,J., and Singh,H. (1994). Requirement of transcription factor PU.1 in the development of multiple hematopoietic lineages. *Science* *265*, 1573-1577.
- Shafizadeh,E., Paw,B.H., Foott,H., Liao,E.C., Barut,B.A., Cope,J.J., Zon,L.I., and Lin,S. (2002). Characterization of zebrafish merlot/chablis as non-mammalian vertebrate models for severe congenital anemia due to protein 4.1 deficiency. *Development* *129*, 4359-4370.
- Shalaby,F., Ho,J., Stanford,W.L., Fischer,K.D., Schuh,A.C., Schwartz,L., Bernstein,A., and Rossant,J. (1997). A requirement for Flk1 in primitive and definitive hematopoiesis and vasculogenesis. *Cell* *89*, 981-990.
- Shalaby,F., Rossant,J., Yamaguchi,T.P., Gertsenstein,M., Wu,X.F., Breitman,M.L., and Schuh,A.C.

- (1995). Failure of blood-island formation and vasculogenesis in Flk-1-deficient mice. *Nature* 376, 62-66.
- Shi, Y., Lee, J.S., and Galvin, K.M. (1997). Everything you have ever wanted to know about Yin Yang 1..... *Biochim Biophys Acta* 1332, F49-F66.
- Shivdasani, R.A., Mayer, E.L., and Orkin, S.H. (1995). Absence of blood formation in mice lacking the T-cell leukaemia oncogene tal-1/SCL. *Nature* 373, 432-434.
- Silverstein, R.A. and Ekwall, K. (2005). Sin3: a flexible regulator of global gene expression and genome stability. *Curr Genet* 47, 1-17.
- Smith, L.G., Weissman, I.L., and Heimfeld, S. (1991). Clonal analysis of hematopoietic stem-cell differentiation in vivo. *Proc Natl Acad Sci U S A* 88, 2788-2792.
- Socolovsky, M., Lodish, H.F., and Daley, G.Q. (1998). Control of hematopoietic differentiation: lack of specificity in signaling by cytokine receptors. *Proc. Natl. Acad. Sci. U. S. A* 95, 6573-6575.
- Solnica-Krezel, L., Schier, A.F., and Driever, W. (1994). Efficient recovery of ENU-induced mutations from the zebrafish germline. *Genetics* 136, 1401-1420.
- Souabni, A., Cobaleda, C., Schebesta, M., and Busslinger, M. (2002). Pax5 promotes B lymphopoiesis and blocks T cell development by repressing Notch1. *Immunity* 17, 781-793.
- Spronk, C.A., Tessari, M., Kaan, A.M., Jansen, J.F., Vermeulen, M., Stunnenberg, H.G., and Vuister, G.W. (2000). The Mad1-Sin3B interaction involves a novel helical fold. *Nat Struct. Biol* 7, 1100-1104.
- Stainier, D.Y., Weinstein, B.M., Detrich, H.W., III, Zon, L.I., and Fishman, M.C. (1995). Cloche, an early acting zebrafish gene, is required by both the endothelial and hematopoietic lineages. *Development* 121, 3141-3150.
- Su, D.M. and Manley, N.R. (2000). Hoxa3 and pax1 transcription factors regulate the ability of fetal thymic epithelial cells to promote thymocyte development. *J. Immunol.* 164, 5753-5760.
- Sui, G., Affar, e.B., Shi, Y., Brignone, C., Wall, N.R., Yin, P., Donohoe, M., Luke, M.P., Calvo, D., Grossman, S.R., and Shi, Y. (2004). Yin Yang 1 is a negative regulator of p53. *Cell* 117, 859-872.
- Tenen, D.G., Hromas, R., Licht, J.D., and Zhang, D.E. (1997). Transcription factors, normal myeloid development, and leukemia. *Blood* 90, 489-519.
- Thomas, M.J. and Seto, E. (1999). Unlocking the mechanisms of transcription factor YY1: are chromatin modifying enzymes the key? *Gene* 236, 197-208.
- Thompson, M.A., Ransom, D.G., Pratt, S.J., MacLennan, H., Kieran, M.W., Detrich, H.W., III, Vail, B., Huber, T.L., Paw, B., Brownlie, A.J., Oates, A.C., Fritz, A., Gates, M.A., Amores, A., Bahary, N., Talbot, W.S., Her, H., Beier, D.R., Postlethwait, J.H., and Zon, L.I. (1998). The cloche and spadetail genes differentially affect hematopoiesis and vasculogenesis. *Dev Biol* 197, 248-269.
- Thorsteinsdottir, U., Sauvageau, G., and Humphries, R.K. (1999). Enhanced in vivo regenerative potential of HOXB4-transduced hematopoietic stem cells with regulation of their pool size. *Blood* 94, 2605-2612.
- Till, J.E.M.E.A.a.S.L. (1964). A stochastic model of stem cell proliferation, based on the growth of spleen colony-forming cells. *Proc. Natl. Acad. Sci. U. S. A* 51, 29-36.
- Ting, C.N., Olson, M.C., Barton, K.P., and Leiden, J.M. (1996). Transcription factor GATA-3 is required for development of the T-cell lineage. *Nature* 384, 474-478.
- Traver, D., Paw, B.H., Poss, K.D., Penberthy, W.T., Lin, S., and Zon, L.I. (2003). Transplantation and in

- vivo imaging of multilineage engraftment in zebrafish bloodless mutants. *Nat Immunol* 4, 1238-1246.
- Trede,N.S., Zapata,A., and Zon,L.I. (2001). Fishing for lymphoid genes. *Trends Immunol* 22, 302-307.
- Tsai,F.Y., Keller,G., Kuo,F.C., Weiss,M., Chen,J., Rosenblatt,M., Alt,F.W., and Orkin,S.H. (1994). An early haematopoietic defect in mice lacking the transcription factor GATA-2. *Nature* 371, 221-226.
- Tsang,A.P., Fujiwara,Y., Hom,D.B., and Orkin,S.H. (1998). Failure of megakaryopoiesis and arrested erythropoiesis in mice lacking the GATA-1 transcriptional cofactor FOG. *Genes Dev* 12, 1176-1188.
- Tsang,A.P., Visvader,J.E., Turner,C.A., Fujiwara,Y., Yu,C., Weiss,M.J., Crossley,M., and Orkin,S.H. (1997). FOG, a multitype zinc finger protein, acts as a cofactor for transcription factor GATA-1 in erythroid and megakaryocytic differentiation. *Cell* 90, 109-119.
- Uchida,N., Jerabek,L., and Weissman,I.L. (1996). Searching for hematopoietic stem cells. II. The heterogeneity of Thy-1.1(lin⁻)Sca-1+ mouse hematopoietic stem cells separated by counterflow centrifugal elutriation. *Exp Hematol* 24, 649-659.
- van Eeden,F.J., Granato,M., Odenthal,J., and Haffter,P. (1999). Developmental mutant screens in the zebrafish. *Methods Cell Biol* 60, 21-41.
- Varnum-Finney,B., Xu,L., Brashem-Stein,C., Nourigat,C., Flowers,D., Bakkour,S., Pear,W.S., and Bernstein,I.D. (2000). Pluripotent, cytokine-dependent, hematopoietic stem cells are immortalized by constitutive Notch1 signaling. *Nat. Med.* 6, 1278-1281.
- Vogelstein,B., Lane,D., and Levine,A.J. (2000). Surfing the p53 network. *Nature* 408, 307-310.
- Wagers,A.J., Christensen,J.L., and Weissman,I.L. (2002a). Cell fate determination from stem cells. *Gene Ther.* 9, 606-612.
- Wagers,A.J., Sherwood,R.I., Christensen,J.L., and Weissman,I.L. (2002b). Little evidence for developmental plasticity of adult hematopoietic stem cells. *Science* 297, 2256-2259.
- Wang,C.Y., Liang,Y.J., Lin,Y.S., Shih,H.M., Jou,Y.S., and Yu,W.C. (2004). YY1AP, a novel co-activator of YY1. *J Biol Chem* 279, 17750-17755.
- Wang,H., Clark,I., Nicholson,P.R., Herskowitz,I., and Stillman,D.J. (1990). The *Saccharomyces cerevisiae* SIN3 gene, a negative regulator of HO, contains four paired amphipathic helix motifs. *Mol Cell Biol* 10, 5927-5936.
- Wang,H., Long,Q., Marty,S.D., Sassa,S., and Lin,S. (1998). A zebrafish model for hepatoerythropoietic porphyria. *Nat Genet* 20, 239-243.
- Wang,Q., Stacy,T., Binder,M., Marin-Padilla,M., Sharpe,A.H., and Speck,N.A. (1996). Disruption of the *Cbfa2* gene causes necrosis and hemorrhaging in the central nervous system and blocks definitive hematopoiesis. *Proc Natl Acad Sci U S A* 93, 3444-3449.
- Wang,X., Kua,H.Y., Hu,Y., Guo,K., Zeng,Q., Wu,Q., Ng,H.H., Karsenty,G., de Crombrughe,B., Yeh,J., and Li,B. (2006). p53 functions as a negative regulator of osteoblastogenesis, osteoblast-dependent osteoclastogenesis, and bone remodeling. *J Cell Biol* 172, 115-125.
- Warren,A.J., Colledge,W.H., Carlton,M.B., Evans,M.J., Smith,A.J., and Rabbitts,T.H. (1994). The oncogenic cysteine-rich LIM domain protein *rbt2* is essential for erythroid development. *Cell* 78, 45-57.
- Weinstein,B.M., Schier,A.F., Abdelilah,S., Malicki,J., Solnica-Krezel,L., Stemple,D.L., Stainier,D.Y., Zwartkuis,F., Driever,W., and Fishman,M.C. (1996). Hematopoietic mutations in the zebrafish. *Development* 123, 303-309.

- Weiss,M.J., Keller,G., and Orkin,S.H. (1994). Novel insights into erythroid development revealed through in vitro differentiation of GATA-1 embryonic stem cells. *Genes Dev* 8, 1184-1197.
- Weiss,M.J. and Orkin,S.H. (1995). Transcription factor GATA-1 permits survival and maturation of erythroid precursors by preventing apoptosis. *Proc Natl Acad Sci U S A* 92, 9623-9627.
- Westman,B.J., Mackay,J.P., and Gell,D. (2002). Ikaros: a key regulator of haematopoiesis. *Int. J. Biochem. Cell Biol.* 34, 1304-1307.
- Wienholds,E., Schulte-Merker,S., Walderich,B., and Plasterk,R.H. (2002). Target-selected inactivation of the zebrafish rag1 gene. *Science* 297, 99-102.
- Wienholds,E., van Eeden,F., Kusters,M., Mudde,J., Plasterk,R.H., and Cuppen,E. (2003). Efficient target-selected mutagenesis in zebrafish. *Genome Res* 13, 2700-2707.
- Willert,K., Brown,J.D., Danenberg,E., Duncan,A.W., Weissman,I.L., Reya,T., Yates,J.R., III, and Nusse,R. (2003). Wnt proteins are lipid-modified and can act as stem cell growth factors. *Nature* 423, 448-452.
- Willett,C.E., Cherry,J.J., and Steiner,L.A. (1997). Characterization and expression of the recombination activating genes (rag1 and rag2) of zebrafish. *Immunogenetics* 45, 394-404.
- Willett,C.E., Cortes,A., Zuasti,A., and Zapata,A.G. (1999). Early hematopoiesis and developing lymphoid organs in the zebrafish. *Dev Dyn.* 214, 323-336.
- Willett,C.E., Kawasaki,H., Amemiya,C.T., Lin,S., and Steiner,L.A. (2001). Ikaros expression as a marker for lymphoid progenitors during zebrafish development. *Dev Dyn.* 222, 694-698.
- Wilson,A., MacDonald,H.R., and Radtke,F. (2001). Notch 1-deficient common lymphoid precursors adopt a B cell fate in the thymus. *J. Exp. Med.* 194, 1003-1012.
- Wingert,R.A., Brownlie,A., Galloway,J.L., Dooley,K., Fraenkel,P., Axe,J.L., Davidson,A.J., Barut,B., Noriega,L., Sheng,X., Zhou,Y., and Zon,L.I. (2004). The chianti zebrafish mutant provides a model for erythroid-specific disruption of transferrin receptor 1. *Development* 131, 6225-6235.
- Winnier,G., Blessing,M., Labosky,P.A., and Hogan,B.L. (1995). Bone morphogenetic protein-4 is required for mesoderm formation and patterning in the mouse. *Genes Dev* 9, 2105-2116.
- Wong,N., Chan,A., Lee,S.W., Lam,E., To,K.F., Lai,P.B., Li,X.N., Liew,C.T., and Johnson,P.J. (2003). Positional mapping for amplified DNA sequences on 1q21-q22 in hepatocellular carcinoma indicates candidate genes over-expression. *J Hepatol.* 38, 298-306.
- Wong,N., Lai,P., Lee,S.W., Fan,S., Pang,E., Liew,C.T., Sheng,Z., Lau,J.W., and Johnson,P.J. (1999). Assessment of genetic changes in hepatocellular carcinoma by comparative genomic hybridization analysis: relationship to disease stage, tumor size, and cirrhosis. *Am J Pathol* 154, 37-43.
- Wu,H., Liu,X., Jaenisch,R., and Lodish,H.F. (1995). Generation of committed erythroid BFU-E and CFU-E progenitors does not require erythropoietin or the erythropoietin receptor. *Cell* 83, 59-67.
- Xu,M.J., Matsuoka,S., Yang,F.C., Ebihara,Y., Manabe,A., Tanaka,R., Eguchi,M., Asano,S., Nakahata,T., and Tsuji,K. (2001). Evidence for the presence of murine primitive megakaryocytopoiesis in the early yolk sac. *Blood* 97, 2016-2022.
- Yamanaka,R., Barlow,C., Lekstrom-Himes,J., Castilla,L.H., Liu,P.P., Eckhaus,M., Decker,T., Wynshaw-Boris,A., and Xanthopoulos,K.G. (1997). Impaired granulopoiesis, myelodysplasia, and early lethality in CCAAT/enhancer binding protein epsilon-deficient mice. *Proc. Natl. Acad. Sci. U. S. A* 94, 13187-13192.
- Yoder,M.C. and Hiatt,K. (1997). Engraftment of embryonic hematopoietic cells in conditioned

newborn recipients. *Blood* 89, 2176-2183.

Yoder, M.C., Hiatt, K., Dutt, P., Mukherjee, P., Bodine, D.M., and Orlic, D. (1997a). Characterization of definitive lymphohematopoietic stem cells in the day 9 murine yolk sac. *Immunity* 7, 335-344.

Yoder, M.C., Hiatt, K., and Mukherjee, P. (1997b). In vivo repopulating hematopoietic stem cells are present in the murine yolk sac at day 9.0 postcoitus. *Proc Natl Acad Sci U S A* 94, 6776-6780.

Zan, Y., Haag, J.D., Chen, K.S., Shepel, L.A., Wigington, D., Wang, Y.R., Hu, R., Lopez-Guajardo, C.C., Brose, H.L., Porter, K.I., Leonard, R.A., Hitt, A.A., Schommer, S.L., Elegbede, A.F., and Gould, M.N. (2003). Production of knockout rats using ENU mutagenesis and a yeast-based screening assay. *Nat. Biotechnol.* 21, 645-651.

Zhang, D.E., Zhang, P., Wang, N.D., Hetherington, C.J., Darlington, G.J., and Tenen, D.G. (1997). Absence of granulocyte colony-stimulating factor signaling and neutrophil development in CCAAT enhancer binding protein alpha-deficient mice. *Proc. Natl. Acad. Sci. U. S. A* 94, 569-574.

Zhang, P., Behre, G., Pan, J., Iwama, A., Wara-Aswapati, N., Radomska, H.S., Auron, P.E., Tenen, D.G., and Sun, Z. (1999). Negative cross-talk between hematopoietic regulators: GATA proteins repress PU.1. *Proc Natl Acad Sci U S A* 96, 8705-8710.

Zhang, P., Zhang, X., Iwama, A., Yu, C., Smith, K.A., Mueller, B.U., Narravula, S., Torbett, B.E., Orkin, S.H., and Tenen, D.G. (2000). PU.1 inhibits GATA-1 function and erythroid differentiation by blocking GATA-1 DNA binding. *Blood* 96, 2641-2648.

Zhuang, Y., Cheng, P., and Weintraub, H. (1996). B-lymphocyte development is regulated by the combined dosage of three basic helix-loop-helix genes, E2A, E2-2, and HEB. *Mol. Cell Biol.* 16, 2898-2905.

Zon, L.I. (1995). Developmental biology of hematopoiesis. *Blood* 86, 2876-2891.